UNIVERSIDADE FEDERAL DO PARANÁ

RENATA RANK MIRANDA

EFEITOS CITOTÓXICOS DA INTERAÇÃO ENTRE NANOPARTÍCULAS DE PRATA E METAIS NÃO ESSENCIAIS EM CÉLULAS DE HEPATOCARCINOMA HUMANO (HEPG2)

CURITIBA

2017

RENATA RANK MIRANDA

EFEITOS CITOTÓXICOS DA INTERAÇÃO ENTRE NANOPARTÍCULAS DE PRATA E METAIS NÃO ESSENCIAIS EM CÉLULAS DE HEPATOCARCINOMA HUMANO (HEPG2)

Tese apresentada ao Programa de Pós-Graduação em Biologia Celular e Molecular, Departamento de Biologia Celular, Setor de Ciências Biológicas, Universidade Federal do Paraná como requisito parcial à obtenção de título de Doutor em Biologia Celular

Orientador: Prof. Dr. Francisco Filipak Neto

Coorientador: Prof. Dr. Frank Kjeldsen

CURITIBA

2017

Universidade Federal do Paraná
Sistema de Bibliotecas

Miranda, Renata Rank
Efeitos citotóxicos da interação entre nanopartículas de prata e metais não essenciais em células de hepatocarcinoma humano (HEPG2). / Renata Rank Miranda. – Curitiba, 2017.
117 f.: il. ; 30cm.

Orientador: Prof. Dr. Francisco Filipak Neto
Coorientador: Prof. Dr. Frank Kjeldsen

Tese (Doutorado) - Universidade Federal do Paraná, Setor de Ciências Biológicas. Programa de Pós-Graduação em Biologia Celular e Molecular.

1.Cadmio. 2. Mercúrio. 3. Proteômica. 4. Fígado - Câncer. 5. Nanopartículas. 6. Metais. 7. Prata - nanoestrutura I. Título. II. Filipak Neto, Francisco. III. Kjeldsen, Frank. IV. Universidade Federal do Paraná. Setor de Ciências Biológicas. Programa de Pós-Graduação em Biologia celular e Molecular.

CDD (20. ed.) 615.9253

Programa de Pós-graduação Biologia Celular e Molecular

Departamento de Biologia Celular
Setor de Ciências Biológicas
Universidade Federal do Paraná

PPGBioCelMol
UFPR

PARECER

A banca examinadora, instituída pelo colegiado do Programa de Pós-Graduação em Biologia Celular e Molecular, do Setor de Ciências Biológicas, da Universidade Federal do Paraná, composta por:

Prof. Dr. Francisco Filipak Neto — Aprovado — Francisco Filipak Neto
Orientador e presidente da banca
Universidade Federal do Paraná - UFPR

Profa. Dra. Lia Sumie Nakao — aprovada — Lia Sumie Nakao
Universidade Federal do Paraná - UFPR

Prof. Dr. Paulo Costa Carvalho — Aprovado
Instituto Carlos Chagas - ICC

Profa. Dra. Silvia Maria Suter Correia Cadena — Aprovada — Silvia Maria Suter Correia Cadena
Universidade Federal do Paraná - UFPR

Prof. Dr. Bruno Dallagiovanna Muñiz
Instituo Carlos Chagas - ICC

E tendo como suplente,

Profa. Dra. Carolina Camargo de Oliveira
Universidade Federal do Paraná – UFPR

Profa. Dra. Célia Regina Cavichiolo Franco
Universidade Federal do Paraná – UFPR

Após arguir a candidata ***Renata Rank de Miranda***, em relação ao seu trabalho intitulado: "***Efeitos citotóxicos da interação entre nanopartículas de prata e metais não essenciais em células de hepatocarcinoma humano (HepG2)***", são de parecer favorável à Aprovação da acadêmica, habilitando-a ao título de Doutora em Biologia Celular e Molecular.
A obtenção do título está condicionada à implementação das correções sugeridas pelos membros da banca examinadora, bem como ao cumprimento integral das exigências estabelecidas no Regimento Interno deste Programa de Pós-Graduação.

Curitiba, 28 de Março de 2017.

Centro Politécnico
Rua Heráclito Domingos dos Santos s/n | Jardim das Américas
Caixa Postal: 19031 | CEP: 81.531-980 | Curitiba | Paraná | Brasil
Fone: 55.41.3361-1676

AGRADECIMENTOS

Ao meu querido orientador Prof. Francisco Filipak Neto. Por confiar no meu trabalho, pela dedicação na minha formação, por todos os ensinamentos, pela paciência, disponibilidade e por me incentivar a fazer o meu melhor ao longo desses últimos 6 anos;

Ao meu coorientador dinamarquês Prof. Frank Kjeldsen. Por ter me recebido tão bem no Protein Research Group, por ter acreditado na minha capacidade, me apoiado e aberto novas portas da ciência para mim;

Ao Prof. Arandi Ginane Bezerra Jr, pela disponibilidade, atenção e colaboração ao longo desses anos;

Aos Professores do grupo de toxicologia celular: Ciro A. Oliveira Ribeiro, Marco Randi, Sonia Grötzner, Claudia Ortolani-Machado e Maritana Mela;

Ao Samuel Liebel, que dedicou a mim muito do seu tempo e conhecimento, me ensinando não apenas sobre cultivo celular, mas também organização e paciência;

Ao Vladimir Gorshkov e Stefan Kempf, por todos os ensinamentos no mundo da proteômica e principalmente pela companhia e amizade durante meu período na Dinamarca;

Aos amigos e colegas do Laboratório de Toxicologia Celular: Carola, Flávia, Débora, Dandie, Nilce, Maristela e todos os demais. Obrigada por toda ajuda, apoio e amizade durante os anos;

A Halina, minha amiga de todas as etapas vida;

Um agradecimento especial para as meninas que trabalharam comigo no cultivo celular: Yvanna, Gis, Andressa, Jessica, Ludi e Marcelle;

Aos amigos e colegas do PR Group: Otília, Taewook, Vasco, Veit, Gio, Pia, Pernille, Asif, Barbara, Joy, Soren, Tina, Lilia, Arek e os demais;

À Micaella e a Lívia. Amigas queridas que eu tive muita sorte de ter conhecido durante o doutorado sanduíche, que dividiram comigo seu conhecimento e amizade;

À Profa. Carolina Camargo, pela disponibilidade e ajuda com o citômetro e fluxo e sugestões para melhoria do primeiro capítulo desta tese;

Às técnicas do PR Group, Vibike e Andrea, pelo auxílio nos espectrômetros de massa;

Ao Prof. Kaare Rasmussen e Lilian Skytte, do departamento de química da SDU (DK) pela colaboração nas análises de quantificação de metais;

À Prof. Carmen Voigt, do departamento de química da UEPG pela colaboração ao longo dos anos com análises de caracterização de nanopartículas;

À Profa. Célia Regina e Dilza Trevizan, por todas as contribuições na correção dos relatórios anuais do doutorado;

À secretária do programa de pós-graduação em biologia celular, Marlene;

À secretária do Protein Research Group. Lene, quem facilitou muito todo o processo de ida para Dinamarca, me recebeu de braços abertos e sempre fez com que eu me sentisse em casa no PR group;

Ao Israel Bini, pelo auxílio na obtenção de imagens no microscópio confocal;

Ao Centro de Microscopia Eletrônica da UFPR;

À agencia financiadora CAPES pela bolsa de doutorado no Brasil e pela bolsa de doutorado sanduíche na Dinamarca;

E gostaria de agradecer especialmente aos meus pais, Regina e Fausto, e minha irmã, Fernanda, pelo amor incondicional, por sempre me apoiarem, sempre me incentivarem a dar o meu melhor e sempre me guiarem pelo melhor caminho. Amo muito vocês!;

Enfim, a todos aqueles que de alguma forma contribuíram para o desenvolvimento deste trabalho.

MUITO OBRIGADA!

RESUMO

Devido a intensa produção e incorporação de AgNP em produtos para consumo, espera-se que estas sejam, direta ou indiretamente, liberadas em ambiente naturais, o que representa uma via de exposição em potencial não apenas para a biota, mas também para humanos. Apesar de muitos estudos terem demonstrado o potencial tóxico de AgNP em células e organismos, a co-exposição com contaminantes onipresentes na natureza, como metais, pode induzir efeitos que não podem ser previstos a partir daqueles gerados por exposições isoladas. Nesta tese, as interações toxicológicas entre AgNP e Cd/Hg foram investigadas em células HepG2. No primeiro capítulo, ensaios bioquímicos, microscopia confocal e quantificação intracelular de metais indicaram que as co-exposições resultam em interações toxicológicas, sendo a associação de AgNP+Cd mais tóxica do que AgNP+Hg. Aumentos nos níveis de EROs citosólicas e mitocondrial foram observados após 2-4 h de exposição a AgNP+ Cd/Hg, porém esse efeito foi parcialmente revertido após 24 h de exposição a AgNP+Hg. Ainda, decréscimos da viabilidade celular, metabolismo, proliferação e atividade dos transportadores MDR foram mais pronunciados em células co-expostas aos contaminantes do que aos contaminantes individuais. As co-exposições levaram ao aumento da morte celular, principalmente por necrose, e aumento na concentração intracelular de Hg. Desta forma, interações toxicológicas resultam na potencialização da toxicidade de AgNP, Cd e Hg. Enquanto o aumento intracelular de Hg pode estar relacionado com a maior toxicidade de AgNP+Hg, essa lógica não é válida para os efeitos deletérios observados após a co-exposição a AgNP+Cd. Desta forma, o segundo capítulo foi conduzido de modo a explorar mais aprofundadamente os efeitos celulares e moleculares induzidos pela associação entre as AgNP e Cd. A viabilidade celular e relação ADP/ATP foram pouco alteradas após 4 h de exposição; no entanto, esses parâmetros foram substancialmente alterados após 24 h. Os resultados da análise proteômica seguiram o mesmo padrão: enquanto após 4 h as exposições aos contaminantes o proteoma total das células foi pouco alterado, após 24 h de exposição às AgNP e Cd, cerca de 7% e 2% do proteoma total foi desregulado, respectivamente, enquanto 43% deste foi alterado após co-exposição a AgNP+Cd. Resumidamente, a toxicidade desta associação parece estar envolvida com a inativação de Nrf-2, o que pode resultar na redução dos níveis da defesa antioxidante, e proteínas relacionadas aos proteossomos; redução dos níveis de proteínas envolvidas na via glicolítica e aumento nos níveis de proteínas envolvidas com a fosforilação oxidativa e metabolismo de lipídios, o que pode indicar uma tentativa de retorno às condições de homeostase energética. No entanto, essa estratégia de adaptação celular não foi suficiente para reestabelecer a homeostase de ADP/ATP e impedir a morte celular. De maneira geral, este estudo fornece as primeiras informações a respeito da interação toxicológica entre AgNP e metais não essenciais em modelo *in vitro*.

Palavras-chave: AgNP, cádmio, mercúrio, co-exposição, interação, ensaios bioquímicos, proteômica.

ABSTRACT

Due to the increasing production and applications of AgNP in consumer products, AgNP are expected to be, directly or indirectly, released into natural environments, representing a potential threat to the biota and humans. An increasing number of studies have described the toxic potential of AgNP in cells and organisms. However, co-exposure of AgNP with ubiquitous contaminants, such as metals, may result in non-predictable outcomes. In this thesis, toxicological interactions of AgNP, Cd and Hg were investigated in HepG2 cells. In the first chapter, biochemical endpoints, confocal microscopy and intracellular metal concentration indicated that the co-exposures led to toxicological interactions, with AgNP + Cd being more toxic to HepG2 cells than AgNP + Hg. Early (2-4 h) increases of cytosolic and mitochondrial ROS were observed in the cells co-exposed to AgNP + Cd/Hg, in comparison to the control and individual contaminants, but the effect was partially reverted in AgNP + Hg at the end of 24 h-exposure. In addition, decreases of mitochondrial metabolism, cell viability, cell proliferation and ABC-transporters activity were also more pronounced in the co-exposure groups. Foremost, co-exposure to AgNP and metals potentiated cell death (mainly by necrosis) and Hg (but not Cd) intracellular levels. Therefore, toxicological interactions seem to increase the toxicity of AgNP, Cd and Hg. While an increase of Hg uptake might be related to the increase of toxicity after exposure to AgNP+Hg, this logic is not valid for the high toxicity observed after co-exposure to AgNP+Cd. Therefore, the second chapter was conducted to further explore cellular and molecular effects induced by this co-exposure. Cell viability and ADP/ATP ratio were slightly affected after the 4 h exposure to individual and combined exposures. However, these endpoints were strongly altered after 24 h co-exposure to AgNP+Cd compared to the control and individual exposures. The proteomics data followed the same trend: minor deregulation at 4 h-exposure in all groups and 7% (AgNP), 2% (Cd) and 43% (AgNP+Cd) at 24 h-exposure. Briefly, the toxicity induced by AgNP+Cd seems to be involved the inactivation of Nrf-2, which can result in down-regulation of antioxidant defense and proteasome related proteins, down-regulation of glycolysis related proteins and upregulation of oxidative phosphorylation and lipid metabolism proteins. This may indicate an attempt to reestablish homeostasis. Thus, the adaptation strategy was not able to restore ADP/ATP homeostasis and avoid cell death. Overall, this study provides the first insights into cellular outcomes after the co-exposure to AgNP and non-essential metals.

Key words: AgNP, cadmium, mercury, co-exposure, interaction, biochemical endpoints, proteomics.

LISTA DE FIGURAS

INTRODUÇÃO

FIGURA 1. Representação ilustratrada da definição de nanopartículas. 13
FIGURA 2. Mecanismo proposto da toxicidade de AgNP. 16
FIGURA 3. Células HepG2. 20
FIGURA 4. Fluxograma de um experimento baseado em espectrometria de massas 25
FIGURA 5. Fluxograma de um experimento usando a metodologia iTRAQ 27

CAPÍTULO I

FIGURE 1. AgNP characterization. 40
FIGURE 2. MTT assay in cells exposed for 4 and 24 h. 41
FIGURE 3. Neutral red assay in cells exposed for 4 and 24 h. 42
FIGURE 4. Cell proliferation assay in cells exposed for 24 h. 43
FIGURE 5. ROS production in cells after exposure for 2, 4 and 24 h. 44
FIGURE 6. Superoxide production in mitochondria of cells exposed for and 24 h. 46
FIGURE 7. Rhodamine accumulation assay in cells exposed for 4 and 24 h. 47
FIGURE 8. Intracellular concentration of Ag, Cd and Hg in cells exposed for 4 h. .49

CAPÍTULO II

FIGURE 1. AgNP characterization. 70
FIGURE 2. LDH leakage and trypan blue assays in cells exposed for 4 and 24 h. 71
FIGURE 3. ADP/ATP ratio in cells exposed for 4 and 24 h.. 73
FIGURE 4. Schematic work-flow applied to the study of interaction of AgNP and cadmium in HepG2 cells. 74
FIGURE 5. Quantitative data of proteomic analysis 75
FIGURE 6. Functional interaction networks of deregulated proteins after 24 h 77
FIGURE 7. Upstream regulators and canonical pathways analyis after 24 h 78

LISTA DE TABELAS

CAPÍTULO I

TABLE 1. Experimental design for the toxicity evaluation of the contaminats 36

CAPÍTULO II

TABLE 1. Antioxidant defense proteins differentially regulated after 24 h. 80
TABLE 2. Proteasomal subunits differentially regulated after 24.....81
TABLE 3. Proteins related to ubiquitination differentially regulated after 24 h.....82
TABLE 4. Translation related proteins differentially deregulated after 24 h.....84
TABLE 5. Glycolisis related proteins differentially deregulated after 24 h.....85
TABLE 6. Oxidative phosphorylation related proteins differentially deregulated after 24 h. 86
TABLE 7. TCA cycle and lipid metabolism related proteins differentially deregulated after 24 h. 87

LISTA DAS PRINCIPAIS ABREVIATURAS[1]

ADP – adenosina difosfato

ATP – adenosina trifosfato

AgNP – nanopartículas de prata

ACN – acetonitrila

AGC – controle automático de ganho

Cd – cloreto de cádmio

DCFDA – 2'-7'-diclorofluriscéína diacetato

DLS – espalhamento dinâmico da luz

EROs – espécies reativas de oxigênio

FA – ácido fórmico

Hg – cloreto de mercúrio

HPLC – cromatografia líquida de alta performance

IPA – *ingenuity pathway analysis*

iTRAQ – *isobaric tags for relative and absolute quantification*

LC-MS/MS – cromatografia líquida acoplada a espectrometria de massas tandem

LDH – lactato desidrogenase

MDR – transportadores de resistência à multidrogas

MS – espectrometria de massas

MTT – brometo de [3-(4,5-dimetiltiazol-2-il)-2,5 difeniltetrazólio]

NH_3 – amônia

NP – nanopartícula

PBS – tampão fosfato salino

ROS – *reactive oxygen species* (espécies reativas de oxigênio)

SRING – *search tool for the retrieval of interacting genes/proteins*

TEAB – tampão trietilamonio bicarbonato

TFA – ácido trifluoroacético

---

[1] Abreviações citadas apenas uma vez ou em sequência no texto não estão listadas.

SUMÁRIO

1. INTRODUÇÃO 12
1.1. Nanopartículas, nanotecnologia e nanotoxicologia 12
1.2. Nanopartículas de Prata: aplicações e toxicidade 14
1.3. Misturas complexas e metais tóxicos 17
1.4. Modelo de estudo: células HepG2 19
1.5. Biomarcadores para avaliação *in vitro* de toxicidade 20
1.6. Aplicação de proteômica baseada em espectrometria de massas em toxicologia 24
2. OBJETIVOS 28
2.1. Objetivo geral 28
2.2. Objetivos específicos 28
3. ESTRATÉGIA EXPERIMENTAL 30
CAPITULO I - Toxicological interactions of silver nanoparticles and non-essential metals in human hepatocarcinoma cell line 31
ABSTRACT 32
1. INTRODUCTION 33
2. MATERIALS AND METHODS 35
2.1. Silver nanoparticles synthesis and characterization 35
2.2. HepG2 cell culture 35
2.3. Selection of the concentrations of AgNP, Hg and Cd 35
2.4. Contaminants preparation and exposure protocol 36
2.5. Cytotoxicity and proliferation assays 37
2.6. Reactive Oxygen Species (ROS) levels 37
2.7. Multidrug efflux transporters activity 37
2.11. Cell death 38
2.12. Intracellular metals concentration 38
2.13. Statistical procedures 39
3. RESULTS 40
3.1. AgNP characterization 40

3.2. Cytotoxicity/Viability 40
3.3. Cell Proliferation 42
3.4. ROS production 43
3.6. Multidrug efflux transporters activity 46
3.7. Cell death 48
3.8. Intracellular metals concentration 48
4. DISCUSSION 50
Contaminants affected cell survivor and the mode of cell death after time-dependent toxicological interaction 50
ROS production increased early after the co-exposures 51
*Rhodamine accumulation followed the same pattern of mitochondrial ROS levels*52
Higher accumulation of the metal can explain the higher toxicity of the association containing Hg, but not Cd 53
5. CONCLUSION 54
SUPPLEMENTARY MATERIAL 55
REFERENCES 56
CAPÍTULO II - CO-EXPOSURE TO SILVER NANOPARTICLES AND CADMIUM IONS INDUCES ANTIOXIDANT DEFENSE DEPLETION AND METABOLIC PROTEINS REPROGRAMMING IN HEPG2 CELLS…….....60
ABSTRACT 61
1. INTRODUCTION 62
2. MATERIAL AND METHODS 64
2.1. Silver nanoparticles characterization 64
2.2. HepG2 cell culture 64
2.3. Exposure protocol 64
2.4. Cell viability tests 64
2.5. ADP/ATP ratio assay 65
2.6. Statistical procedures for biochemical assays 66
2.7. Sample preparation for mass spectrometry based proteomics analysis 66
2.8. Desalting with R2/R3 micro-columns 66
2.9. Peptide labeling 67

2.10. Sample fractionation 67
2.11. Reversed-phase NanoLC MS/MS 67
2.12. Database searches and bioinformatics analysis 68
3. RESULTS AND DISCUSSION 70
3.1. Silver nanoparticle characterization 70
3.2. Co-exposure of AgNP and Cd induce loss of cell viability and metabolic depletion 70
3.3. Co-exposure to AgNP+Cd lead to deep changes in HepG2 cell proteome 73
3.4. Molecular mechanisms underlying the toxic response to the contaminants 76
4. CONCLUSION 88
4. DISCUSSÃO GERAL 94
REFERÊNCIAS 100
RESULTADOS COMPLEMENTARES 113

1. INTRODUÇÃO

1.1. Nanopartículas, nanotecnologia e nanotoxicologia

Partículas em nanoescala[2] ocorrem naturalmente no meio ambiente, podendo estar presentes em minérios ou geradas a partir da combustão incompleta de combustíveis fósseis e erupções vulcânicas (NOWACK E BUCHELI, 2007) . No entanto, o termo nanopartícula (NP), ou nanomaterial, é utilizado apenas para definir partículas na escala nanométrica produzidas industrialmente, como os óxidos metálicos, fulerenos, nanotubos de carbono, NP metálicas, entre outros (HOYT E MASON, 2008; FELIU E FADEEL, 2010).

De acordo com a Organização Internacional de Padronização (*International Standadization Organization* – ISO), NP é um material individual que apresenta ao menos uma de suas dimensões na escala nanométrica (fig. 1; ISO, 2015). No entanto, classificações que levam em consideração propriedades como morfologia, composição, dimensionalidade e uniformidade também são aceitas e encontradas na literatura BYSTRZEJEWSKA-PIOTROWSKA et al., 2009). Nessas dimensões, a relação área de superfície por massa aumenta consideravelmente se comparado ao mesmo material em macro ou microescala. Por exemplo, enquanto cerca de 1% dos átomos ocupam a superfície de uma micropartícula, mais de 10% dos átomos ocupam a área de superfície de uma partícula de 10 nm de diâmetro (GRAINGER E CASTNER, 2008). Essa relação entre a porcentagem de átomos na superfície e o volume da partícula gera uma maior reatividade atômica de superfície, conferindo às NP propriedades magnéticas, químicas, físicas, elétricas e catalíticas únicas e fundamentalmente distintas daquelas observadas em materiais em escala não-nanométrica (NEL et al*.,* 2006; SIERRA et al*.,* 2016). Por exemplo: o ponto de fusão do ouro muda em função do decréscimo do seu tamanho, nanopartículas de ferro apresentam propriedades supramagnéticas[3] nessas dimensões, e uma folha de átomos de carbono, quando enrolada de modo a formar um tubo oco,

[2] Nanoescala - intervalo de comprimento de aproximadamente 1 nm a 100 nm (ISO, 2010).
[3] Supramagnetismo - tipo de magnetismo que aparece em partículas férricas em escala nanométrica.

produz um novo material, mais leve e resistente do que o aço e mais duro que o diamante (FELIU E FADEEL, 2010).

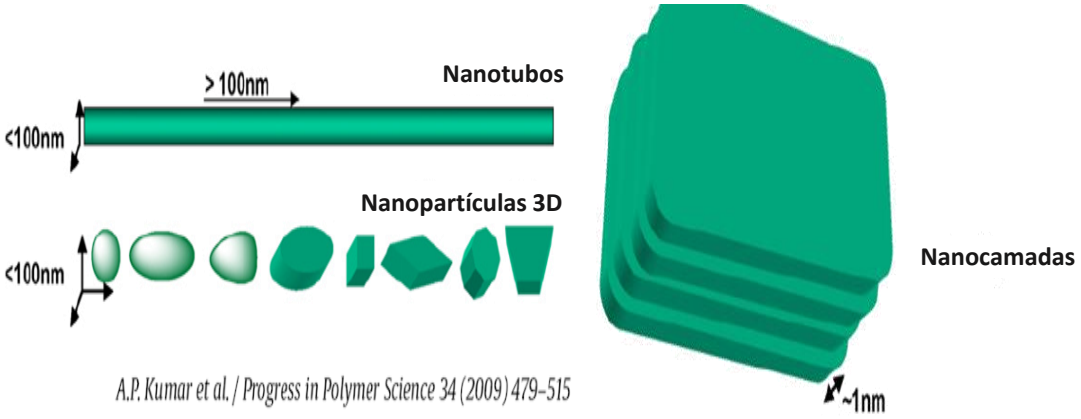

FIGURA 1. Representação ilustrada da definição de nanomateriais de acordo com suas dimensões (Fonte: figura adaptada de Kumar et al.,, 2009).

A exploração e aplicação das propriedades inovadoras encontradas em nanopartículas têm possibilitado o avanço tecnológico e científico de áreas diversas como biomédica, farmacêutica, eletrônica, agricultura e biorremediação ambiental (CONTRERAS et al., 2016; KUMARI E SINGH, 2016; PETERS et al., 2016; WANG et al., 2015). Por esta razão, atualmente a nanotecnologia[4] é um dos campos mais promissores da ciência e tecnologia, com uma taxa de crescimento anual de aproximadamente 20%, estima-se que seu mercado global deverá crescer para cerca de 90 bilhões de dólares até 2021 (BCC, 2016). De acordo com o *Nanotech Project*, até o momento 1827 produtos cadastrados apresentam algum tipo de nanopartícula incorporada (VANCE et al., 2015). No entanto, o uso crescente de nanomateriais na sociedade vem sendo acompanhado da preocupação com potenciais efeitos adversos para humanos e meio ambiente (FELIU E FADEEL, 2010).

O termo nanotoxicologia surgiu recentemente, quando Donaldson e coautores (2004) sugeriram a criação desta nova disciplina em resposta ao avanço da

[4] Nanotecnologia - desenvolvimento da pesquisa e tecnologia, ao processo de fabricação e manipulação da matéria em escala atômica (EPA, 2007).

nanotecnologia, a fim de abordar os potenciais efeitos nocivos do uso generalizado e produção em larga escala de nanopartículas. Desta forma, a nanotoxicologia surge como uma contribuição importante para o desenvolvimento sustentável e seguro da nanotecnologia (DONALDSON, 2004). Segundo Shvedova et al., (2016), dois fatores fazem com que o estudo da nanotoxicologia seja de extrema importância: (1) produção em larga escala de diferentes nanomateriais e (2) rápido desenvolvimento de nanomateriais com características físicas e químicas únicas e inesperadas.

Historicamente, a toxicologia é associada a *Paracelsus*[5] e ao conceito de dose e dose-resposta. No entanto, diferentemente do que ocorre para contaminantes clássicos, a toxicidade das NPs não depende apenas da dose ou concentração, mas também de suas propriedades físico-químicas. Apesar do potencial tóxico de matérias em escala convencional e/ou de químicos a nível molecular serem amplamente conhecidos, os de materiais em nanoescala ainda estão sendo descobertos (ELSAESSER E HOWARD, 2012). Vários grupos de pesquisa têm demonstrado o potencial tóxico de nanopartículas tanto em células quanto em organismos complexos (TAKEDA et al., 2009; NGUYEN et al., 2013; WU et al., 2013; MIRANDA et al*.,* 2016). De modo geral, observa-se que a medida que o tamanho da partícula decresce, há um aumento na sua reatividade de superfície e uma tendência no aumento de sua toxicidade, mesmo nos casos onde o tamanho não nanométrico do material for relativamente inerte, como ocorre, para o carbono negro e óxido de titânio (FARRÉ et al., 2009). No entanto, outras características das NP também determinam seu potencial tóxico (*e.g.* composição, forma, taxa de dissolução oxidativa ou capeamento), bem como o meio que essas partículas encontram-se (*e.g.* alterando a biodisponibilidade e/ou carga das NP) (MISRA et al*.,* 2012).

1.2. Nanopartículas de Prata: aplicações e toxicidade

As nanopartículas de prata (AgNP) são as NP mais amplamente empregadas em produtos de consumo humano, sendo incorporadas em aproximadamente 25% dos produtos cadastrados no banco de dados *Nanotech Project* (VANCE et al., 2015). Suas

[5] *Paracelsus* – intelectual suíço do século XVI, considerado o fundador da toxicologia clássica. A ele é atribuída a frase “a dose faz o veneno”.

aplicações incluem uma grande variedade de produtos alimentícios, vestuário, domésticos, cosméticos, eletrônicos e aparelhos médicos (ZANETTE et al., 2011). A principal característica que permite o sucesso das AgNP é sua ação germicida, com atividade comprovada contra bactérias, fungos e até mesmo alguns tipos de vírus, incluindo HIV e SARS (LARA et al., 2011; YOU et al., 2012).

No entanto, os efeitos adversos que AgNP podem induzir têm sido reportados em diferentes níveis de organização biológica (GLIGA et al., 2014; MONFARED et al., 2015; MORONES et al., 2005; WU et al., 2010; TANG et al., 2008), o que tem despertado preocupação no meio científico. Publicações com modelos *in vivo* e *in vitro* demonstram que a toxicidade das AgNP está relacionada não apenas com a concentração administrada (CARLSON et al., 2008; WU et al., 2010), mas também com o tamanho da partícula (MIETHLING-GRAFF et al., 2014; KUMAR et al., 2015) e tipo de capeamento (NALLANTHIGHAL et al., 2017).

As principais consequências *in vitro* da exposição às AgNP são a produção de espécies reativas de oxigênio, alterações no ciclo celular, danos ao material genético, processos inflamatórios e morte celular (ASHARANI et al., 2009; SINGH E RAMARAO 2012; MIETHLING-GRAFF et al., 2014).

A figura 2 apresenta um resumo ilustrado dos principais efeitos *in vitro* provocados após a exposição à AgNP.

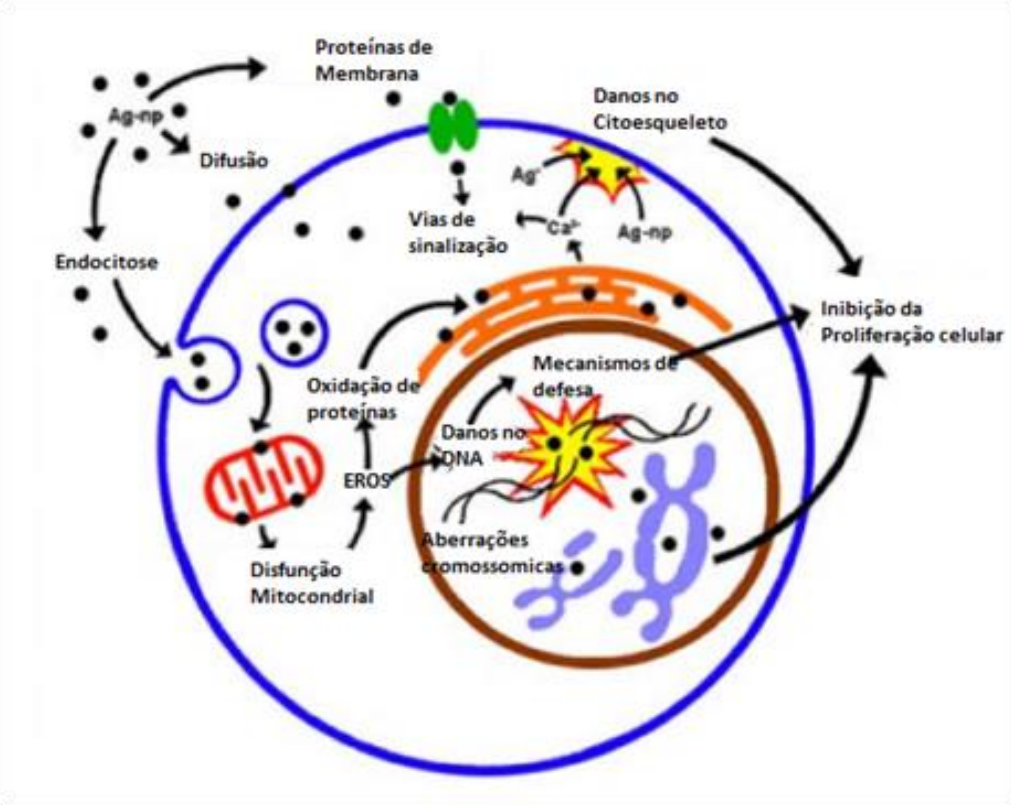

FIGURA 2. Mecanismo de toxicidade de AgNP (Fonte: figura adaptada de ASHARANI et al., 2009).

Ainda, a toxicidade das AgNP também está associada com a liberação de íons prata (Ag^+; efeito conhecido como "cavalo de Tróia[6]") e a combinação de ambos, partícula e íons (GLIGA et al., 2014). No entanto, a entrada de Ag nas células é maior quando estas são expostas às AgNP em comparação a exposição somente aos íons Ag^+, e as respostas provocadas por AgNP, apesar de relacionadas com Ag^+ são ainda mais complexas (como por exemplo, alteração da expressão de genes relacionados com a proliferação celular (FOLDBJERG et al., 2012; VERANO-BRAGA et al., 2014; KARLSSON et a*L.,* 2014).

Devido a produção e aplicações extensivas espera-se que altos níveis de AgNP sejam liberadas em ambientes naturais (BYSTRZEJEWSKA-PIOTROWSKA et al., 2009;

[6] Efeito cavalo de Tróia – Nanopartículas servem como carreadores, que ao atingirem o interior celular, liberam íons tóxicos. No caso das AgNP, ocorre a liberação de íons Ag^+ (HSIAO et al., 2015).

CLEVELAND et al., 2012). No entanto, poucos estudos têm atentado para o potencial de liberação de NP no ambiente a partir de produtos no mercado. Alguns modelos propostos (CLEVELAND et al., 2012) apontam que esses nanomateriais são capazes de adentrar águas superficiais, onde podem interagir com organismos e/ou levar à exposição humana através do contato direto ou consumo da água (CHRISTENSEN et al., 2010; WEIR et al., 2012; MARKUS et al., 2013). Além disso, estimativas indicam que a concentração de AgNP prevista para ambientes naturais seja na faixa de 0.088-10.000 ng l^{-1} (MAURER-JONES et al., 2013; KIM et al., 2015). Desta forma, sendo as AgNP as nanopartículas mais utilizadas em produtos comerciais, sua presença no ambiente poderá tornar-se uma potencial via de contaminação humana.

1.3. Misturas complexas e metais tóxicos

O meio ambiente recebe continuamente substâncias químicas não essenciais ao funcionamento biológico (xenobióticos), liberadas a partir das mais diversas atividades antrópicas, como agrícolas, industriais e urbanas. Entre eles, pode-se citar poluentes orgânicos e inorgânicos, como bifenilas policloradas, compostos organoclorados, hidrocarbonetos policíclicos aromáticos, policlorodibenzofuranos, policlorobenzodioxinas, metais (VAN DER OOST et al., 2003) e, mais recentemente, nanorresíduos provenientes da nanotecnologia (BISWAS E WU, 2005; KLAINE et al., 2008). Apesar de muitos estudos demonstrarem os efeitos biológicos de contaminantes isolados, a presença simultânea destes muitas vezes pode induzir interações toxicológicas levando a respostas que não podem ser previstas a partir das exposições isoladas (SHENG et al., 2013; ADEBAMBO et al., 2015; CANESI et al., 2015). Desta forma, o estudo de interações entre contaminantes tem uma enorme importância prática para toxicologia (GOLDONI E JOHANSSON, 2007), particularmente para novos contaminantes, como as nanopartículas.

Entre os xenobióticos introduzidos no ambiente, os mais intensamente estudados são os metais. O cádmio (Cd) é um elemento não essencial onipresente na Terra e amplamente distribuído no meio ambiente, e tem sido considerado um carcinogênico tipo I pela *Internacional Agency for Cancer Research* (IARC). Esse metal de transição tóxico

ocorre naturalmente em minas de zinco, chumbo e cobre. As fontes naturais de cádmio na atmosfera incluem erupções vulcânicas e incêndios florestais, sendo que este pode aderir em partículas e ser transportado pelo ar. Entre as fontes antropogênicas, destacam-se as baterias, estabilizadores, pigmentos, ligas metálicas e fertilizantes, os quais podem conter altas concentrações de cádmio (FILIPIČ, 2012). Este metal é prontamente absorvido pelos organismos, sendo bioacumulado[7] e biomagnificado[8] ao longo da cadeia trófica, podendo ser encontrado preferencialmente, no caso de vertebrados, no fígado e rins (IPCS).

O mercúrio (Hg), assim como o cádmio, é um metal que não tem função biológica conhecida e seus efeitos sobre a biota normalmente são deletérios. Em vertebrados, esse metal pode afetar células especializadas como células renais, neurônios e hepatócitos. Quanto às fontes naturais, o Hg pode ser liberado devido à lixiviação de rochas contendo mercúrio ou da emissão de gases em áreas vulcânicas. Contudo, as concentrações desse metal na atmosfera, hidrosfera, solo e biota têm aumentado muito em função das atividades antrópicas (SYVERSEN E KAUR, 2012). Tais atividades englobam queimadas de floresta, produção de cloro e soda cáustica por eletrólise do cloreto de sódio, empregando células de mercúrio como catodo, mineração, produção de compostos organomercuriais com ação bactericida e fungicida utilizados na agricultura e na indústria de tintas; síntese de reagentes, formulações dentarias, soluções desinfetantes e esterilizantes contendo mercúrio (SAHU et al., 2014; SYVERSEN E KAUR, 2012).

Desta maneira, tendo em mente a grande produção, consumo e provável liberação de nanopartículas no ambiente (levando a sua presença conjunta com contaminantes clássicos como metais), bem como alta reatividade de sua superfície, é importante investigar se as nanopartículas são capazes de alterar/potencializar a toxicidade de metais, em modelos biológicos. Recentemente, alguns grupos de pesquisa têm abordado essa questão e avaliado efeitos *in vivo* e *in vitro* da associação de NP e

[7] Bioacumulação – Absorção de um químico, proveniente do meio abiótico/biótico, por um organismo numa taxa superior a sua capacidade de eliminação.
[8] Biomagnificação – Processo onde uma substância química é transferida ao longo da cadeia alimentar, com aumento da concentração da substância no organismo em função de sua posição na cadeia.

contaminantes ambientais clássicos, como metais tóxicos e hidrocarbonetos policíclicos aromáticos (FERREIRA et al., 2014; DELLA TORRE et al., 2015; GLINSKI et al., 2016). Apesar disso, o conhecimento que se tem hoje sobre a interação entre NP e outros contaminantes ambientais clássicos em sistemas biológicos ainda é limitado.

1.4. Modelo de estudo: células HepG2

O fígado é um alvo importante de toxicidade de contaminantes orgânicos e metais devido ao seu papel central em vários processos metabólicos essenciais para homeostase de vertebrados e reações de biotransformação de moléculas endobióicas e xenobióticos (SEGNER, 1998). Por essa razão, diversas linhagens celulares humanas originadas do fígado foram estabelecidas e são utilizadas na pesquisa biomédica envolvendo xenobióticos. Uma dessas linhagens de hepatócitos mais utilizadas e versáteis é a HepG2, estabelecida por Aden em 1972, por (ADEN, 1979.) A partir de um hepatocarcinoma humano (fig. 3).

Essa linhagem é considerada uma ferramenta útil na determinação de riscos causados por compostos químicos, uma vez que mantém a expressão endógena de diversas enzimas antioxidantes. Por essa razão, tem sido utilizada rotineiramente no estudo de citotoxidade de diversos compostos (KNASMÜLLER et al., 2004; MERSCH-SUNDERMANN et al., 2004; URANI, 2005; AHAMED et al., 2013).

As células HepG2 apresentam-se justapostas em monocamada contínua, com morfologia semelhante à de células epiteliais e tendem a formar aglomerados/cordões celulares (Figura 3).

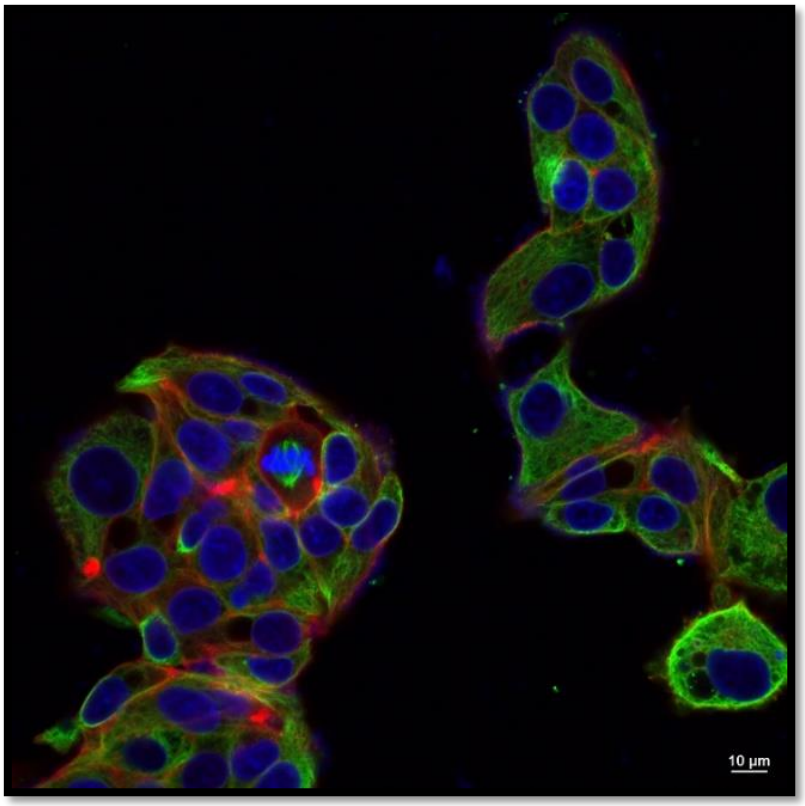

FIGURA 3. Microscopia confocal de células HepG2. Núcleo das células marcados em azul (DAPI), microtúbulos marcados em verde (Anti-tubulina – Alexa Fluor ® 488) e filamentos de actina marcados em vermelho (faloidina conjugada com alexa Fluor® 546) (fonte: LIEBEL, 2015).

1.5. Biomarcadores para avaliação *in vitro* de toxicidade

O uso de modelos de estudo não animais, como abordagens *in vitro*, é uma ferramenta importante para aprofundar o conhecimento sobre os efeitos tóxicos induzidos por contaminantes, bem como para inferir esses efeitos em humanos (BROADHEAD E COMBES, 2001; EISENBRAND et al*.,* 2002). Além de um modelo de estudo apropriado, a escolha de parâmetros biológicos, ou de biomarcadores, relevantes é crucial para garantir a qualidade da análise toxicológica (BLAAUBOER et al*.,* 2012).

Biomarcadores podem ser definidos como parâmetros (farmacológicos, fisiológicos, celulares, moleculares etc.) que podem ser usados para prever um efeito nocivo em um determinado sistema biológico (GUPTA, 2014). Um biomarcador ideal é considerado acessível, não invasivo, sensível, específico e de baixo custo.

Os estudos de efeitos citotóxicos são o primeiro passo para a avaliação da toxicidade de compostos potencialmente nocivos *in vitro.* Os biomarcadores mais frequentemente utilizados nos testes de toxicidade celular baseiam-se nos seguintes parâmetros (EISENBRAND et al*.,* 2002; RISS E MORAVEC, 2004; VINKEN E BLAAUBOER, 2016):

- Danos a membranas celulares;
- Redução do metabolismo celular:
- Alterações na taxa de proliferação celular;
- Morfologia celular;
- Mecanismos de morte celular.

Os danos à membrana plasmática podem ser avaliados através de diferentes ensaios. O azul de tripan avalia a integridade da membrana celular, uma vez que este corante não é permeável em células viáveis cujas membranas estão íntegras, ao passo que em células não viáveis, o corante é capaz de permear a célula, corando o citoplasma e núcleo em azul (PHILIPS, 1973). O comprometimento da integridade da membrana plasmática também pode ser avaliado através da detecção de moléculas intracelulares presentes no meio extracelular, entre estas, a enzima lactato desidrogenase (LDH). Danos na membrana plasmática permitem que esta enzima extravase do citosol para o meio extracelular em quantidades relativamente altas. Desta forma, sua quantificação pode ser relacionada com a viabilidade celular (VINKEN E BLAAUBOER 2016).

A integridade do sistema endolisossomal também pode fornecer informações sobre a viabilidade celular. O ensaio do vermelho neutro baseia-se na capacidade das células viáveis de incorporar e assimilar o corante dentro dos endossomos e lisossomos. Danos à superfície celular ou na membrana lisossômica, e alterações no bombeamento de prótons do citosol para o lúmen de endossomos e lisossomos resultam numa diminuição da retenção do corante. Desta forma, a quantidade de corante incorporado às células é diretamente proporcional ao número de células com sistema endolisossomal funcional.

Dado seu papel indispensável na iniciação e perpetuação da citotoxidade, as alterações em mitocôndrias são biomarcadores ideais na avaliação do estresse químico

induzido por contaminantes (VINKEN E BLAAUBOER, 2016). A atividade mitocondrial pode ser avaliada através da capacidade da enzima succinato desidrogenase (presente no complexo II da membrana mitocondrial interna) em reduzir do MTT (3- (4,5-dimetiltiazol-2yl) -2,5-difenil brometo de tetrazolina). Este ensaio baseia-se na capacidade das células em reduzir o MTT em formazan, e assim pode ser interpretada como uma medida da viabilidade/número de células ou metabolismo mitocondrial.

A determinação do mecanismo de morte celular, através da localização da fosfatidilserina (com marcador fluorescente anexina V-FITC) e a capacidade do iodeto de propídio em intercalar o DNA celular também são muito utilizados em ensaios de citotoxidade após a exposição a xenobióticos (WEN et al*.,* 2010). Neste trabalho, a detecção destes marcadores fluorescentes por microscopia confocal clássica em *time-lapse* permitiu analisar os mecanismos de morte celular e sua progressão durante o curso de 24 h de exposição aos contaminantes.

As espécies reativas de oxigênio (EROs) são produzidas naturalmente durante diversos processos celulares *e.g.*, cadeia transportadora de elétrons, atividade de enzimas oxido-redutases, atividade do citocromo P450 e em reações imunológicas, como fagocitose (HALLIWELL E GUTTERIDGE, 2007). Em concentrações baixas ou moderadas, as EROs desempenham funções fisiológicas, mas em altas concentrações podem induzir efeitos deletérios, desde leves até irreversíveis como a morte celular (BIRBEN et al*.,* 2012; RAJESH et al*.,* 2016). Sob condições homeostáticas, os efeitos nocivos induzidos por EROs são contrabalanceados pelo sistema de defesa antioxidante, que consiste em uma ampla gama de moléculas capazes de neutralizar as EROs por ligação direta a elas (*scavengers*[9], como a glutationa e vitaminas) ou catalisando reações altamente específicas (enzimas antioxidantes como superóxido dismutase, catalase e glutationa peroxidase) (REGOLI E GIULIANI, 2014). As mitocôndrias são umas das principais fontes de EROs na célula, produzindo principalmente o ânion superóxido, no sítio ubiquinona no complexo respiratório III. Este radical é convertido a peróxido de hidrogênio, que pode difundir-se livremente para o citoplasma (FLEURY et al*.,* 2002).

[9] *Scavengers* – antioxidantes não enzimáticos de baixo peso molecular, como vitaminas (vitaminas C e E), β-caroteno, ácido úrico e GSH (BIRBEN et al*.,* 2012),

Metais pesados, como Cd e Hg, e AgNP são capazes de induzir estresse oxidativo tanto através da depleção de enzimas antioxidantes como pela geração de EROs, via reação de Habber-Weis/Fenton[10] (BIRBEN et al., 2012; MASSARSKY et al., 2014; AGUADO et al., 2013; NZENGUE et al., 2008). Uma forma de verificar uma possível desequilíbrio redox induzida por contaminantes é a quantificação de EROs, que pode ser feita através de marcadores fluorescentes para EROs específicas (*e.g.* diclorofluriceína diacetato para EROs como o peróxido de hidrogênio ou Mitosox® para ânion superóxido).

Os transportadores envolvidos com resistência a multidrogas ou multixenobióticos são uma superfamília de transportadores transmembranares que utiliza a energia proveniente da hidrólise do ATP para translocar um amplo espectro de moléculas, tanto endógenas como xenobióticos, através da membrana plasmática (Rodrigues *et al.,* 2009). Alguns membros desta família de transportadores excretam compostos tóxicos de células como parte integral de seu mecanismo de defesa contra agentes citotóxicos. Entre estes, o transportador mais relevantes toxicologicamente é a glicoproteína-P (P-gp, ABCB1) (LESLIE et al., 2005). Alguns trabalhos na literatura reportam que nanopartículas podem atenuar o funcionamento destes transportadores e que estes parecem estar relacionados à toxicidade induzida pelas partículas (SALOMON E EHRHARDT 2011; CHEN et al., 2016). Já os metais tóxicos Cd e Hg podem induzir o aumento na expressão destes transportadores, mas causar a redução de sua atividade em linhagem celular de peixes (DELLA TORRE et al., 2012).

Análise desses parâmetros é importante principalmente em situações nas quais o efeito final de um agente químico é desconhecido, como é o caso de misturas de contaminantes, ainda que os efeitos individuais sejam bem elucidados. Ainda, a análise

---

[10] Reação de Fenton / Habber-Weiss – o peróxido de hidrogênio (H_2O_2) pode reagir com alguns metais de transição, como cobre e ferro, e formar radicais hidroxila (•OH) pela reação de Fenton. No processo, o metal oxidado pode ser reduzido ao reagir com ânion superóxido ($O_2^{\bullet-}$), tornando-se disponível para novas reações de Fenton (BIRBEN et al., 2012). A reação de Habber-Weiss é o conjunto de ambas as reações:

$Cu^{+}/Fe^{2+} + H_2O_2 \rightarrow Cu^{2+}/Fe^{3+} + OH^{-} + \bullet OH$ (Reação de Fenton)

$Cu^{2+}/Fe^{3+} + O_2^{\bullet-} \rightarrow Cu^{+}/Fe^{2+} + O_2$

desses biomarcadores pode ser complementada com abordagens *high-throughput*, como genômica, transcriptômica ou proteômica.

1.6. Aplicação de proteômica baseada em espectrometria de massas em toxicologia

As proteínas formam a estrutura das células e estão envolvidas em todos os seus processos metabólicos e mecanismos regulatórios. As propriedades das proteínas, como abundância, interações proteína-proteína, modificações pós traducionais, localização subcelular e degradação são dinâmicas e podem mudar rapidamente durante o curso de processos celulares, como por exemplo a proliferação, migração celular ou endocitose (LARANCE E LAMOND, 2015). A espectrometria de massas (MS[11]) é uma das técnicas mais sensíveis para identificação e quantificação relativa de proteínas em amostras complexas e em larga escala. Por essa razão, a proteômica baseada em MS tem sido considerada uma das ferramentas analíticas mais importantes no estudo de metabolismo de drogas, farmacocinética e toxicologia (KANG, 2012).

A abordagem *bottom-up* é a estratégia mais comumente utilizada para avaliação de amostras complexas de proteínas. Esta técnica se baseia na digestão enzimática de uma mistura de proteínas em peptídeos antes da análise de massas, e as massas e sequencias dos peptídeos gerados são utilizadas para identificar as proteínas correspondentes (YATES et al., 2009). Quando a complexidade da mistura de peptídeos é alta, a amostra é separada/fracionada por cromatografia líquida de alta performance (HPLC) antes de ser analisada no espectrômetro de massas. Essa etapa permite a detecção de peptídeos com baixa abundância, que de outra forma seriam ocultados por um sinal de maior abundância (YATES et al., 2009). Ao eluir da coluna de cromatografia liquida, o solvente contendo os peptídeos passa por um fino capilar com um potencial elétrico alto, e então é vaporizado e disperso em pequenas gotículas carregadas. Estas evaporam e transferem os peptídeos ionizados para o espectrômetro de massas, esse processo é chamado de ionização *eletrospray* (AEBERSOLD E MANN, 2003).

[11] MS – Abreviação do termo em inglês *Mass Spectometry*.

Em um experimento tandem MS, o instrumento inicialmente adquire a razão massa/carga (*m/z)* de cada peptídeo ionizado eluindo para o espectrômetro de massas em um dado momento, gerando os espectros MS. Subsequentemente, peptídeos ionizados alvo, com uma *m/z* definida, são selecionados, isolados e fragmentados, produzindo fragmentos de ions que são adquiridos para gerar espectros MS/MS. Após a aquisição dos dados, os espectros MS/MS são então comparados com bancos de dados para identificação de peptídeos e proteínas (ENG et al*.,* 2011; MEYER E SELBACH, 2015).

Um fluxograma genérico de um experimento baseado em espectrometria de massas está esquematizado na figura 4.

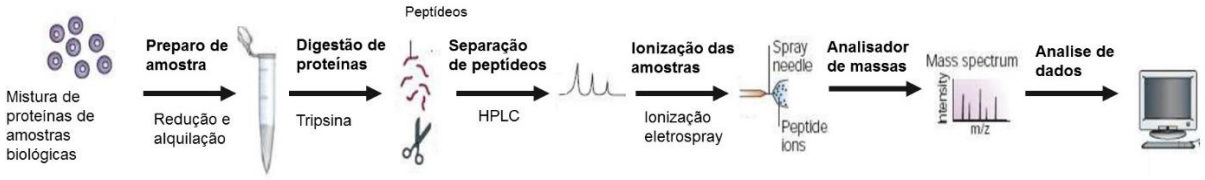

FIGURA 4. Fluxograma genérico de um experimento baseado em espectrometria de massas (Fonte: figura adaptada de STEEN E MANN, 2004).

A maioria dos estudos tem utilizado uma entre três metodologias principais para quantificação relativa de proteínas: (1) quantificação *labble free*, (2) marcação metabólica *in vivo* com isótopos estáveis (marcação de isótopos estáveis em aminoácidos em cultura de células (SILAC – *stable isotope labbeling by aminoacid in cell culture*), N-marcação e NeuCode SILAC), ou (3) marcação com isótopos estáveis usando tags químicas covalentemente ligadas *in vitro* (*tandem mass tags* (TMT) e marcador isobárico para quantificação relativa e absoluta (iTRAQ) (LARANCE E LAMOND, 2015). Nesta última abordagem, a quantificação com iTRAQ[12] é uma das metodologias mais utilizadas (ILIUK et al., 2009; HULTIN-ROSENBERG et al*.,* 2013). Esses reagentes podem ser usados para marcar até 8 amostras biológicas diferentes que, subsequentemente, são combinadas em um único experimento. Os marcadores do iTRAQ reagem com todos os

[12] iTRAQ – abreviação do termo em inglês *Isobaric Tags for Relative and Absolute Quantification*

grupos funcionais de aminas primárias, incluindo a região N-terminal e grupamentos ε-amino da cadeia lateral de lisinas. Isso significa que quase todos os peptídeos de uma amostra serão marcados com iTRAQ. Cada marcador tem um grupo reativo de peptídeo, um grupo repórter e um balanço que mantém constante a massa total do marcador de 305 Da (no caso do *kit iTRAQ 8-plex* e 145 Da no *kit iTRAQ 4-plex*). A fragmentação MS/MS resulta na liberação do grupo repórter do iTRAQ e produz íons distintos de m/z 113, 114, 115, 116, 117, 118, 119 e 121. A abundância dos íons repórteres é diretamente proporcional às abundâncias relativas de cada peptídeo marcado na amostra (CHAHROUR et al., 2015). A figura 5 ilustra um experimento no qual a metodologia empregada para quantificação relativa de proteínas com iTRAQ 8-plex foi utilizada (fig. 5A) e a estrutura do marcador (fig. 5B).

O monitoramento do perfil proteico, a partir de técnicas tandem-MS, associadas a ferramentas de bioinformática, tem sido utilizado para obter informações sobre possíveis mecanismos de ação de compostos potencialmente tóxicos, incluindo nanopartículas (VERANO-BRAGA et al., 2014; GIORIA et al., 2016; MAURER et al., 2016). Desta forma, a aplicação destas técnicas no presente modelo de estudo fornece informações importantes a respeito de moléculas e mecanismo de toxicidade envolvidos na coexposição de contaminantes em células HepG2.

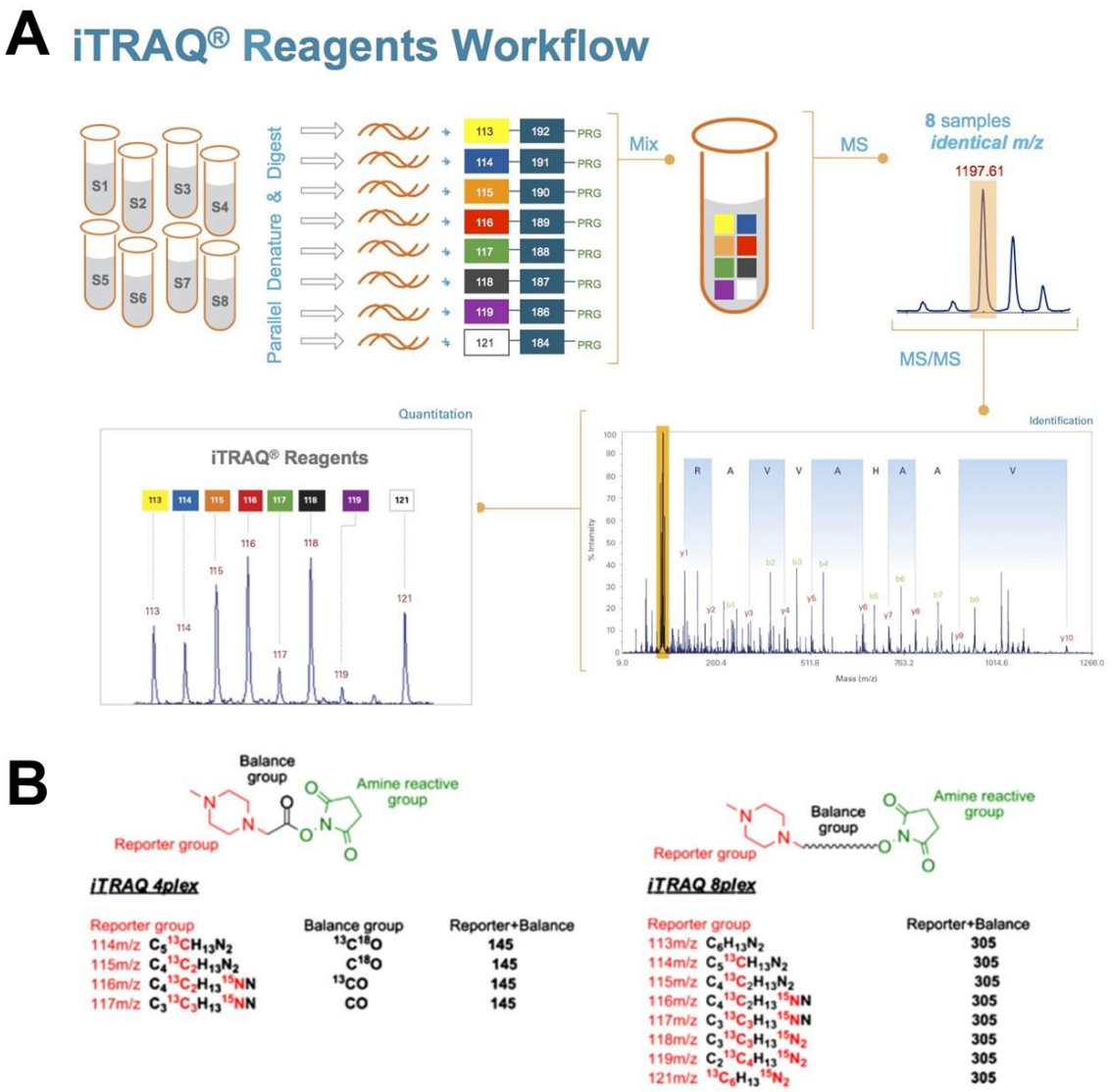

FIGURA 5. Metodologia iTRAQ para quantificação de proteínas. (A) os peptídeos de cada amostra biológica são marcados com etiquetas específicas. Essas amostras são combinadas e analisadas juntas por MS/MS. A fragmentação MS/MS resulta na liberação dos repórteres e sua abundância é diretamente proporcional ao peptídeo ao qual estava ligado. Desta forma é feita a quantificação dos peptídeos em cada amostra biológica (fonte: Sciex®). (B) Estrutura dos reagentes iTRAQ 4- e 8-plex (fonte: Chahrour *et al.*,, 2015).

2. OBJETIVOS

2.1. Objetivo geral

Avaliar o efeito e possíveis mecanismos moleculares envolvidos na resposta celular à mistura de nanopartículas de prata e metais não essenciais na linhagem de carcinoma humano, HepG2.

2.2. Objetivos específicos

Capítulo 1

- Expor a linhagem humana de hepatócitos, HepG2, a uma mistura de nanopartículas de prata (2 nm, não capeadas) e metais não essenciais ($CdCl_2$ e $HgCl_2$) durante 4 e 24 h, avaliando efeitos da mistura de contaminantes sobre:
  - ✓ a viabilidade celular (teste de vermelho neutro e MTT);
  - ✓ o número de células aderidas/ proliferação celular (teste cristal violeta);
  - ✓ o ambiente redox celular (níveis de espécies reativas de oxigênio no citosol (ensaio DCF) e na mitocôndria (ensaio Mitosox Red);
  - ✓ a atividade dos transportadores de multixenobióticos (ensaio de exclusão da rodamina B);
  - ✓ o mecanismo de morte celular (em microscopia confocal);
  - ✓ a concentração intracelular de AgNP e metais

Capítulo 2

- Expor a linhagem humana de hepatócitos, HepG2, a uma mistura de nanopartículas de prata (10 nm, em tampão citrato) e metal não essencial ($CdCl_2$) durante 4 e 24 h, avaliando efeitos da mistura de contaminantes sobre:

- ✓ a viabilidade celular (ensaios de liberação da enzima lactato desidrogenase e permeabilidade ao corante azul de tripan);
- ✓ o mecanismo de morte celular e *status* metabólico das células (relação ADP/ATP intracelular);
- ✓ o perfil proteico das células (espectrometria de massas);

- Utilizar ferramentas de bioinformática para entender os mecanismos moleculares induzidos pela exposição aos contaminantes.

3. ESTRATÉGIA EXPERIMENTAL

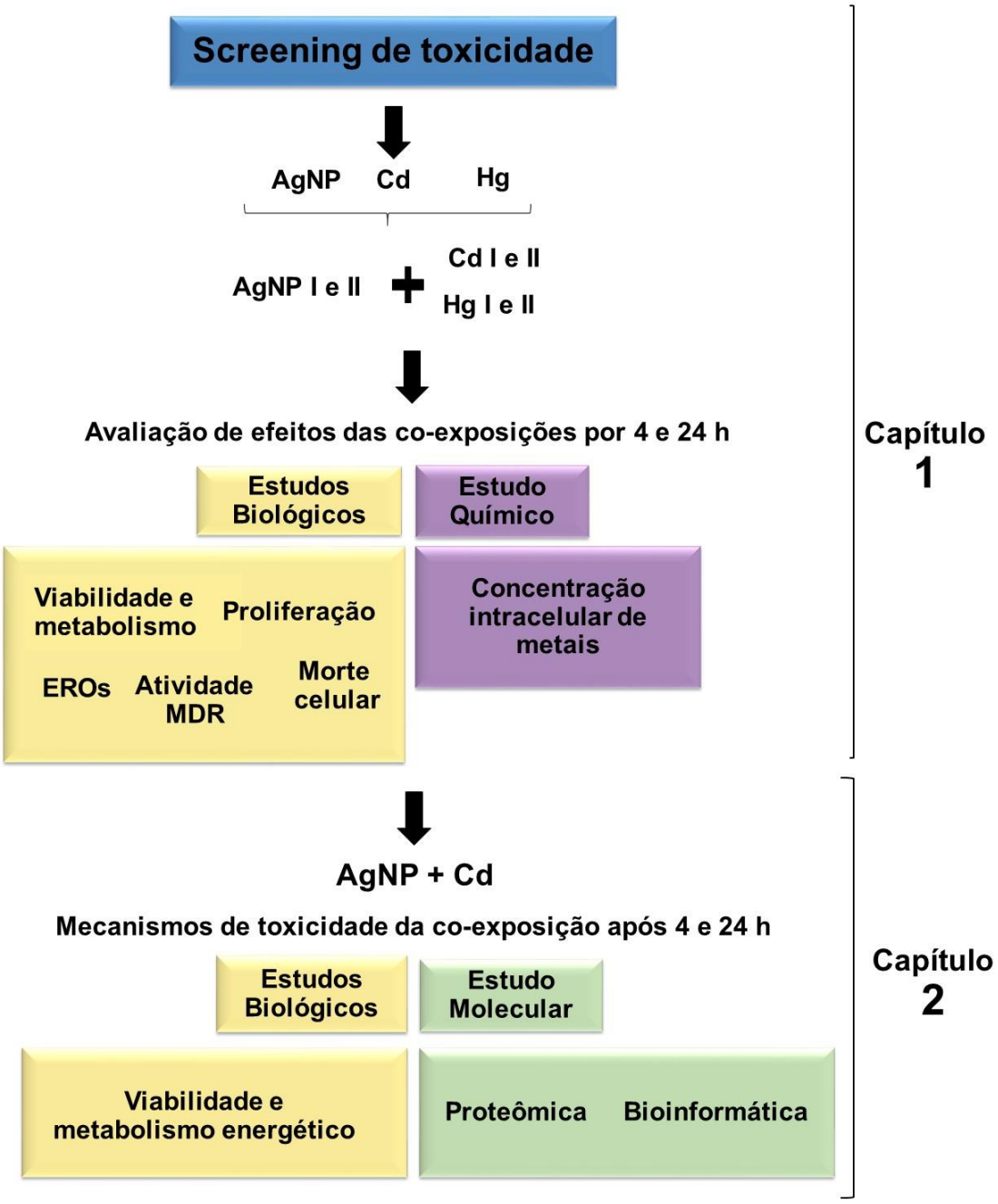

CAPITULO I

Toxicological interactions of silver nanoparticles and non-essential metals in human hepatocarcinoma cell line

Publicado na revista Toxicology in vitro

doi:10.1016/j.tiv.2017.01.003

Renata Rank de Miranda[a], Arandi Ginane Bezerra Jr[b], Ciro Alberto Oliveira Ribeiro[a], Marco Antônio Ferreira Randi[a], Carmen Lúcia Voigt[c], Lilian Skytte[d], Kaare Lund Rasmussen[d], Frank Kjeldsen[e], Francisco Filipak Neto[a*]

[a] *Departamento de Biologia Celular, Universidade Federal do Paraná, CEP 81.531-980, Curitiba, PR, Brazil*

[b] *Departamento de Física, Universidade Tecnológica Federal do Paraná, DAFIS, CEP 80.230-901, Curitiba, PR, Brazil*

[c] *Universidade Estadual de Ponta Grossa, Programa Associado de Pós-Graduação em Química, Setor de Ciências Exatas e Naturais, CEP 84.030-900 Ponta Grossa, PR, Brazil*

[d] *Department of Physics, Chemistry and Pharmacy, University of Southern Denmark, Campusvej 55, DK-5230 Odense M, Denmark*

[e] *Protein Research Group, Department of Biochemistry and Molecular Biology, University of Southern Denmark, Odense, Denmark*

Abstract

Toxicological interaction represents a challenge to toxicology, particularly for novel contaminants. There are no data whether silver nanoparticles (AgNPs), present in a wide variety of products, can interact and modulate the toxicity of ubiquitous contaminants, such as nonessential metals. In the current study, we investigated the toxicological interactions of AgNP (size = 1-2 nm; zeta potential = -23 mV), cadmium and mercury in human hepatoma HepG2 cells. The results indicated that the co-exposures led to toxicological interactions, with AgNP + Cd being more toxic than AgNP + Hg. Early (2-4 h) increases of ROS (DCF assay) and mitochondrial $O_2^{\bullet-}$ levels (Mitosox® assay) were observed in the cells co-exposed to AgNP + Cd/Hg, in comparison to control and individual contaminants, but the effect was partially reverted in AgNP + Hg at the end of 24 h-exposure. In addition, decreases of mitochondrial metabolism (MTT), cell viability (neutral red uptake assay), cell proliferation (crystal violet assay) and ABC-transporters activity (rhodamine accumulation assay) were also more pronounced in the co-exposure groups. Foremost, co-exposure to AgNP and metals potentiated cell death (mainly by necrosis) and Hg^{2+} (but not Cd^{2+}) intracellular levels (ICP-MS). Therefore, toxicological interactions seems to increase the toxicity of AgNP, cadmium and mercury.

Keywords: HepG2, silver nanoparticles, mercury, cadmium, co-exposure, interaction

1. Introduction

Silver nanoparticles (AgNP) are present in about 24% of all products listed in the Woodrow Wilson Database (Vance *et al.,* 2015), such as food products, fabrics, cosmetics and medical devices (Seltenrich, 2013; Gaillet and Rouanet, 2015). Due to the extensive production and applications of AgNP, increased amounts of nanowaste will be generated and released into the environment (Bystrzejewska-Piotrowska *et al.,*, 2009; Cleveland *et al.,*, 2012). It has been already estimated that the predicted environment concentrations (PEC) of AgNP in surface waters is 0.088-10,000 ng l^{-1} and the maximum estimated PEC in wastewater treatment plant effluent is 17 µg l^{-1} (Maurer-Jones *et al.,* 2013, Kim *et al.,* 2015), representing a potential danger to the biota and human health. AgNP can cause adverse effects on a variety of biological models (Morones *et al.,*, 2005; Wu *et al.,*, 2010; Gliga *et al.,*, 2014; Monfared *et al.,*, 2015). However, it is not clear whether they represent a threat to the health of vertebrates (Fabrega *et al.,*, 2011; Della Torre *et al.,*, 2015), particularly when the interactions of AgNP and other environmental contaminants are considered. For example, AgNP, cadmium and mercury can disrupt cell antioxidant defense and induce the production of ROS, DNA damage, apoptosis and promote cell proliferation (Aguado *et al.,*, 2013; Chen *et al.,*, 2014; Vergilio *et al.,*, 2014; Lee *et al.,*, 2014; Kim *et al.,*, 2015; Kumar *et al.,*, 2015), but the effects of the combination of these metals and AgNP are unknown.

Cadmium and mercury are non-essential metals and ubiquitous contaminants of natural environments and dietary products (Monroe and Halvorsen, 2009; Guo *et al.,*, 2013; Arbuckle *et al.,*, 2016). These metals enter the environment through different anthropogenic sources. Cadmium is used in battery production, fertilizers, paints and plastic stabilizers (Capaldo *et al.,* 2016) and mercury applications include soda chlorine production, coal combustion, paints and seed treatment (Syversen and Kaur 2012, Sahu *et al.,* 2014). Some studies reported that nanoparticles can modulate the toxicity of environmental contaminants, such as metals, polycyclic aromatic hydrocarbons (PAH) and organochlorinated pesticides (OCP), leading to unexpected results (Guo *et al.,*, 2013; Ferreira *et al.,*, 2014; Kim *et al.,*, 2015; Glinski *et al.,*, 2016). Guo *et al.,* (2013), for instance, observed positive synergetic interaction of SiNP + $CdCl_2$ for hepatic biochemical

and histopathological parameters, as well as the distribution of $CdCl_2$ in the liver and kidneys of mice. Likewise, Kim *et al.,* (2015) reported that co-exposure with citrate coated-AgNP increased the bioaccumulation of Cd in *Daphnia magna*.

Considering the increasing use of AgNP, the widespread metal contamination and therefore, the possibility of these contaminants coexist in natural environments, we investigated the biological effects of combination of AgNP, Cd and Hg in human hepatoma (HepG2) cells through viability, metabolism, proliferation, efflux transporters activity, reactive oxygen species production and cell death parameters, to answer whether the co-exposure increase toxicity. HepG2 cells were selected, since liver is an important target organ of the three contaminants (Fowler 2009; Stacchiotti *et al.,*, 2009; Elsaesser and Howard, 2012). Also, this cell line has been routinely used to investigate the toxicity of several compounds, because it preserves most of the phenotypic characteristics of normal hepatocytes (Knasmüller *et al.,*, 2004; Mersch-Sundermann *et al.,*, 2004; Urani *et al.,*, 2005).

2. Materials and methods

2.1. Silver nanoparticles synthesis and characterization

We synthesized silver nanoparticles through laser ablation in liquid medium (water as solvent) and determined the concentration of the stock solution through flame absorption spectrometry. Shape, diameter, size distribution, zeta potential and spectral properties of AgNP were determined by electron transmission microscopy JEOL 1200 EXII, *Zeta-sizer* (MALVERN®), Dynamic light scattering (DLS) and UV-VIS, respectively.

2.2. HepG2 cell culture

Human hepatoma cells HepG2 (Rio de Janeiro Cell bank - Brazil) were cultured as a monolayer in high glucose DMEM medium supplemented with 10% inactivated fetal bovine serum (FBS) and antibiotics (10 U ml^{-1} penicillin and 10 µg ml^{-1} streptomycin), at 37 °C and 5% CO_2. Cells at passages 100-110 were utilized in the current study.

2.3. Selection of the concentrations of AgNP, Hg and Cd

Initially, toxicity-screening tests (MTT metabolism and neutral red uptake; complementary results fig.2 and 3) were performed, in different concentrations and periods of exposure, for AgNP (0.005-6.66 µg ml^{-1}), Hg^{2+} (20-640 µM) and Cd^{2+} (0.5-50 µM) to determine two test concentrations of each contaminant: one that did not induce toxicity and one that induced pronounced toxicity. Based on these results, two concentrations for each contaminant at 24 h time-point were selected (table 1; complementary results fig. 2 and 3).

TABLE 1. Experimental design used in the evaluation of the toxicity of AgNP, metals and its

Groups	Concentration
Control	-
AgNP (I)	0.35 µg/ml
AgNP (II)	3.5 µg/ml
$CdCl_2$ (I)	0.15 µM
$CdCl_2$ (II)	1.5 µM
$HgCl_2$ (I)	2.8 µM
$HgCl_2$ (II)	28 µM
AgNP (I) + $CdCl_2$ (I)	0.35 µg/ml + 0.15 µM
AgNP (I) + $CdCl_2$ (II)	0.35 µg/ml + 1.5 µM
AgNP (II) + $CdCl_2$ (I)	3.5 µg/ml + 0.15 µM
AgNP (II) + $CdCl_2$ (II)	3.5 µg/ml + 1.5 µM
AgNP (I) + HgC_{l2} (I)	0.35 µg/ml + 2.8 µM
AgNP (I) + $HgCl_2$ (II)	0.35 µg/ml + 28 µM
AgNP (II) + $HgCl_2$ (I)	3.5 µg/ml + 2.8 µM
AgNP (II) + $HgCl_2$ (II)	3.5 µg/ml + 28 µM

1.4. Contaminants preparation and exposure protocol

AgNP were synthesized in H_2O and both metals ions stock solutions were prepared in 0.01 M HCl to avoid adsorption to the glass. For the exposure, the contaminants were added to fresh culture medium. In the case of co-exposures, first one contaminant was added to the medium, mixed and then the other contaminant was added. At final, all groups (control, AgNP, metal ions and mixtures) have the same concentration of HCl (buffered by culture medium) and water. Metal ions concentrations are expressed in µM and AgNP concentration is expressed in µg ml^{-}.

Cells were seeded onto 96-well microplate ($4x10^4$ cells per well) for cytotoxicity, proliferation, reactive oxygen species production and multidrug efflux transporters assays,

and onto 6-well plates ($1.2x10^6$ cells per well) for metal uptake assays. After 24 h, the medium was replaced by fresh DMEM medium with antibiotics and 2% fetal bovine serum containing AgNP ((I) 0.35 µg ml^{-1}; (II) 3.5 µg ml^{-1}), $CdCl_2$ ((I) 0.15 µM; (II) 1.5 µM) and $HgCl_2$ ((I) 2.8 µM; (II) 28 µM) or the combination of AgNP and each metal. Cells were exposed to these contaminants for 4 and 24 h, and an appropriate control group was kept in parallel. 'I' and 'II' stand, respectively, for the lowest and highest concentrations of AgNP and metals.

2.5. Cytotoxicity and proliferation assays

Neutral red (NR) uptake assay was determined after incubation of cells with 50 µg ml^{-1} of neutral red for 3 h. MTT assay was determined after incubation of cells with 0.5 mg 1^{-1} of MTT (3- (4,5-dimethylthiazol- 2-yl)-2,5-diphenyltetrazolium bromide) for 2 h.

Cell proliferation was determined after DNA staining with 50 µl $well^{-1}$ of 0.25 mg ml^{-1} of violet crystal solution, according to previously published protocols for HepG2 cells (Liebel *et al.,*, 2015).

2.6. Reactive Oxygen Species (ROS) levels

Intracellular ROS levels were evaluated with H_2DCF-DA (2', 7'-dichlorodihydro-fluorescein diacetate) and MitoSOX™ Red (Invitrogen). After exposure, cells were incubated with either 10 µM of H_2DCF-DA or 5 µM of MitoSOX™, in fresh culture medium, (15 min, 37 °C, protected from light), washed with PBS and suspended in 250 µl of PBS. Fluorescence was measured at 488/530 nm (H_2DCF-DA) and 514/580 nm (MitoSOX; Benov *et al.,*, 1998).

2.7. Multidrug efflux transporters activity

The activity of ABC transporters was determined by Rhodamine 123 efflux assay (Pessatti *et al.,*, 2002, with modifications for cell culture). Culture medium was replaced by 200 µl of PBS containing 1 µM of rhodamine B, and cells were incubated. Cells were

incubated (30 min, 37 °C, protected from light), washed twice with PBS and frozen at -76 °C in 250 µl well^{-1} of PBS. Then, cells were thawed and 200 µl of the lysate were transferred to a black microplate for fluorescence quantification (540/580 nm). Verapamil (20 µM) was utilized as a positive control.

2.11. Cell death

Apoptotic and necrotic cells were detected using the FITC-Annexin V/propidium iodide (PI) Apoptosis Detection Kit (BD Biosciences, Heidelberg, Germany) and analyzed by time-lapse confocal microscopy (during 0-24 h exposure), according to the manufacturer's instructions.

2.12. Intracellular metals concentration

Intracellular content of metals were quantified by inductively coupled plasma mass spectrometry - ICP-MS (Bruker 820-MS + SPS 3 autosampler) (for Ag and Cd) and FIMS (Perkin Elmer FIMS 400 + S 10 autosampler) (for Hg). Cells were seeded onto 6-well plates (1.2x10^6 cells well^{-1}), cultured for 24 h and exposed to the highest concentrations of Hg, Cd, AgNP and their association for 4 h. After exposure, cells were washed 3 times with PBS (to remove AgNP and metals from cell's surface), trypsinized (0.25% trypsin, 0.02% EDTA in PBS, pH 7.2), harvested to tubes with 5 ml culture medium, pelleted (500 *g* for 5 min) and suspended in 1 ml culture medium for cell counting. Tubes received 200 µl HNO_3 and 100 µl H_2O_2 (both ICP-MS grade), and remained at -20°C until the analysis by ICP-MS and FIMS. Metals were quantified in the cells' pellets, exposure culture media and PBS washes. HCl was added to all samples to remove excess H_2O_2, and the samples were left to react overnight. The following morning all samples were diluted and divided into two subsamples, which were then analyzed on either the ICP-MS or the FIMS. Five-point calibration curves were used for quantification, and NIST 1486 (for the ICP-MS) and NIST 1515 (for the FIMS) were used for quality control. Three independent replicates were carried out, and the results are expressed in ppm/10^6 cells.

2.13. Statistical procedures

Three independent experiments were performed. A total of 12 replicates per experiment were utilized for biomarkers analyzed in 96-well microplates. Data distribution was tested and parametric (one-way ANOVA) or nonparametric (Kruskall-Wallis) tests were performed, followed by Dunnett's or Dunns post-tests (when appropriate). Effects of contaminants were verified by the comparison of the control *vs* AgNP I and II, Cd I and II, Hg I and II, the four mixtures of AgNP + Cd, or the four mixtures of AgNP + Hg. Toxicological interactions were verified by the comparison of each co-exposure group *vs* the contaminants alone present in it. Thus, there is only one variable in the statistical comparisons, i.e., the absence/presence of a certain ion/particle. Therefore, it was possible to verify, whether AgNP + Cd/Hg was different from Cd/Hg (variable = presence of AgNP) and AgNP + Cd/Hg was different from AgNP (variable = presence of Cd/Hg). P-values lower than 0.05 were considered statistically significant.

3. Results

3.1. AgNP characterization

Silver nanoparticles, synthesized by laser ablation, had spherical shape, diameter of 1-2 nm (fig. 1A and 1B), zeta potential of -23 mV (Zeta-sizer analysis, complementary results fig.1) and absorption peak at 400 nm (fig. 1C).

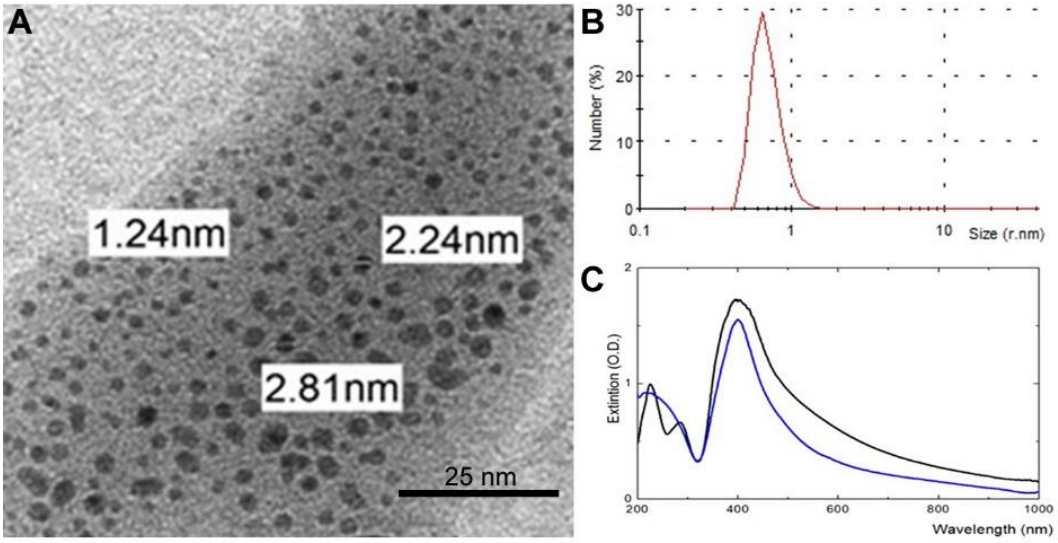

FIGURE 1. AgNP characterization. A) TEM image of AgNP suspension. B) Particle distribution according to size (Zetasizer). C) UV-Vis analysis of two AgNP suspensions indicating light peak absorption at 400 nm.

3.2. Cytotoxicity/Viability

The mitochondrial dehydrogenases activity, measured by MTT assay, decreased >20% in cells exposed to the highest AgNP concentration (AgNP II) and the mixtures AgNP II + Hg I/II and AgNP II + Cd I/II for 4 h-experiment (fig. 2A and B). Decrease of mitochondrial metabolism also occurred in the cells exposed to Cd II (30%), 3 groups of AgNP + Cd and AgNP + Hg II (30%) for 24 h-experiment (fig. 2C and D). For AgNP II + Cd II (decrease of 60%) and AgNP II + Hg II, the effects were more pronounced than those of individual contaminants (# symbol).

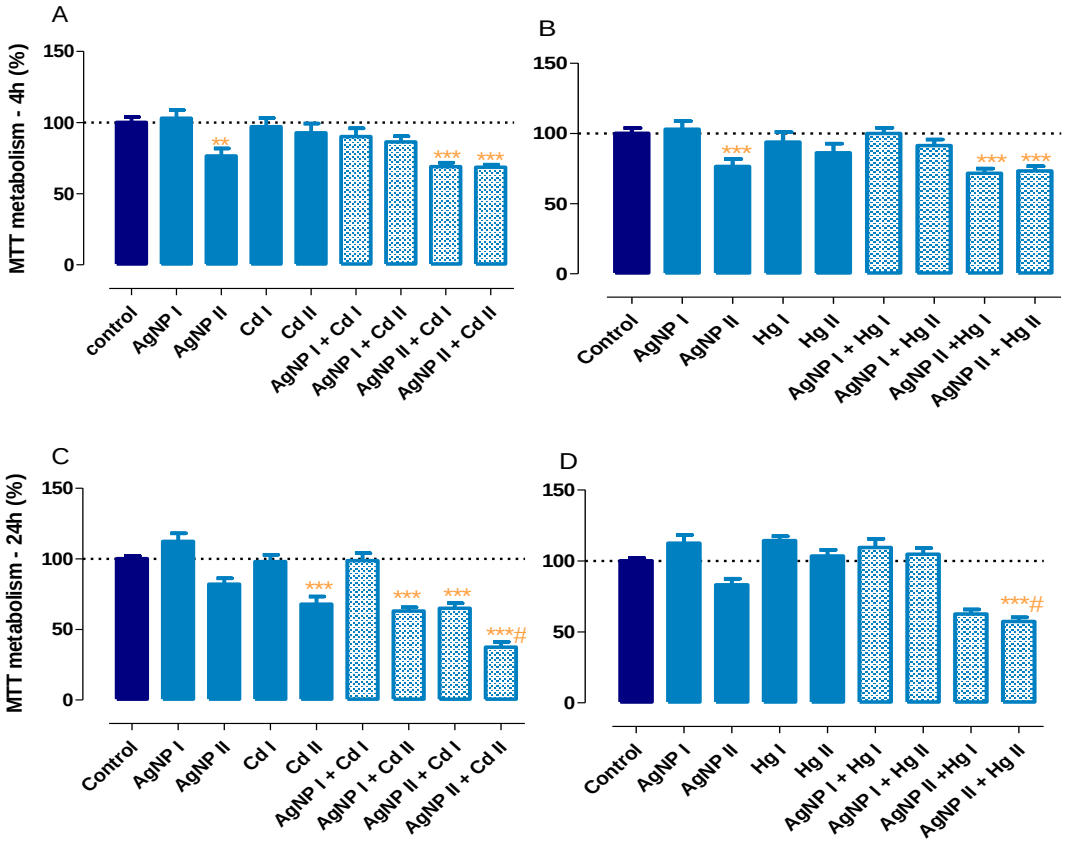

FIGURE 2. MTT assay in HepG2 cells exposed for 4 h (A-B) and 24 h (C-D). Values in % compared to control group. Data are presented as the mean + SEM of three independent experiments. Asterisks indicate effects in comparison to control (**p<0.01, ***p<0.001); sharp symbol (#) indicates toxicological interaction.

Endosome-lysosome system stability, measured by neutral red assay, decreased after exposure to AgNP II (30%) and Cd II (15%), as well as in the majority of groups containing the association of AgNP + Cd and AgNP + Hg for 4 h-experiment (fig. 3A and B). However, the effects occurred because of the association of AgNP and metals only for AgNP II + Cd II (50%) and AgNP II + Hg I/II (≈ 40%; fig. 3A and B). At 24 h-experiment, neutral red uptake decreased after the exposure to AgNP II and Cd II (25-45%), but not Hg, with effects due to the association only for AgNP II + Cd II (decrease of 80%; fig. 3C and D). Interestingly, an increase of 20% of NR uptake was observed for Hg I and AgNP I + Hg II (fig. 3D).

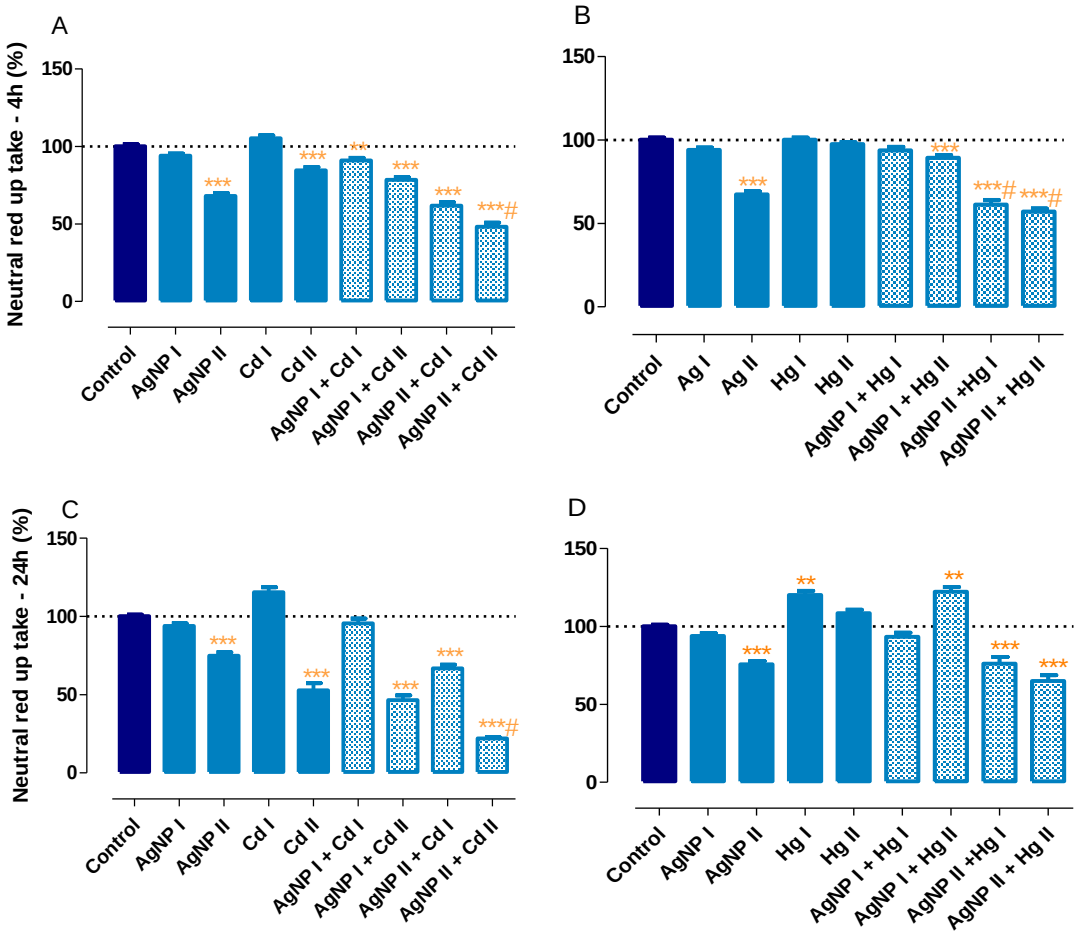

FIGURE 3. Neutral red assay in HepG2 cells exposed for 4 h (A-B) and 24 h (C-D). Values in % compared to control group. Data are presented as the mean + SEM of three independent experiments. Asterisks indicate effects in comparison to control (**p<0.01, ***p<0.001); sharp symbol (#) indicates toxicological interaction.

3.3. Cell Proliferation

The effect of AgNP and its association with Cd and Hg on cell proliferation was investigated by the crystal violet assay, a cationic dye for DNA. After 24 h, groups exposed to Cd I and Hg I had a slight (10%) increase of cell proliferation. However, co-exposure to AgNP II + Cd II and AgNP II + Hg II led to decreases of cell proliferation (40% and 20%, respectively), which were not observed in the cells exposed to the individual contaminants (fig. 4A and B).

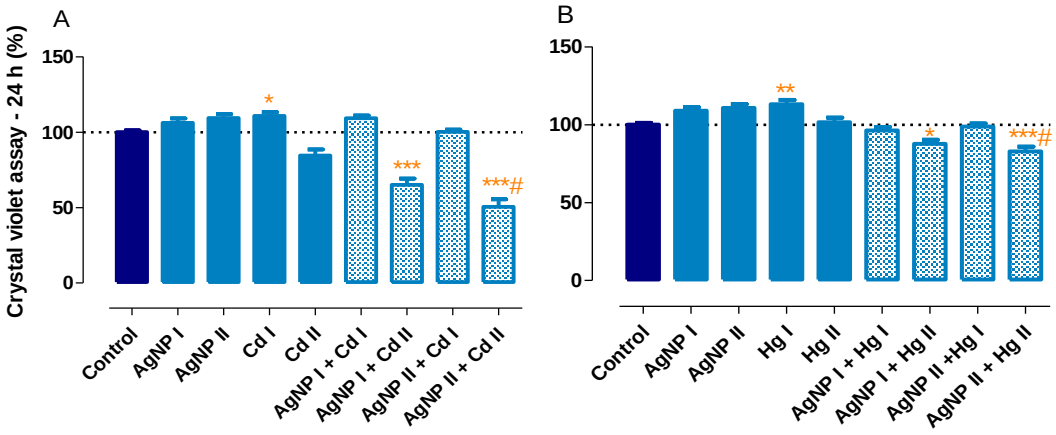

FIGURE 4. Cell proliferation assay in HepG2 cells exposed for 24 h. Values in % compared to control group. Data are presented as the mean + SEM of three independent experiments. Asterisks indicate effects in comparison to control (*p<0.05, **p<0.01, ***p<0.001); sharp symbol (#) indicates toxicological interaction.

3.4. ROS production

The DCFH-DA probe detected increases of >30% of ROS in the cytoplasm of almost all co-exposed groups short after exposure (at 2 h-experiment), while the individual contaminants did not affect ROS production compared to control (fig. 5A and B). At 4 h-experiment, ROS concentration increased in the AgNP II group (40%) and, foremost, in the AgNP I/II + Cd II (40-100%) and AgNP II + Hg I/II (70%) groups (fig. 5C and D).

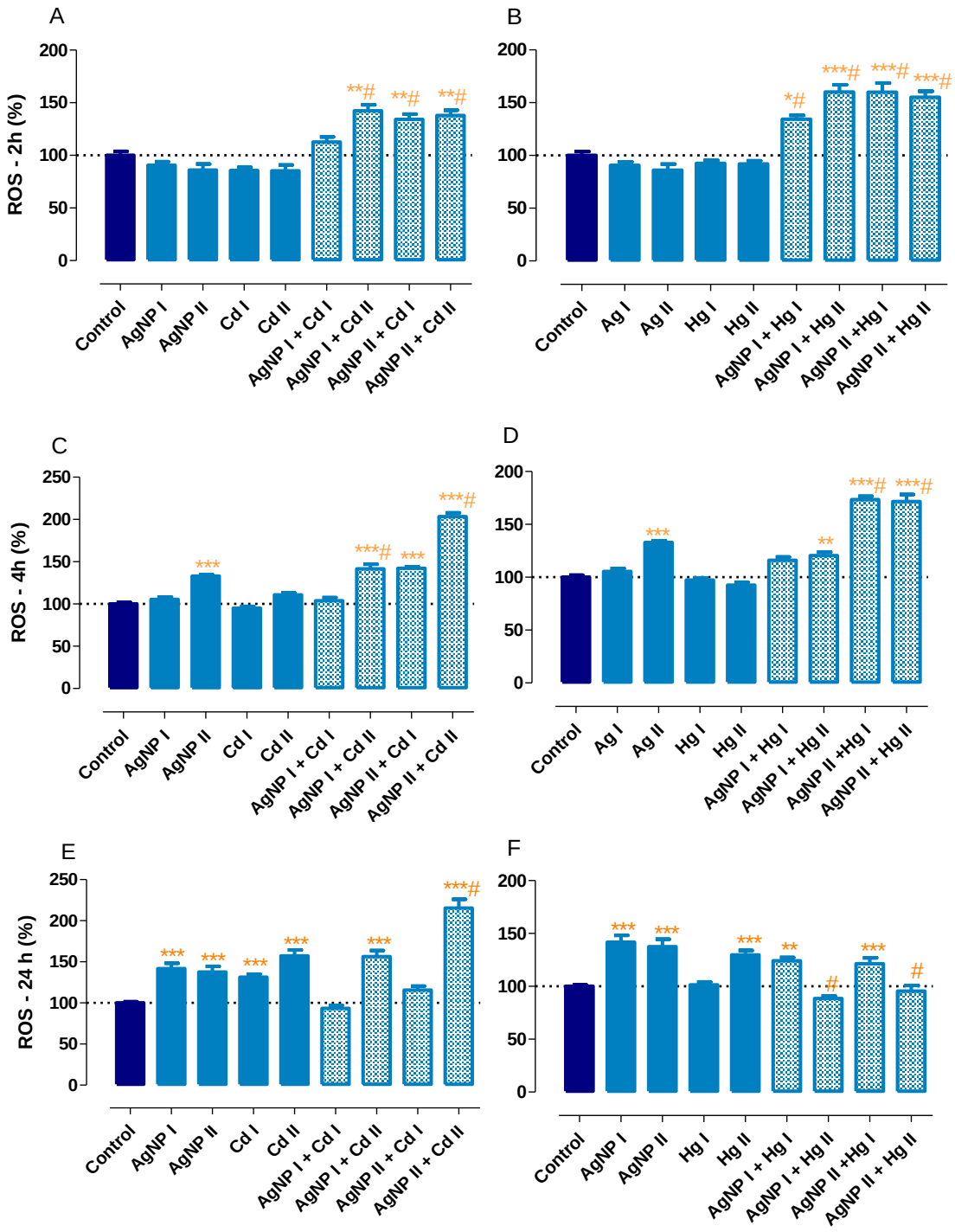

FIGURE 5. ROS production relative to cell viability in HepG2 cells after exposure for 2 h (A-B), 4 h (C-D) and 24 h (E-F). Data are presented as the mean + SEM of three independent experiments. Asterisks indicate effects in comparison to control (*p<0.05, **p<0.01, *** p<0.001); sharp symbol (#) indicates toxicological interaction.

At 24 h-experiment, all the individual contaminants, except for Hg I, induced ROS increases (25-60%). However, only AgNP II + Cd II caused increase of ROS (110%) (fig. 5E). Co-exposure of AgNP and Hg II for 24 h led to decreases of ROS levels (5% *vs* control; >20% *vs* individual contaminants; fig. 5F).

3.5. Mitochondrial Superoxide production

The role of mitochondria in free radical production was also investigated in HepG2 cells. At 4 h-experiment, increases of $O_2^{\bullet-}$ production were observed for AgNP II (95%), Cd II (45%), AgNP II + Cd II (195%) and AgNP II + Hg I/II (50-105%) groups, but not for Hg I/II groups (fig. 6A and B). For AgNP II + Cd II, the effect can be attributed to the association of contaminants (fig. 6A). For 24 h-experiment, the contaminants alone did not cause increase of superoxide, except for AgNP II (100% increase). Nevertheless, the co-exposure of AgNP II + Cd II led to 970% increase of $O_2^{\bullet-}$ production (fig. 6C). Like for 4 h-experiment, some mixtures of AgNP + Cd and AgNP + Hg led to levels of $O_2^{\bullet-}$ different from that of the control, but those effects were not caused by toxicological interaction of the contaminants (fig. 6C and D; groups have asterisks but not sharp symbols).

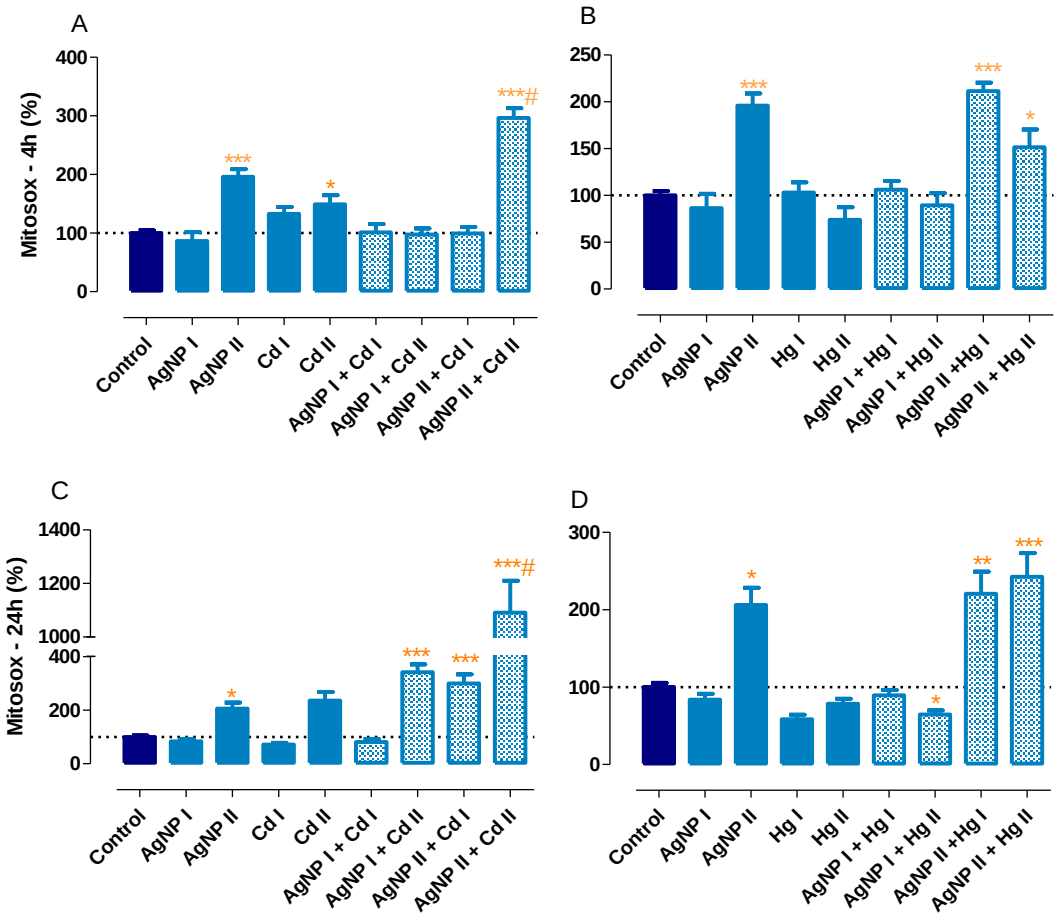

FIGURE 6. Superoxide production in mitochondria of HepG2 cells exposed for 4 h (A-B) and 24 h (C-D). Values in % compared to control group. Data are presented as the mean + SEM of three independent experiments. Asterisks indicate effects in comparison to control (*p<0.05, **p<0.01, ***p<0.001); sharp symbol (#) indicates toxicological interaction.

3.6. Multidrug efflux transporters activity

The activity of the multidrug efflux transporters was evaluated by rhodamine B accumulation assay: the greater the accumulation, the lower the transporters activity. At 4 h-experiment, the exposure to the contaminants in isolation did not affect rhodamine B accumulation in HepG2 cells. However, levels of rhodamine B were higher in cells exposed to AgNP II + Cd I/II (130-150%) and AgNP II + Hg I/II (90%) than those of control (fig. 7A and B). At 24 h-experiment, rhodamine B accumulation was higher in AgNP II (30%), Cd II (90%), AgNP I + Cd II (105%) and, foremost, AgNP II + Cd II (415%) groups (fig. 7C). In both experiments, the effect can be attributed to the association of

contaminants only for AgNP II + Cd I/II groups. The co-exposure to AgNP and Hg also led to increases of rhodamine B accumulation at 24 h-experiment (25-60%), but they were statistically equal to at least one of the individual contaminants present in the respective association (fig. 7D) and so do not characterize an effect of interaction.

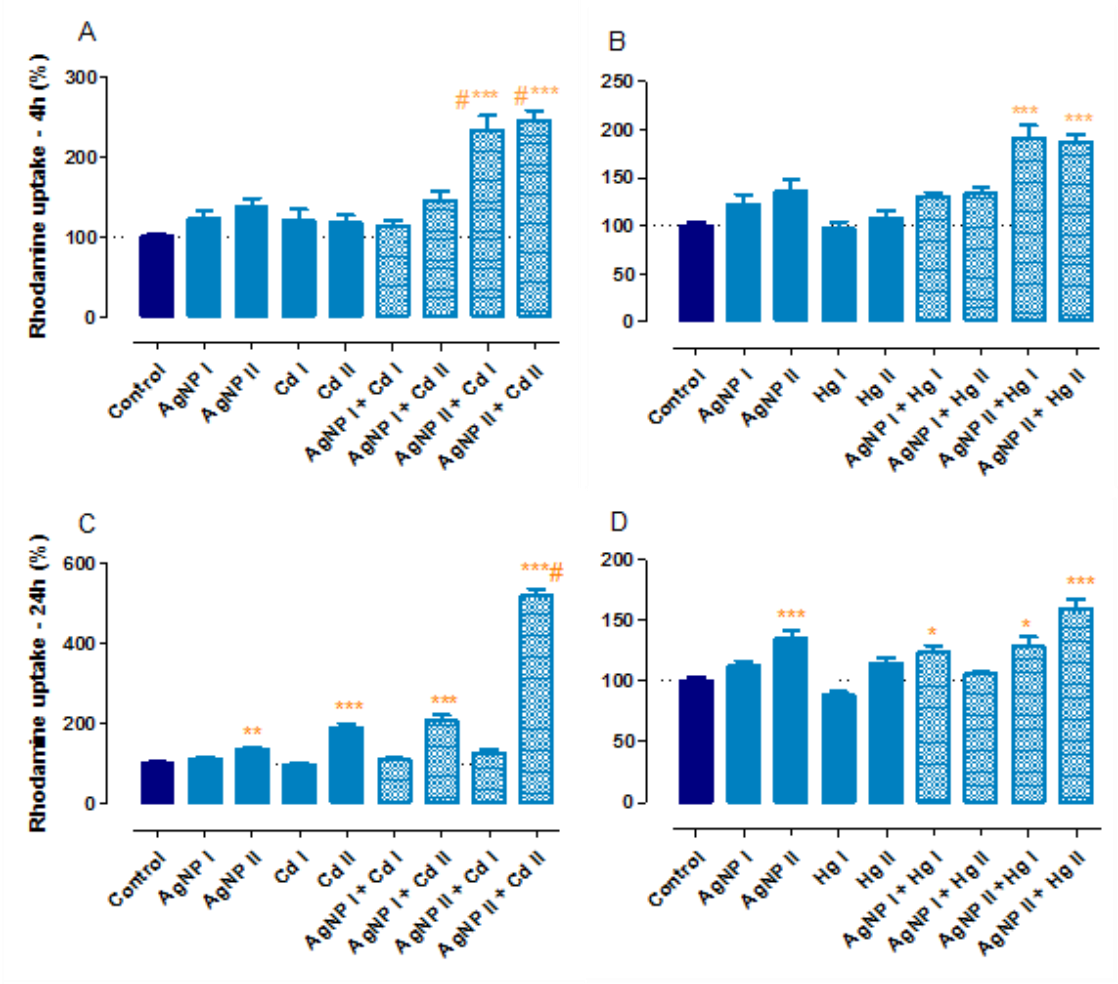

FIGURE 7. Rhodamine accumulation assay in HepG2 cells exposed for 4 h (A-B) and 24 h (C-D). Values in % compared to control group. Data are presented as the mean + SEM of three independent experiments. Asterisks indicate effects in comparison to control (*p<0.05, **p<0.01, ***p<0.001); sharp symbol (#) indicates toxicological interaction. The greater the rhodamine accumulation, the lower the activity of the xenobiotic efflux transporters.

3.7. Cell death

To verify whether apoptosis and necrosis were associated with early toxicity of AgNP, Cd and Hg, Annexin V/PI staining was performed in HepG2 cells. Time-lapse images in confocal microscopy showed the progression of cell death during 24 h, with the co-exposure to AgNP II + Cd II, but not to AgNP + Hg II, inducing earlier cellular damage than the individual contaminants (video in supplementary material; complementary results fig. 4 and 5). Interestingly, at the first 12 h, cells seemed to start the apoptotic program, with changes in the cell shape (cells became round), detachment of neighboring cells and decrease of nucleus volume. However, later on, most of the same cells exhibited changes that are characteristic of necrosis. Cells lost the appropriate osmotic balance and swelled up, and plasma membrane became permeable to hydrophilic molecules such as propidium iodide (nucleus that were stained in blue by Hoechst became pink/purple by Hoechst + iodide propidium), with rapid and subsequent phosphatidylserine labeling (in green), and some cells even bursting.

3.8. Intracellular metals concentration

To find whether the higher toxicity observed in cells co-exposed to AgNP and metals was due to higher uptake, intracellular concentrations of Ag, Cd and Hg were determined by ICP-MS and FIMS, after 4 h of exposure. Co-exposure of AgNP and Cd did not result in a higher uptake of neither the contaminants (fig. 8A). However, co-exposure of AgNP and Hg resulted in a 2.8-fold increase of Hg concentration in HepG2 cells (fig. 8B).

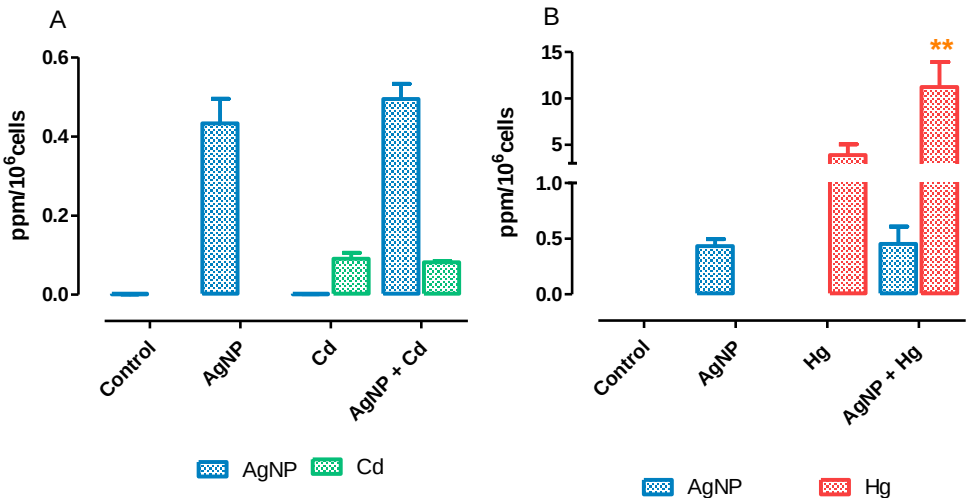

FIGURE 8. Intracellular concentration of Ag, Cd and Hg in HepG2 cells exposed for 4 h (A-B). Results are expressed in ppm/10^6 cells. Data are presented as the mean + SEM of three independent experiments. **p<0.01.

4. Discussion

Toxicological interactions occurred in HepG2 cells co-exposed to AgNP + Cd and AgNP + Hg, as follow.

Contaminants affected cell survivor and the mode of cell death after time-dependent toxicological interaction

The MTT metabolism of cells co-exposed to AgNP II + Hg II for 24 h decreased more than expected, considering the effects the contaminants alone, while AgNP II + Cd II induced a predicted effect (i.e., similar to the sum of individual contaminants). Both AgNP and Cd can disturb mitochondrial structure and activity of mitochondrial dehydrogenases (responsible for MTT metabolism), leading to ATP depletion (Yano and Marcondes, 2005; Chairuangkitti *et al.,*, 2013; Aueviriyavit *et al.,*, 2014). This disturb occurred as soon as at 4 h-exposure for AgNP, but not for Cd and Hg, and so AgNP can cause a toxic effect on mitochondria faster than those two toxic metals. Later (24 h), the situation changed as Cd effects on MTT metabolism and cell viability became more pronounced than those of AgNP.

The effect of the association of AgNP + Cd on cell viability varied in a time-dependent manner. At 4 h-exposure, the effect of AgNP II + Cd II was less pronounced than that of 24 h, but induction of lysosomal membrane instability can cause the decrease of neutral red retention observed in both cases, as reported in HepG2 and other cell types (Fotakis and Timbrell, 2006; Messner *et al.,*, 2012; Grosse *et al.,*, 2013). Conversely, a different trend occurred for the AgNP + Hg groups. Hg was not able to impair cell viability after 4 and 24 h-exposure, but the association AgNP II + Hg II reduced it at 4 h, with a partial recovery of neutral red uptake capacity at 24 h. Activation of the defense systems are time-dependent, so that an initial stress can be balanced thereafter, with partial or even overcompensation. The latter situation occurred for Hg I and AgNP I + Hg II groups (decrease of cell viability at 4 h and increased viability/ number of attached cells at 24 h). Else, if defenses are not able to reestablish homeostasis, the toxicity can increase with time, as observed for Cd II. On this regard, though Cd and Hg are both nonessential and electrophilic metals, Cd^{+2} was much more toxic than Hg^{+2} for HepG2 cells.

Co-exposures to the highest concentrations of the contaminants can induce cell death earlier (time-lapse imaging) than the individual contaminants. Cells seem to start apoptosis program with chromatin condensation, but latter plasma membrane usually became permeable to small molecules (*e.g.*, propidium iodide) before phosphatidylserine labeling (with annexin V-FITC), which is typical for necrosis. Thus, it is possible that chemical stress induced a change of the mode of cell death, from apoptosis to necrosis. Apoptosis requires chemical energy (ATP) which is provided mostly by mitochondria in aerobic eukaryotic cells. AgNP, Cd and Hg can impair mitochondrial membrane potential and ATP synthesis (Monroe and Halvorsen, 2009; Tomankova *et al.,*, 2015), leading to ATP depletion and necrosis; necrosis is a passive process and does not require ATP.

Changes in cell proliferation after contaminant exposure depends on many factors, such as time of exposure and concentration. Many studies reported the ability of AgNP and both metal ions (Cd and Hg) to reduce cell proliferation (Templeton and Liu, 2010; Vergilio *et al.,*, 2014; Miethling-Graff *et al.,*, 2014). In this study, contaminants alone did not impair cell proliferation, though co-exposures seem to induce an inhibitory effect that could not be predicted based on the results from the lone exposures. Decreased metabolic status of the cells (MTT assay) and cell death after exposure to AgNP II + Cd II or to AgNP II + Hg II could explain, at least in part, the decrease of the number of attached cells (determined through crystal violet assay). Conversely, activation of cell defense mechanisms could lead to the increases of cell number observed in the cells exposed to the lowest Cd and Hg concentrations.

ROS production increased early after the co-exposures

Oxidative stress is one of the hallmarks of AgNP toxicity (Asharani *et al.,*, 2008; Kim *et al.,*, 2009; Liu *et al.,*, 2010). Cadmium and mercury can also induce the increase of ROS levels, by binding to sulfhydryl groups of antioxidants such as glutathione, inhibiting antioxidant enzymes (Nzengue *et al.,*, 2008; Aguado *et al.,*, 2013) and blocking electron flow in mitochondria (Monroe and Halvorsen, 2009). In the current study, increase of ROS production was an early response (observed from 2 h-experiment on) in cells co-exposed to AgNP and Cd/Hg, but not in cells exposed to the individual contaminants. For

longer exposures, individual contaminants were able to unbalance redox milieu, and the effects of the associations became less evident (4 h-experiment) until being only observed in AgNP II + Cd II and AgNP I/II + Hg II groups (24 h-experiment). Thus, cellular defense systems may be efficient to avoid oxidative stress at very short-term exposures, but not at longer-term ones for individual contaminants. For the associations of AgNP and Cd/Hg, defenses were not enough to deal with ROS at 2 h-exposures and avoid cell death during the course of 24 h-exposure.

Mitochondria were one important source of ROS in the cells exposed to AgNP and Cd, but not Hg, as well as in cells co-exposed to AgNP II + Cd II; for the latter group, superoxide levels increased with the exposure time. Excess of ROS in mitochondria can lead to organelle malfunction (*e.g.*, decreased enzymatic activity and MTT metabolism) and ATP depletion, as well as malfunction or damage to the other cell compartments, as unstable superoxide can be converted to much more stable and membrane-permeable hydrogen peroxide (Fleury *et al.*,, 2002). Decrease of ATP levels can, in turn, impair active transport processes such as proton transport into endosomes and lysosomes (decreasing neutral red retention) and rhodamine transport out the cell (by ABC efflux transporters), as well as impair the execution of apoptosis program.

Rhodamine accumulation followed the same pattern of mitochondrial ROS levels

ABC transporters are a superfamily of membrane transporters that use energy from ATP hydrolysis to translocate a broad-spectrum of molecules across cell membranes (Rodrigues *et al.*,, 2009). One of these transporters, P-glycoprotein (P-gp), is involved with the transport of cell lipids and drugs (Klein *et al.*,, 1999), being important for cell detoxification. In HepG2 cells, accumulation of rhodamine B, associated with the malfunction of the efflux system, occurred in all AgNP II-containing associations (AgNP II + Cd I/II; AgNP II + Hg I/II) as early as at 4 h-experiment, with no effect on the individual exposures. However, as observed for mitochondrial ROS levels, even individual contaminants affected rhodamine B accumulation after 24 h-exposure. Regardless of the exact cause of efflux transporters impairment, i.e. decrease of ATP levels or direct damage to the transporters (by metals or ROS), cells may become more sensitive to

additional chemical stressors that are substrates for the transporters, as they might remain longer inside the cells.

Higher accumulation of the metal can explain the higher toxicity of the association containing Hg, but not Cd

Metals such as Cd and Pb can adsorb onto AgNP surface due to the nanoparticle's highly reactive surface and charge difference (Alqudami *et al.,*, 2012). Since AgNP used in the experiments exhibit negative charge, as showed by zeta potential, and both Cd and Hg ions are positively charged, it is possible that AgNP absorbed these ions.

ICP-MS analysis were performed in order to find if the increase of toxicity, observed in co-exposed cells, was the outcome of a higher intracellular concentration of one or both contaminants. In the presence of AgNP, concentration of Hg ions increased about 2.8 fold in HepG2 cells after 4 h-exposure. This might explain the increased toxic effect of AgNP + Hg groups in some parameters, such as cell metabolism, viability, and proliferation, as well as ROS production. However, this logic is not valid for Cd ions, since the presence of AgNP did not affect intracellular Cd ions concentration, but co-exposures AgNP + Cd were much more toxic. For AgNP + Cd, each contaminant may independently interfere with converting toxic pathways (*e.g.*, mitochondrial ATP synthesis) resulting in a toxicological interaction. An alternative hypothesis, that needs investigation, is that the interaction was only a consequence of the fact that a cell under some level of stress (by a contaminant) may be able to deal with it but not with additional stress (by the other contaminant) because the sum of both stresses exceeds cells defenses, independent of the nature of the contaminants.

5. Conclusion

Taken together, these results provide important information about the toxicological interaction of AgNP, cadmium and mercury in HepG2 cells. Associations of AgNP and the metal ions were more toxic than the individual contaminants. Expected effects were observed in most co-exposures, whereas in few cases the effects of the mixtures were higher than the sum of the effects observed for the individual contaminants. ROS production was an early effect of the co-exposures, with important contribution of mitochondria. Decrease of mitochondrial metabolism and ATP levels can, in principle, explain the other findings in HepG2 cells: the accumulation of rhodamine B (decreased efflux transporters activity), decreased viability (decreased neutral red retention) and change of the mode of cell death (apoptosis to necrosis). Highest intracellular concentration of Hg in the presence of AgNP can explain the highest toxicity of AgNP + Hg association. For AgNP + Cd groups, AgNP had no effect on Cd uptake.

Conflict of interest statement

The authors declare that there are no conflicts of interest.

Acknowledgements

CNPq (Brazilian Agency for Science and Technology) and CAPES (PhD scholarship) supported the work described in the current paper. The authors thank Israel Henrique Bini for the assistance with the confocal microscope. The authors also gratefully acknowledge financial support by the European Research Council (ERC) under the European Union's Horizon 2020 Research and Innovation Programme (grant agreement No 646603) as well the VILLUM Center for Bioanalytical Sciences at the University of Southern Denmark.

Supplementary Material

Supplementary data to this article can be found online at http://dx.doi.org/10.1016/j.tiv.2017.01.003.

Video 1. Supplementary material. Time-lapse video of HepG2 cells exposed to Cd II, AgNP II and AgNP II + Cd II during 24 h in DMEM culture medium, 5% CO_2 and 37 °C. Hoechst stains the nucleus of viable cells in blue. Annexin V-FITC labels phosphatidylserine at the plasma membrane (PM) in green of cells in apoptosis (in the outer surface of PM) and necrosis (in the inner surface of PM). Propidium iodide stains the nucleus of non-viable cells (cells with damaged PM) in orange. Overlap of Hoechst and propidium iodide is pink/purple. Images were captured with laser scanning confocal multiphoton microscope; model A1 MP+ (NIKON Instruments Inc., Tokyo, Japan).

References

Alqudami, A., Alhemiary, N. a., Munassar, S., 2012. Removal of Pb(II) and Cd(II) ions from water by Fe and Ag nanoparticles prepared using electro-exploding wire technique. Environ. Sci. Pollut. Res. 19, 2832–2841.

Arbuckle, T.E., Liang, C.L., Morisset, A.-S., Fisher, M., Weiler, H., Cirtiu, C.M., Legrand, M., Davis, K., Ettinger, A.S., Fraser, W.D., 2016. Maternal and fetal exposure to cadmium, lead, manganese and mercury: The MIREC study. Chemosphere 163, 270–282.

Asharani, P. V, Wu, Y.L., Gong, Z., Valiyaveettil, S., 2008. Toxicity of silver nanoparticles in zebrafish models 255102.

Aueviriyavit, S., Phummiratch, D., Maniratanachote, R., 2014. Mechanistic study on the biological effects of silver and gold nanoparticles in Caco-2 cells--induction of the Nrf2/HO-1 pathway by high concentrations of silver nanoparticles. Toxicol. Lett. 224, 73–83.

Benov, L., Sztejnberg, L., Fridovich, I., Enov, L.U.B., Ztejnberg, L.A.S., 1998. Critical evaluation of the use of hydroethidine as a measure of superoxide anion radical. Free Radic. Biol. Med. 25, 826–831.

Bystrzejewska-Piotrowska, G., Golimowski, J., Urban, P.L., 2009. Nanoparticles: their potential toxicity, waste and environmental management. Waste Manag. 29, 2587–2595.

Capaldo, A., Gay, F., Scudiero, R., Trinchella, F., Caputo, I., Lepretti, M., Marabotti, A., Esposito, C., Laforgia, V., 2016. Histological changes, apoptosis and metallothionein levels in Triturus carnifex (Amphibia, Urodela) exposed to environmental cadmium concentrations. Aquat. Toxicol. 173, 63-73.

Chairuangkitti, P., Lawanprasert, S., Roytrakul, S., Aueviriyavit, S., Phummiratch, D., Kulthong, K., Chanvorachote, P., Maniratanachote, R., 2013. Silver nanoparticles induce toxicity in A549 cells via ROS-dependent and ROS-independent pathways. Toxicol. In Vitro. 27, 330–338.

Chen, Y.Y., Zhu, J.Y., Chan, K.M., 2014. Effects of cadmium on cell proliferation , apoptosis , and proto-oncogene expression in zebrafish liver cells. Aquat. Toxicol. 157, 196–206.

Cleveland, D., Long, S.E., Pennington, P.L., Cooper, E., Fulton, M.H., Scott, G.I., Brewer, T., Davis, J., Petersen, E.J., Wood, L., 2012. Pilot estuarine mesocosm study on the environmental fate of Silver nanomaterials leached from consumer products. Sci. Total Environ. 421-422, 267–272.

Della Torre, C., Balbi, T., Grassi, G., Frenzilli, G., Bernardeschi, M., Smerilli, A., Guidi, P., Canesi, L., Nigro, M., Monaci, F., Scarcelli, V., Rocco, L., Focardi, S., Monopoli, M., Corsi, I., 2015. Titanium dioxide nanoparticles modulate the toxicological response to cadmium in the gills of Mytilus galloprovincialis. J. Hazard. Mater. 297, 92–100

Elsaesser, A., Howard, C.V., 2012. Toxicology of nanoparticles. Adv. Drug Deliv. Rev. 64, 129–137.

Fabrega, J., Luoma, S.N., Tyler, C.R., Galloway, T.S., Lead, J.R., 2011. Silver nanoparticles: behaviour and effects in the aquatic environment. Environ. Int. 37, 517–531.

Ferreira, J.L.R., Lonné, M.N., França, T. A., Maximilla, N.R., Lugokenski, T.H., Costa, P.G., Fillmann, G., Antunes Soares, F. A., de la Torre, F.R., Monserrat, J.M., 2014. Co-exposure of the organic nanomaterial fullerene C60 with benzo[a]pyrene in Danio rerio (zebrafish) hepatocytes: Evidence of toxicological interactions. Aquat. Toxicol. 147, 76–83.

Fleury, C., Mignotte, B., Vayssière, J.-L., 2002. Mitochondrial reactive oxygen species in cell death signaling. Biochimie 84, 131–141.

Fotakis, G., Timbrell, J. a, 2006. Role of trace elements in cadmium chloride uptake in hepatoma cell lines. Toxicol. Lett. 164, 97–103.

Fowler, B. a, 2009. Monitoring of human populations for early markers of cadmium toxicity: a review. Toxicol. Appl. Pharmacol. 238, 294–300.

Gaillet, S., Rouanet, J.-M., 2015. Silver nanoparticles: their potential toxic effects after oral exposure and underlying mechanisms--a review. Food Chem. Toxicol. 77, 58–63.

Gliga, A.R., Skoglund, S., Wallinder, I.O., Fadeel, B., Karlsson, H.L., 2014. Size-dependent cytotoxicity of silver nanoparticles in human lung cells: the role of cellular uptake, agglomeration and Ag release. Part. Fibre Toxicol. 11, 11.

Glinski, A., Liebel, S., Pelletier, È., Voigt, C.L., Randi, M.A.F., Campos, S.X., Oliveira Ribeiro, C.A., Filipak Neto, F., 2016. Toxicological interactions of silver nanoparticles and organochlorine pesticides in mouse peritoneal macrophages. Toxicol. Mech. Methods 26, 251–259.

Grosse, S., Evje, L., Syversen, T., 2013. Silver nanoparticle-induced cytotoxicity in rat brain endothelial cell culture. Toxicol. In Vitro 27, 305–313.

Guo, M., Xu, X., Yan, X., Wang, S., Gao, S., Zhu, S., 2013. In vivo biodistribution and synergistic toxicity of silica nanoparticles and cadmium chloride in mice. J. Hazard. Mater. 260, 780–788.

Kim, I., Lee, B.-T., Kim, H.-A., Kim, K.-W., Kim, S.D., Hwang, Y.-S., 2015. Citrate coated silver nanoparticles change heavy metal toxicities and bioaccumulation of Daphnia magna. Chemosphere. 143,99-105.

Kim, S., Choi, J.E., Choi, J., Chung, K.-H., Park, K., Yi, J., Ryu, D.-Y., 2009. Oxidative stress-dependent toxicity of silver nanoparticles in human hepatoma cells. Toxicol. In Vitro 23, 1076–1084.

Klein, I., Sarkadi, B., Váradi, A., 1999. An inventory of the human ABC proteins. Biochim. Biophys. Acta - Biomembr. 1461, 237–262.

Knasmüller, S., Mersch-Sundermann, V., Kevekordes, S., Darroudi, F., Huber, W.W., Hoelzl, C., Bichler, J., Majer, B.J., 2004. Use of human-derived liver cell lines for the detection of environmental and dietary genotoxicants; Current state of knowledge. Toxicology 198, 315–328.

Kumar, G., Degheidy, H., Casey, B.J., Goering, P.L., 2015. Flow cytometry evaluation of in vitro cellular necrosis and apoptosis induced by silver nanoparticles. Food Chem. Toxicol. 85, 45–51.

Liebel, S., de Oliveira Ribeiro, C.A., de Magalhães, V.F., da Silva, R.D.C., Rossi, S.C., Randi, M.A.F., Filipak Neto, F., 2015. Low concentrations of cylindrospermopsin induce increases of reactive oxygen species levels, metabolism and proliferation in human hepatoma cells (HepG2). Toxicol. Vitr. 29, 479–488.

Liu, W., Wu, Y., Wang, C., Li, H.C., Wang, T., Liao, C.Y., Cui, L., Zhou, Q.F., Yan, B., Jiang, G.B., 2010. Impact of silver nanoparticles on human cells: effect of particle size. Nanotoxicology. 4, 319–330.

Maurer-Jones, M. a., Gunsolus, I.L., Murphy, C.J., Haynes, C.L., 2013. Toxicity of engineered nanoparticles in the environment. Anal. Chem. 85. 3036–3049.

Mersch-Sundermann, V., Knasmüller, S., Wu, X.J., Darroudi, F., Kassie, F., 2004. Use of a human-derived liver cell line for the detection of cytoprotective, antigenotoxic and cogenotoxic agents. Toxicology 198, 329–340.

Messner, B., Ploner, C., Laufer, G., Bernhard, D., 2012. Cadmium activates a programmed, lysosomal membrane permeabilization-dependent necrosis pathway. Toxicol. Lett. 212, 268–75.

Miethling-Graff, R., Rumpker, R., Richter, M., Verano-Braga, T., Kjeldsen, F., Brewer, J., Hoyland, J., Rubahn, H.-G., Erdmann, H., 2014. Exposure to silver nanoparticles induces size- and dose-dependent oxidative stress and cytotoxicity in human colon carcinoma cells. Toxicol. In Vitro 28, 1280–1289.

Monfared, A.L., Bahrami, A.M., Hosseini, E., Soltani, S., Shaddel, M., 2015. Effects of Nano-particles on Histo-pathological changes of the fish. J. Environ. Heal. Sci. Eng. 13, 62.

Monroe, R.K., Halvorsen, S.W., 2009. Environmental toxicants inhibit neuronal Jak tyrosine kinase by mitochondrial disruption. Neurotoxicology 30, 589–598.

Morones, J.R., Elechiguerra, J.L., Camacho, A., Holt, K., Kouri, J.B., Ramírez, J.T., Yacaman, M.J., 2005. The bactericidal effect of silver nanoparticles. Nanotechnology 16, 2346–2353.

Nzengue, Y., Steiman, R., Garrel, C., Lefèbvre, E., Guiraud, P., 2008. Oxidative stress and DNA damage induced by cadmium in the human keratinocyte HaCaT cell line: role of glutathione in the resistance to cadmium. Toxicology 243, 193–206.

Pessatti, M.L., Resgalla Jr., C., Reis, F.R.W., Kuehn, J., Salomão, L.C., Fontana, J.D., 2002. Variability of rates of filtration, respiration and assimilation and multixenobiotic mechanism resistance (MXR) of mussel Perna perna under lead influence. Br. J. Biol. 62, 651–656.

Rodrigues, A.C., Curi, R., Hirata, M.H., Hirata, R.D.C., 2009. Decreased ABCB1 mRNA expression induced by atorvastatin results from enhanced mRNA degradation in HepG2 cells. Eur. J. Pharm. Sci. 37, 486–491.

Sahu, S.K., Bhangare, R.C., Tiwari, M., Ajmal, P.Y., Pandit, G.G., 2014. Depth profiles of lithogenic and anthropogenic mercury in the sediments from Thane Creek, Mumbai, India. Int. J. Sediment Res.29, 131-139.

Seltenrich, N., 2013. Nanosilver: Weighing the risks and benefits. Environ. Health Perspect. 121, 220–225.

Stacchiotti, A., Morandini, F., Bettoni, F., Schena, I., Lavazza, A., Giovanni, P., Apostoli, P., Rezzani, R., Francesca, M., 2009. Stress proteins and oxidative damage in a renal derived cell line exposed to inorganic mercury and lead. Toxicology. 264, 215–224.

Syversen, T., Kaur, P., 2012. The toxicology of mercury and its compounds. J. Trace Elem. Med. Biol. 26, 115-126.

Templeton, D.M., Liu, Y., 2010. Chemico-Biological Interactions Multiple roles of cadmium in cell death and survival. Chem. Biol. Interact. 188, 267–275.

Tomankova, K., Horakova, J., Harvanova, M., Malina, L., Soukupova, J., Hradilova, S., Kejlova, K., Malohlava, J., Licman, L., Dvorakova, M., Jirova, D., Kolarova, H., 2015. Cytotoxicity, cell uptake and microscopic analysis of titanium dioxide and silver nanoparticles in vitro. Food Chem. Toxicol. 82, 106-115.

Vance, M.E., Kuiken, T., Vejerano, E.P., McGinnis, S.P., Hochella, M.F., Hull, D.R., 2015. Nanotechnology in the real world: Redeveloping the nanomaterial consumer products inventory. Beilstein J. Nanotechnol. 6, 1769–1780.

Vergilio, C.S., Carvalho, C.E. V, Melo, E.J.T., 2014. Mercury-induced dysfunctions in multiple organelles leading to cell death. Toxicol. In Vitro 29, 63–71.

Wu, Y., Zhou, Q., Li, H., Liu, W., Wang, T., Jiang, G., 2010. Effects of silver nanoparticles on the development and histopathology biomarkers of Japanese medaka (Oryzias latipes) using the partial-life test. Aquat. Toxicol. 100, 160–167.

Yano, C.L., Marcondes, M.C.C.G., 2005. Cadmium chloride-induced oxidative stress in skeletal muscle cells in vitro. Free Radic. Biol. Med. 39, 1378–1384.

CAPÍTULO II

Co-exposure to silver nanoparticles and cadmium ions induces antioxidant defense depletion and metabolic proteins reprogramming in HepG2 cells

Manuscrito a ser submetido para revista Nanotoxicology

Renata Rank Miranda[a], Vladimir Gorshkov[b], Stefan J Kempf[b], Barbara Korzeniowska[b], Francisco Filipak Neto[a], Frank Kjeldsen[b*]

[a] *Department of Cell Biology, Federal University of Parana, Curitiba, PR, Brazil*

[b] *Department of Biochemistry and Molecular Biology, University of Southern Denmark, Odense, Denmark*

Abstract

Although many studies have reported the deleterious effects and mechanism of toxicity of AgNP in a variety of organisms, the possible toxicological interactions of AgNP and ubiquitous environment contaminants, such as cadmium, remains poorly understood. In this study, biochemical assays and mass spectrometry-based proteomics were performed in HepG2 cells after the co-exposure to AgNP+Cd to explore cellular and molecular effects induced by the combination of these contaminants. Cell viability (trypan blue and LDH leakage) and energetic levels (ADP/ATP) were slightly affected after the 4 h exposure to individual and combined contaminants; however, these endpoints were substantially altered after 24 h co-exposure to AgNP+Cd compared to control and individual exposures, which led to minor changes. The proteomics results followed the same trend: while 4 h exposure to contaminants induced minor protein deregulation, after 24 h cells exposed to AgNP and Cd had circa 7 and 2% protein deregulation respectively, while 43% of the proteome of cells co-exposed to AgNP+Cd was deregulated. Briefly, the toxicity induced by AgNP+Cd involved (1) inactivation of Nrf-2, which resulted in antioxidant defense and proteasome related proteins down-regulation, (2) metabolic reprograming in response to ADP/ATP unbalance and (3) increased protein synthesis in order to reestablish homeostasis. Thus, the adaptation strategy was not able to restore ADP/ATP homeostasis and to avoid cell death.

Keywords: HepG2, silver nanoparticles, cadmium, co-exposure, interaction, proteomics

1. Introduction

Production and applications of silver nanoparticles (AgNP) have grown substantially over the past decades, being the most widely used nanoparticles among engineered nanomaterials (Vance *et al.,* 2015). AgNP have an enormous potential to improve current technologies, from medicine and pharmacology to consumer products and bioremediation (Zhang *et al.,* 2016), but not without the release of nanowastes into natural environment (Cleveland *et al.,* 2012a, Furman *et al.,* 2013). According to estimations, the predicted environment concentrations of AgNP in surface waters, which is a potential exposure route to humans, is 0.088-10,000 ng l^{-1}; yet it is difficult to estimate concentrations of nanoparticles that will be released at any given time, due to current and future nanoparticle prevalence in commercial products (Maurer-Jones *et al.,* 2013).

Many research groups have demonstrated the extend of toxicity in cells and tissues of AgNP using controlled experiments (Navarro *et al.,* 2008, Govindasamy and Rahuman 2012, Wildt *et al.,* 2015). However, natural environments continuously receive complex mixtures of contaminants of different chemical properties. Therefore, the study of interactions among toxicants has an enormous practical importance in toxicology (Goldoni and Johansson 2007), particularly for novel contaminants such as AgNP. Recently, an increasing number of studies have addressed this issue by investigating interactions of nanoparticles and widespread environmental xenobiotics, such as metals, polycyclic aromatic hydrocarbons and pesticides in different biological organization levels (Guo *et al.,* 2013, Ferreira *et al.,* 2014, Della Torre *et al.,* 2015, Deville *et al.,* 2016, Glinski *et al.,* 2016). Deville and co-authors (2016), for instance, showed that interaction of gold nanoparticles with niquel led to competitive effect on dendritic cells maturation, and differently from lone exposures, led to cells inactivation. Guo (2013) observed synergistic interaction of silica nanoparticles and cadmium in mice, resulting in enhanced biochemical response and metal biodistribution. Cadmium (Cd) is non-essential metal and ubiquitous contaminant of natural environments and dietary products (Arbuckle *et al.,* 2016). Due to its application in battery production, fertilizers and plastic stabilizers (Capaldo *et al.,* 2016), this metal enters natural

environments and induce deleterious effects not only to the biota, but also to humans (Cuypers *et al.,* 2010).

In a previous study, we showed that mercury uptake by HepG2 cells was enhanced by the co-exposure with 2 nm AgNP, and co-exposure of cadmium with AgNP induced greater toxicity (*e.g.* viability, ROS production and proliferation) despite that AgNP did not add to a higher intracellular cadmium levels (Miranda *et al.,* 2017). Based on these observations we have now used MS-based proteomics in order to infer to greater detail the molecular processes underlying the toxic biological outcomes induced by AgNP+Cd in HepG2 cells. The proteomics results obtained here are compared to the analysis of cell viability and ADP/ATP ratio also conducted. Since liver is a target organ to these contaminants (Fowler 2009, Elsaesser and Howard 2012b), human hepatocarcinoma cell line HepG2 was used as the study model once it preserves most of the phenotypic characteristics of normal hepatocytes and it is routinely used in toxicity assessments (Knasmüller *et al.,* 2004, Urani 2005).

2. Material and Methods

2.1. Silver nanoparticles characterization

Spherical silver nanoparticles, 10 nm, in citrate buffer were commercially obtained from Sigma Aldrich®. The mass concentration was 0.02 mg/ml in 2mM citrate buffer. Suspension was characterized according to NPs size distribution (DelsaMax Pro, Beckman Coulter, CA).

2.2. HepG2 cell culture

Human hepatoma cells HepG2 (Sigma Aldrich®) were cultured as a monolayer in high glucose Dulbecco's Modified Eagle's Medium (DMEM) supplemented with 10% inactivated fetal bovine serum (FBS) and antibiotics (10 U ml^{-1} penicillin and 10 µg ml^{-1} streptomycin), at 37 °C and 5% CO_2. Cells at passages 110-118 were utilized in the current study.

2.3. Exposure protocol

Cells were seeded onto 96-well microplate ($4x10^4$ cells per well) for LDH leakage (cell viability) and ADP/ATP ratio (energy metabolism) analysis and onto 60 mm petri dishes ($1.5x10^6$ cells per well) for trypan blue (cell viability) and proteomics analysis. Contaminants concentrations used in this study were chosen based on a previous study published by the group (Miranda *et al.,* 2017).

After 24 h, the medium was replaced by fresh DMEM medium with antibiotics and 2% fetal bovine serum containing either AgNP (3.5 µg ml^{-1}), or $CdCl_2$ (1.5 µM), or the combination of AgNP and $CdCl_2$. Cells were exposed to these contaminants for 4 h and 24 h using appropriate controls.

2.4. Cell viability tests

The lactate dehydrogenase (LDH) assay is used to access the degree of cellular membrane damage, based on the leakage of the cytosolic enzyme LDH to the extracellular media. CytotoxOne (Promega) cell viability test was performed in a 96

well plate format according to manufactures instructions. Briefly, cells were exposed to the contaminants for 4 and 24 h at a final volume of 100 µl and then stabilized at 22 ºC. Next, 100 µl CytotoxOne reagent was added to each experimental well and incubated for 10 min. In the positive control wells, 2 µl of lysis solution was added. By the end of the incubation, 50 µl of Stop solution was added to all wells and fluorescence was measured at 560/590. Cytotoxicity is expressed in %/maximum LDH release.

Trypan blue assay was also performed to access the viability of cells after exposures. Therefore, cells were seeded onto 60 mm petri dishes ($1.5x10^6$ cells per well) and, after 24 h of plating, exposed to the contaminants for 4 and 24 h. After these periods, cells were detached with 0.5 ml of trypsin (0.25% trypsin, 0.02% EDTA in PBS, pH 7.2), harvested to tubes with 5 ml culture medium, pelleted (500 g for 5 min) and resuspended in 1 ml of total culture medium. Next, 30 µl of each sample were stained with 30 µl of Trypan blue (Sigma Aldrich) and counted with the aid of a Neubauer chamber, under an inverted light microscope. Results are expressed in % viability/control.

2.5. ADP/ATP ratio assay

ADP/ATP ratio is commonly used to accesses cellular energetic status and viability. Therefore, the ADP/ATP kit (Sigma Aldrich) was used in a 96 well plate format, according to the manufacturer's instructions. Briefly, in the first step cells were lysed in order to release ATP and ADP. In the presence of luciferase, ATP imideiatly reacts with the substrate luciferin-D and this reaction generates light. Which is measured in a luminometer and indicates ATP levels (RLU_A).

$$ATP + luciferin\text{-}D + O_2 \xrightarrow{Luciferase} Oxiluciferin + AMP + PP_i + CO_2 + LIGHT$$

Prior to the second step, ATP levels are measured once again (RLU_B). Subsequently, ADP is converted to ATP through an enzymatic reaction. Recently formed ATP reacts with luciferin-D and generates light. This third light intensity is once again measured and it represents the total of ADP and ATP (RLU_C) in the cells. The ratio ADP/ATP is calculated by dividing ADP levels ($RLU_C - RLU_B$) by ATP levels (RLU_A) and normalized by cell viability (trypan blue).

2.6. Statistical procedures for biochemical assays

Three independent experiments were performed. A total of three replicates per experiment were utilized for biomarkers analyzed in 96-well microplates. Data distribution was tested and parametric (one-way ANOVA) tests were performed, followed by Dunnett's post-test. Effects of contaminants were verified by the comparison of the control vs AgNP, Cd or AgNP+Cd. Toxicological interactions were verified the comparison of the co-exposure group vs singly contaminant experiments were performed. p-values lower than 0.05 were considered statistically significant.

2.7. Sample preparation for mass spectrometry based proteomics analysis

After the exposure periods, medium was removed and cells were carefully washed three times with ice-cold PBS. Next, 1 ml of ice-cold PBS, plus protease and phosphatase inhibitors (ProtoSTOP and PhosSTOP, Roche) was added to the plates for cell harvest using a cell scraper. Cell suspensions were transferred to 1.5 ml tubes, centrifuged for 5 min at 600 g and kept at -80 ºC until further analysis.

Lysis buffer (Urea (6M), Tiourea (2M), protease and phosphatase inhibitors cocktail) and 20 mM triethylammonium bicarbonate (TEAB)) plus reducing agent (10 mM DTT) were added to each tube at room temperature for 2 h. Subsequently, samples were diluted 10 times with 20 mM TEAB pH 7.5, cell lysis was enhanced and DNA filaments were sheared by tip sonication on ice. Protein concentration was measured by colorimetric quantification (Qubit™ – LifeTechnologies) and 50 µg of proteins were alkylated in 20 mM iodoacetamide (IAA) for 30 min in the dark. Following incubation, the samples were digested with trypsin (50:1 (w/w) protein: trypsin) overnight at room temperature. Peptides were acidified with 5% formic acid to stop trypsin digestion and dried prior to desalting.

2.8. Desalting with R2/R3 micro-columns

Samples were resuspended in 0.1% TFA and desalted using a home-made p200 columns made with a C8 plug (Empore, 3M purification) packed with equal ratios of Poros R2 and R3 (Applied Biosystems) resins materials in 100% ACN. The column was prepared by short centrifugation (100 g), equilibrated with 0.1% TFA and centrifuged again, this procedure was repeated twice. Next, samples were loaded to

the columns and washed twice with 0.1% TFA. Peptides were eluted with 60% ACN, 0.1% TFA.

2.9. Peptide labeling

A total of 50 µg of tryptic peptides were labeled with iTRAQ 8-plex, according to the manufacturer's instructions. In the three independent experiments, the tags used to label each experimental condition were as follows: control 4 h (113), AgNP 4 h (114), Cd 4 h (115), AgNP + Cd 4 h (116), control 24 h (117), AgNP 24 h (118), Cd 24 h (119) and AgNP + Cd 24 h (121). Peptides were combined 1:1:1:1:1:1:1:1, dried under vacuum and stored at – 20 ºC.

2.10. Sample fractionation

Prior to LC-MS/MS analysis, samples were prefractionated in order to reduce complexity and to remove unbound iTRAQ reagents. The prefractionation methods applied were high pH and HILIC chromatography. In the first method, R3 micro-columns in 100% ACN were prepared (as previously described for R2/R3 columns) and equilibrated with 0.1% NH_3. Samples were resuspended in 1% NH_3, loaded to the columns and washed twice with 0.1% NH_3. Finally, peptides were eluted using different concentrations of ACN. Ten fractions were collected and dried.

Separately for HILIC fractionation, samples were resuspended in 90% ACN, 0.1% TFA and loaded to a TSKGel Amide 80 HILIC HPLC column (length, 15 cm; diameter, 2 mm; particle size, 3 µm). Peptides were eluted at 6 µL/min by decreasing solvent B from 100-60% over 30 min. A total of 9 fractions were collected and subsequently dried in vacuum.

2.11. Reversed-phase NanoLC MS/MS

Each HILIC and high pH sample was resuspended in 0.1% formic acid (FA) and loaded on an in-house packed trap column (2 cm x 100 µm inner diameter; 5 µm) filled with ReproSil-Pur C18 AQ (Dr. Maisch, Ammerbuch-Entringen, Germany). Peptides were separated on an analytical column (17 cm x 75 µm; 3 µm) packed in-house with ReproSil-Pur C18 AQ (Dr. Maisch, Ammerbuch-Entringen, Germany) by reversed

phase chromatography on an EASY-nanoLC system (Thermo Fisher Scientific, Odense, Denmark). To avoid the supercharged effect of the iTRAQ 8-plex, a 5% ammonia solution was placed under the electrospray needle. The chromatography gradient was as follows: 0 – 7 %B in 1 minute; 7 – 30 %B in 79 minutes, 30 – 50 %B in 10 minutes, 50 – 100 %B in 5 minutes, followed by 8 minute was at 100 %B (A: 0.1% FA, B: 95% ACN, 0.1% FA) at a constant flow rate of 250 nl/min. The nanoLC was connected to a Q Exactive high-field Hybrid Quadrupole-Orbitrap mass spectrometer (Thermo Fisher Scientific) operating in positive ion mode and using data- dependent acquisition. The full scan was acquired with an automatic gain control (AGC) target value of $3x10^6$ and a maximum injection time of 100 ms. Each MS scan was acquired at a resolution of 60000 at m/z 200 with a mass range of m/z 400 – 1400. The 12 most intense precursor ions having charge from 2 to 5 were selected to be fragmented with higher-energy collisional dissociation (HCD). Fragmentation was performed at normalized collision energy (NCE) of 30% using an isolation width of 1.2 Da and a dynamic exclusion duration of 20 s. MS^2 spectra were acquired at 30000 resolution at m/z 200, with AGC $1x10^5$ and maximum injection time of 200 ms.

2.12. Database searches and bioinformatics analysis

Raw data were processed using Proteome Discoverer v1.4 (Thermo Fisher Scientific) and searched against SwissProt human database using Mascot search engine. Trypsin was chosen as the enzyme allowing 2 missed cleavage sites. A precursor mass tolerance of 10 ppm and a product ion mass tolerance of 0.02 Da were used. Fixed modifications included carbamidomethylation of cysteines and iTRAQ8-plex labeling for lysines and N-termini. Dynamic modifications contained methionine oxidation and N-terminal acetylation. False discovery rates were calculated using Percolator algorithm (q-value filter set to 0.01). Reporter ion intensities were log2-transformed and normalized in each channel using median. The R Rollup function from DanteR package was used to build protein intensities from peptide. Protein regulations were determined using Limma-Ranked Product approach (Schwämmle *et al.,* 2013). Only proteins with p-values ≤ 0.05 were considered regulated.

Regulated proteins were submitted to STRING (Search Tool for the Retrieval of Interacting Genes/Proteins) (Franceschini *et al.,* 2013) and IPA (Ingenuity Pathway

Analysis) software in order to infer cellular protein responses induced by the exposures to the contaminants.

3. Results and Discussion

3.1. Silver nanoparticle characterization

DLS measurements indicated that most of the particles (70%) had diameter of 14 nm (Fig. 1A).

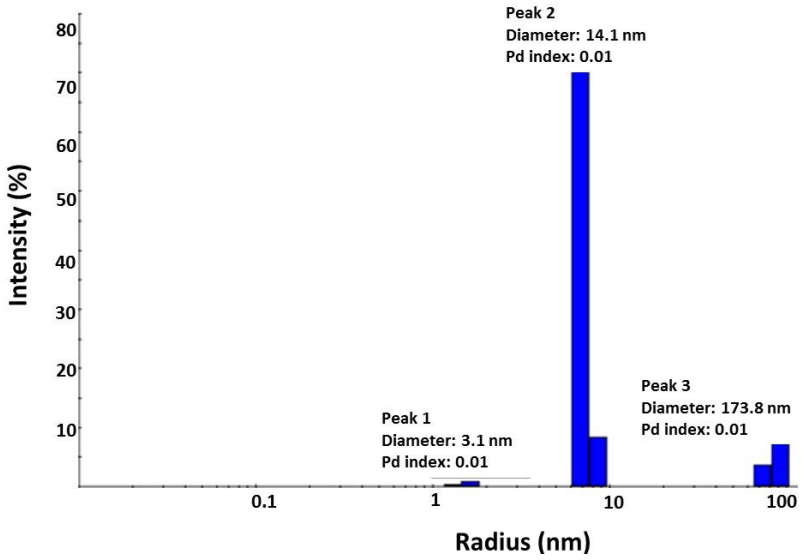

FIGURE 1. AgNP characterization. Particle distribution according to size (DelsaMax Pro).

3.2. Co-exposure of AgNP and Cd induce loss of cell viability and energy unbalance

The effects of AgNP, Cd and AgNP+Cd on cell viability and energy balance were evaluated through trypan blue, LDH leakage (plasma membrane permeability) and ADP/ATP ratios (energy balance). At 4 h-experiment, increases of 1.5 to 5-fold in LDH levels were observed for all groups compared to the control (fig. 2A). After 24 h, the situation was similar for exposure to singly contaminants: AgNP and Cd 1.5 to 5-fold increase in LDH levels compared to the control (fig. 2B), while co-exposure to AgNP+Cd led to an increase of 7-fold increase in LDH compared to the control group (fig. 2B).

However, some studies have demonstrated that AgNP might interact with LDH assay via enzyme inhibition or biding (Han *et al.,* 2011, Gliga *et al.,* 2014), masking viability decrease. Therefore, trypan blue assay was also conducted. Although with some differences from LDH in terms of sensitivity, a more pronounced effect of AgNP+Cd was also observed in trypan blue assay after 24 h (fig. 2C and D). In addition, the effects on cell viability had the same pattern as that observed in our previous study for MTT and neutral red assays after 24 h-exposure (Miranda *et al.,* 2017). Trypan blue assay indicated no effects of contaminants at 4 h-experiment (fig. 2C), but decreases of cell viability at 24 h-experiment occurred for AgNP (34%), Cd (18%) and foremost, AgNP+Cd (77%; fig. 2D).

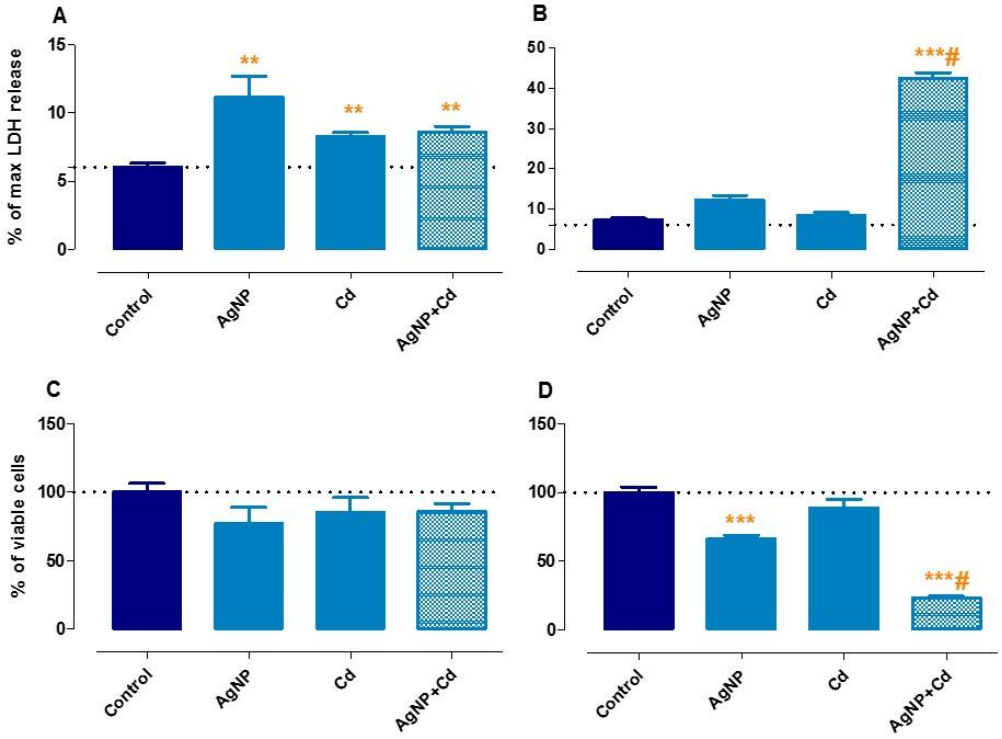

FIGURE 2. Cell viability test. LDH leakage (A, B) and trypan blue (C, D) assays in HepG2 cells exposed for 4 h (A, C) and 24 h (B, D) to AgNP (3.5 µg/ml), Cd (1.5 µM) and AgNP+Cd (3.5 µg/ml + 1.5 µM). Mean + SEM of three independent experiments in triplicate. Asterisks indicate effects in comparison to the control (**p<0.01, ***p<0.001); sharp symbol (#) indicates toxicological interaction.

Comparison of viability data of the present study and the previous one suggests that toxicological interaction of AgNP with Cd depends on the particle's characteristics, such as coating and size, as well as the period of exposure. Non-coated 2 nm AgNP

interaction with Cd induced earlier toxic effects (*e.g.* decreased cell viability and increased ROS levels already after 4 h) than 10 nm citrate coated AgNP. However, after 24 h these endpoints reached similar values after co-exposure of both nanoparticles with Cd.

ADP/ATP ratio is commonly used to gain insights about the mode of cell death as well as the cellular energetic status. For instance, high levels of ATP and low levels of ADP are characteristic of cell proliferation, while the opposite situation indicates apoptosis or necrosis. ADP/ATP ratios increased 52%, 36% and 40% for AgNP, Cd and AgNP+Cd, respectively, in the 4 h-experiment (fig. 3A). After 24 h, the percent increase of ADP/ATP ratios for AgNP and Cd were of 70%, and 61%, respectively. However, a substantial increase of 396% was observed for AgNP+Cd in comparison to the control (fig. 3B). Although energetic unbalance occurred after 4 h exposure to the contaminants, cells were able to survive and viability loss was minor (LDH assay) or not observed (trypan blue assay). As for the 24 h-experiment, ADP/ATP ratio unbalance was followed by loss of cell viability. Considering that the energy production was hampered by the contaminant, cells may not undergo apoptosis, at least in the AgNP+Cd group, which may explain the harsh increase of LHD leakage (characteristic of necrosis) observed in here (Riss and Moravec 2004). In addition, we have previously reported a change of the cells death mechanism from apoptosis to necrosis, by time-lapse confocal microscopy, for HepG2 cells exposed to AgNP+Cd (Miranda *et al.,* 2017). From the above data, it is substantiated that the co-exposure of AgNP+Cd induce significantly more harm to HepG2 cells than any of the two contaminant individually.

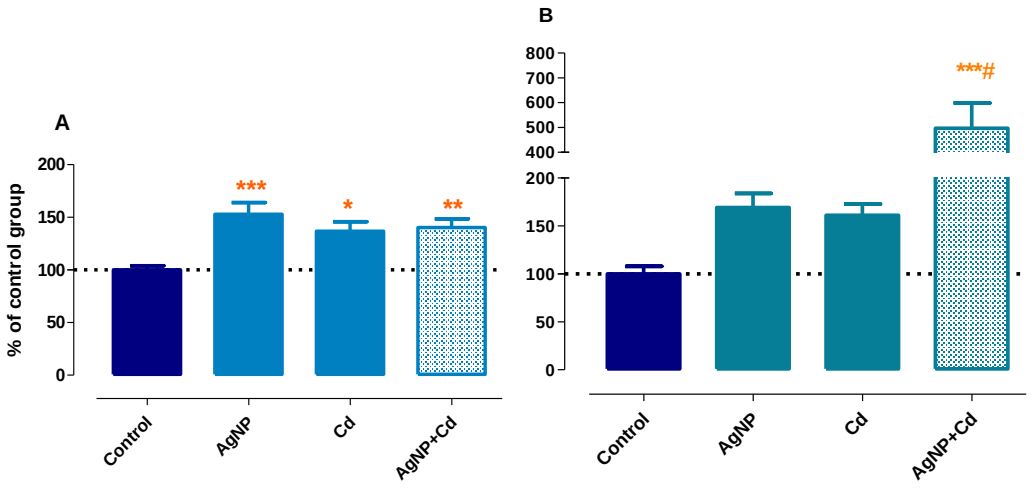

FIGURE 3. Energetic status. ADP/ATP ratio in HepG2 cells exposed for 4 h (A) and 24 h (B) to AgNP (3.5 µg/ml), Cd (1.5 µM) and AgNP+Cd (3.5 µg/ml + 1.5 µM). Mean + SEM of three independent experiments in triplicate. Asterisks indicate effects in comparison to control (**p<0.01, ***p<0.001); sharp symbol (#) indicates toxicological interaction.

3.3. Co-exposure to AgNP+Cd lead to deep changes in HepG2 cell proteome

Quantitative proteomics approach was performed in order to infer the proteomics basis for the observed toxicity effects induced by the co-exposure of AgNP+Cd in HepG2 cells. Following the experimental design illustrated in figure 4, LC-MS/MS analysis allowed the identification and quantification of 4,522 proteins across all experiments (2 high confidence peptides per protein) according to maximum parsimony.

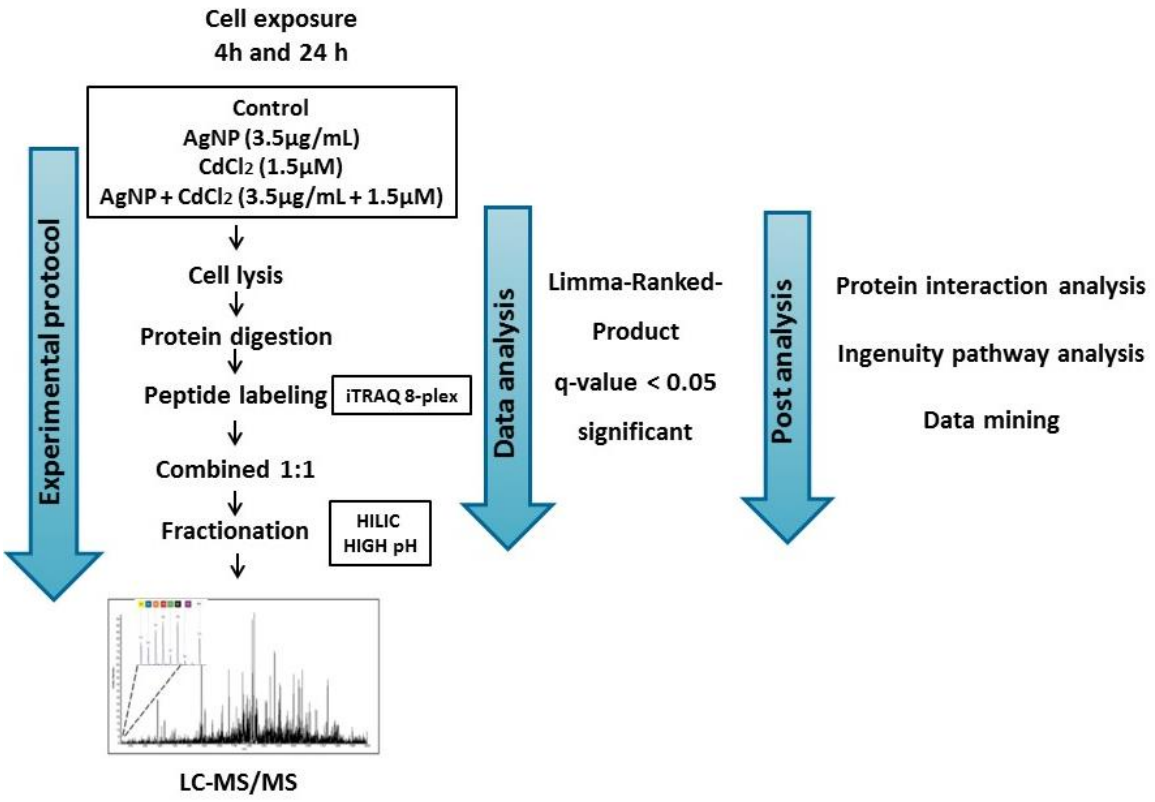

FIGURE 4. Schematic work-flow applied to the study of interaction of AgNP and cadmium in HepG2 cells. The effect AgNP and cadmium in HepG2 cells was tested using cell viability and cell death assays. Regulated proteins were identified and quantified using mass spectrometry-based proteomics combined with bioinformatics analysis.

Here, we have used the term “upregulated” to describe proteins more abundant after exposure to the contaminants, while “downregulated” refers to those less abundant after exposure. Figure 5 shows the number of up and downregulated proteins after 4 h (A) and 24 h (B) of exposure to the contaminants in reference to the control. After 4 h-exposure, a total of 54 proteins were differently regulated for AgNP (30 up and 24 downregulated), 50 proteins for Cd (25 up and 25 downregulated) and 14 proteins for AgNP+Cd (5 up- and 9 down-regulated). From these proteins, some suffered contaminant-specific regulation, i.e., they were up or downregulated only in one of the three-contaminant groups: 47 proteins for AgNP, 40 for Cd and 9 for AgNP+Cd (fig. 5C).

After 24 h-exposure (fig. 5B), 310 proteins were differently regulated for AgNP (105 up and 205 downregulated), 85 proteins for Cd (41 up and 44 downregulated) and foremost 1949 proteins for AgNP+Cd (1151 up and 799 downregulated). From

these proteins, contaminant-specific regulation occurred in 26 proteins for AgNP, 9 for Cd and 1663 for AgNP + Cd (fig. 5D).

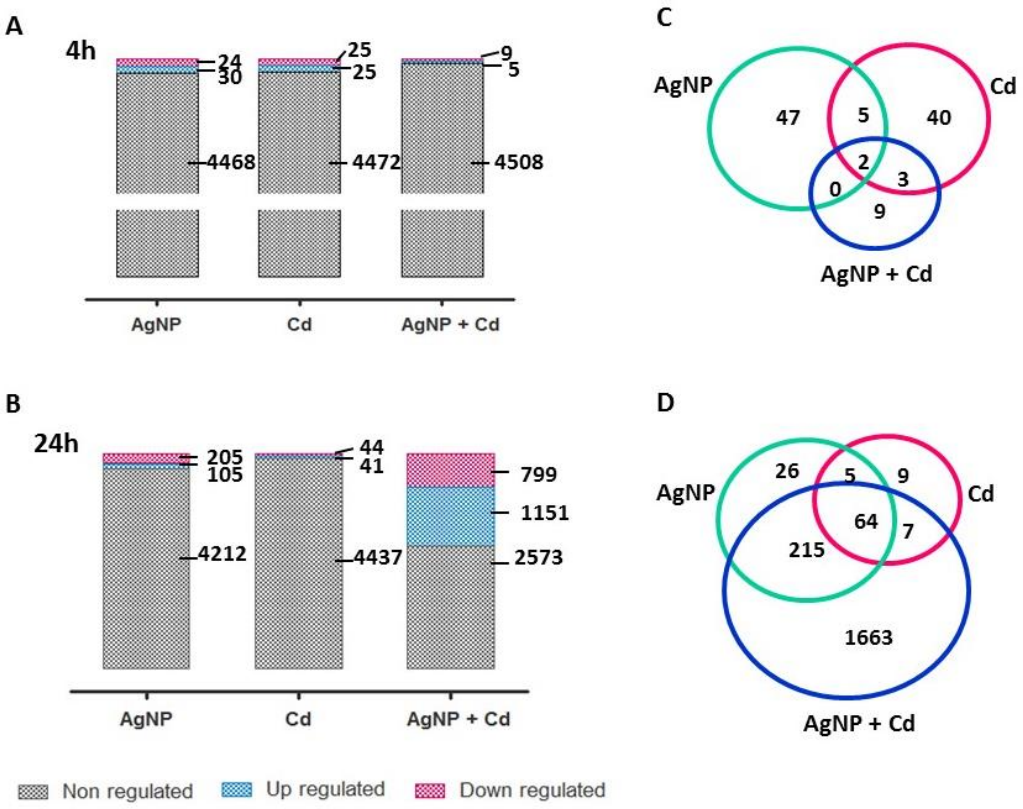

FIGURE 5. Quantitative data of proteomic analysis of three independent experiments. A total of 4522 proteins were identified in all experimental conditions. (A-B) Up- and down- regulated proteins after 4 and 24 h exposure, respectively, to AgNP (3.5 µg/ml), Cd (1.5 µM) and AgNP+Cd (3.5 µg/ml + 1.5 µM). (C-D) Overlap among proteins regulated by each contaminant after 4 and 24 h of exposure.

For all groups, the global cellular response to these contaminants were in the range of few hours and intensified over 24 h, with pronounced difference in protein regulation, particularly for cells co-exposed to AgNP+Cd (alteration of 43% of proteome after 24 h-exposure *vs* 0.3% after 4 h-exposure). In addition, the deregulation after 24 h of co-exposure to the contaminants could not be predicted based on the results from the individual exposures (i.e., ~6.5% and 2% for AgNP and Cd, respectively).

3.4. Molecular mechanisms underlying the toxic response to the contaminants

To better understand the molecular mechanisms caused by exposure to AgNP, Cd and AgNP+Cd, protein-protein interaction networks were built using STRING algorithm for 24 h-exposure experiment (fig. 6; for the 4 h-experiment, protein-protein interaction networks were not formed). AgNP induced the upregulation of mitochondrial proteins related to the respiratory chain and ribosomes, as well as heat shock and cell-cell/matrix adhesion proteins (fig. 6A). A great number of proteins involved with translation initiation and ribosome structure were downregulated. In addition, defined clusters of proteins involved with glucose metabolism, antioxidant defense and cell signaling were observed (fig. 6B). For Cd exposure, clusters of protein-protein interactions were only observed for proteins that were downregulated, indicating that nutrient metabolism and antioxidant defense depletion are related to the cell response (fig. 6C). Protein-protein interactions in the co-exposure group were more related to AgNP than Cd. Upregulation occurred for mitochondrial and respiratory chain proteins, as well as for proteins involved in lipid metabolism, DNA transcription, RNA processing, ribosomes formation and mRNA translation (fig. 6D). Conversely, downregulation occurred for chaperones, heat shock proteins, proteasome subunits, antioxidant defense proteins and proteins involved in glycolysis (fig. 6E).

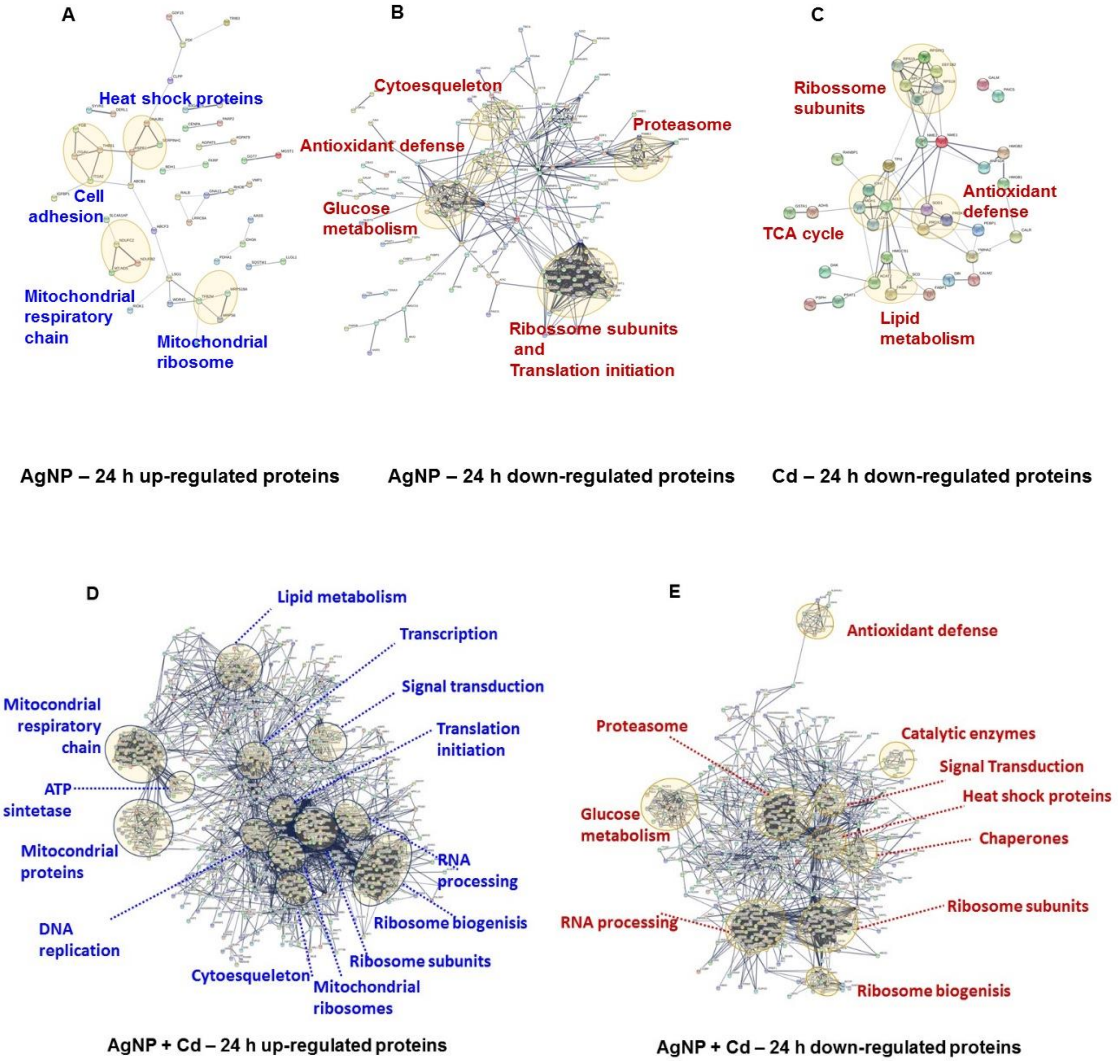

FIGURE 6. Protein-protein interaction networks. Functional interaction networks of deregulated proteins by AgNP and Cd after 24 h were built with STRING algorithm. Thicker lines represent stronger interactions and only interactions with high confidence (score ≥ 0.7) are shown. Up (A) and downregulated (B) proteins after 24 h exposure to AgNP. Proteins down-regulated by Cd after 24 h exposure (C). Proteins up (D) and downregulated (E) after co-exposure to AgNP+Cd.

Pathway analysis was performed to gain an overview on the possible upstream regulators (z-score > 2) involved in the deregulation of proteins after the exposure to the contaminants (fig. 7A). Significant changes of upstream regulators were only observed after 24 h-exposure to AgNP, Cd and AgNP+Cd. Inhibition of the transcription factor Nrf-2 and the activation of RICTOR (subunit of mTORC2) were pointed out as upstream regulators for AgNP. Inhibition of lipid homeostasis regulators, PPAR-γ and SREBF1 were observed for Cd. For AgNP+Cd, 12 upstream regulators

may be involved in the response: 7 were inhibited (such as Nrf-2 and PCK1 involved in gluconeogenesis) and 5 were activated (such as lipid homeostasis related proteins: PPARGC1A, CPI1 and NR1H4). Finally, canonical pathway analysis (p≤0.05) indicated that signaling pathways were mainly associated with cell signaling, glucose and lipid metabolism and oxidative stress–related responses (fig. 7B).

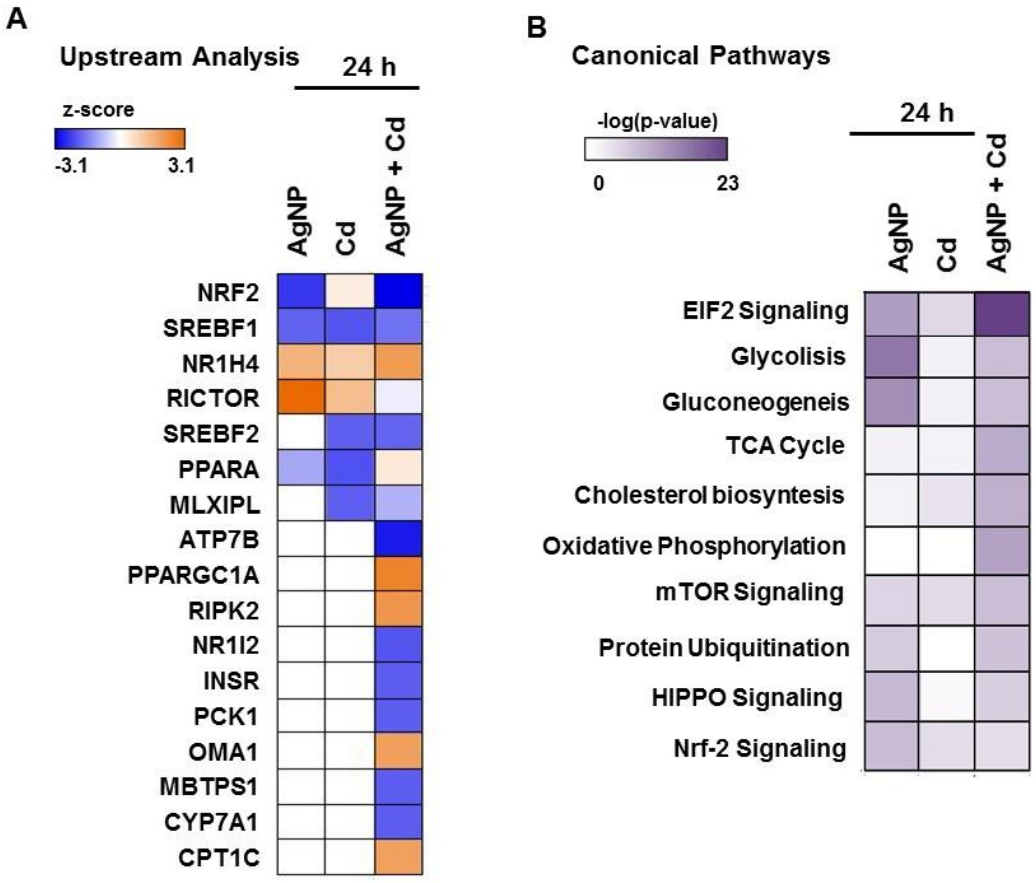

FIGURE 7. Ingenuity Pathway Analysis (IPA). (A) Upstream regulators analysis (z score > 2) of groups exposed to AgNP (RICTOR and NFE2L2), Cd (PPAR-α and SREBF1) and AgNP+Cd (ATP7B, MBTPS1, PCK1, NFE2L2, NR1I2, INSR, CYP7A1, OMA1, CPT1C, RIPK2, NR1H4 and PPARGC1A) after 24 h. (B) Canonical pathway analysis (p value ≤ 0.05) of groups exposed to AgNP, Cd and AgNP + Cd after 24 h.

Toxicity associated with the inactivation of Nrf-2 transcription factor

Oxidative stress results from the unbalance of pro-oxidants and antioxidant defenses. Cells deal with this situation by increasing the expression of antioxidant proteins and activating pathways related to survival and stress adaptation (Holmström and Finkel 2014).

Downregulation of antioxidant enzymes such as superoxide dismutase (SOD) and peroxirredoxin (PRDX), observed after 24 h exposure to all contaminants (fig. 6; table 1) and to AgNP after 4 h (data not shown), may impair antioxidant cell responses leading to increased ROS levels, which was observed after exposure to AgNP, Cd and AgNP+Cd (Miranda *et al*., 2017). Thioredoxins (TXR) were also downregulated after 24 h exposure to AgNP and AgNP+Cd (fig. 6B and E; table 1). This enzyme has an important role in protein repair after oxidative damage, being responsible for reducing oxidized proteins, including peroxirredoxin (after hydrogen peroxide reduction). Exposure for 24 h to AgNP and AgNP+Cd hampered antioxidant defense system in a wider range (fig. 6E), inducing also the downregulation of proteins involved in the glutathione metabolism, such as glutathione synthetase (GSS), glutathione disulphide reductase (GSR) and glutathione *S*-transferase (GST). As shown in table 1, although AgNP and AgNP+Cd disturbed similar antioxidant defense proteins after 24 h, this proteins were more downregulated in the latter case. This situation might have contributed to the increase of ROS levels in the AgNP+Cd group, as observed in our previous study.

Nrf-2 is a transcription factor that binds to the promoter region of antioxidant response elements target genes, having a major role in the redox cell status (de Vries *et al.,* 2008; Vriend and Reiter, 2015). Under homeostatic conditions, Nrf2 is repressed by its negative regulator, KEAP1. However, when intracellular environment becomes more oxidant, this complex dissociates and Nrf2 migrates to the nucleus, promoting the transcription of antioxidant defense related genes (Itoh *et al.,* 2003). The inactivation of this factor was indicated as an upstream regulator after exposure to AgNP and AgNP+Cd (fig. 7A), and the Nrf-2 canonical pathway was significantly affected by all contaminants (fig. 7B), resulting in the downregulation of antioxidant defense proteins mentioned above and, consequently, increased ROS levels.

TABLE 1. Proteins involved in antioxidant defense differentially regulated after 24 h exposure to the contaminants. Ratio represents the experimental group *vs* control mean log-ratio of three independent experiments.

Symbol	Gene Name	Accession Number	RATIO		
			AgNP	Cd	AgNP+Cd
CAT	Catalase	P04040			0.265
GSR	Glutathione-disulfide reductase	P00390			-0.239
GSS	Glutathione synthetase	P48637	-0.4		-0.5
GSTA1	Glutathione S-transferase alpha 1	P08263	-0.68	-0.45	-0.96
GSTM3	Glutathione S-transferase mu 3	P21266			-0.64
GSTO1	Glutathione S-transferase omega 1	P78417	-0.36		-0.36
PRDX	Peroxiredoxin	Q06830	-0.58	-0.31	-0.77
SOD1	Superoxide dismutase 1	P00441	-0.58	-0.41	-0.48
TXN	Thioredoxin	P10599	-0.71		-0.95

Transcription factor Nrf-2 also regulates the expression of proteasomal subunits genes, which contributes to the removal of oxidized proteins following oxidative insult (Chapple *et al.,* 2012, Lee *et al.,* 2012). Moreover, the proteasome has an important role in timely and orderly degradation of cellular proteins, thus regulating many cellular process (Glickman and Ciechanover 2002). Therefore, inactivation of Nrf2 may also be involved with the downregulation of proteasome subunits after exposure to AgNP and, at a higher extend, to AgNP+Cd (fig. 6B; table 2). This situation contributed to the significant alteration of protein ubiquitylation canonical pathway alteration (fig. 7B) and, possibly, the increased toxicity.

In addition, the alteration of protein ubiquitylation canonical pathway (fig. 7B) due to downregulation of ubiquitin, chaperones, heat shock proteins and thioredoxins (table 3) may contribute to this scenario, since proteins may neither be tagged to degradation and degraded in the proteasomes, nor be repaired after the damage caused by the co-exposure to AgNP+Cd.

TABLE 2. Proteasomal subunits differentially regulated after 24 h exposure to the contaminants. Ratio represents the experimental group vs control mean log-ratio of three independent experiments.

Symbol	Gene Name	Accession Number	RATIO		
			AgNP	Cd	AgNP+Cd
PSMA1	proteasome subunit alpha 1	P25786			-0.493
PSMA4	proteasome subunit alpha 4	P25789	-0.418		-0.454
PSMA5	proteasome subunit alpha 5	P28066	-0.413		-0.587
PSMA6	proteasome subunit alpha 6	P60900			-0.541
PSMA7	proteasome subunit alpha 7	O14818			-0.385
PSMB1	proteasome subunit beta 1	P20618			-0.289
PSMB2	proteasome subunit beta 2	P49721			-0.494
PSMB3	proteasome subunit beta 3	P49720			-0.49
PSMB4	proteasome subunit beta 4	P28070	-0.356		-0.55
PSMB6	proteasome subunit beta 6	P28072			-0.47
PSMC3	proteasome 26S subunit. ATPase 3	P17980			-0.803
PSMD5	proteasome 26S subunit. non-ATPase 5	Q16401			-0.538
PSMD7	proteasome 26S subunit. non-ATPase 7	P51665			-0.341
PSMD12	proteasome 26S subunit. non-ATPase 12	O00232			-0.407

.

TABLE 3. Proteins related to ubiquitylation and protein repair differentially regulated after 24 h exposure to the contaminants. Ratio represents the experimental group *vs* control mean log-ratio of three independent experiments.

Symbol	Gene Name	Accession Number	RATIO		
			AgNP	Cd	AgNP+Cd
DNAJB4	DnaJ heat shock protein family (Hsp40) member B4	Q9UDY4			-0,761
DNAJC7	DnaJ heat shock protein family (Hsp40) member C7	Q99615			0,338
DNAJC8	DnaJ heat shock protein family (Hsp40) member C8	O75937	-0,401		-0,509
HSP90AA1	heat shock protein 90 alpha family class A member 1	P07900	-0,421		-0,654
HSPA4	heat shock protein family A (Hsp70) member 4	P34932	-0,346		-0,78
HSPA8	heat shock protein family A (Hsp70) member 8	P11142	-0,41		-0,549
HSPA9	heat shock protein family A (Hsp70) member 9	P38646			0,212
HSPB1	heat shock protein family B (small) member 1	P04792	0,696	0,8	0,314
HSPH1	heat shock protein family H (Hsp110) member 1	Q92598			-0,331
UBA1	ubiquitin like modifier activating enzyme 1	P22314			-0,282
UBE2B	ubiquitin conjugating enzyme E2 B	P63146			-0,814
UBE2I	ubiquitin conjugating enzyme E2 I	P63279			-0,917
UBE2N	ubiquitin conjugating enzyme E2 N	P61088			-0,534
UBE2Q1	ubiquitin conjugating enzyme E2 Q1	Q7Z7E8			0,897
UBE2V1	ubiquitin conjugating enzyme E2 V1	Q13404			-0,575
UCHL5	ubiquitin C-terminal hydrolase L5	Q9Y5K5			-0,156
USP14	ubiquitin specific peptidase 14	P54578			-0,316
USP36	ubiquitin specific peptidase 36	Q9P275			0,446
USP9X	ubiquitin specific peptidase 9, X-linked	Q93008			0,464

Co-exposure to AgNP+Cd strongly deregulates mRNA translation related proteins

Attenuation of mRNA translation, via phosphorylation of eIF2, is an initial cell response to a wide range of stressors, such as nutrient deprivation and accumulation of miss-folded proteins. By this way, cells can save resources while a new program of gene expression is being adopted to prevent further cell damages (Baird and Wek 2012, Donnelly *et al.,* 2013). eIF2 canonical pathway was significantly altered after 24 h-exposure to AgNP and Cd (fig. 7B), due to the downregulation of proteins involved in translation initiation and/or ribosome subunits (fig. 6B and C; table 4). However, a different situation was observed for the combination of both contaminants. Although downregulation of proteins involved in translation initiation and ribosomes also occurred, a greater number of these proteins were found to be upregulated (fig. 6D and E; table 4). Moreover, more up than downregulated proteins were identified and quantified (fig 5B). Supposedly, cells co-exposed to contaminants might have activated transcription and translation of key proteins at 24 h in response to cellular stress. In particular, proteins normally required for reestablishment of energy status, such as those involved in oxidative phosphorylation and mitochondrial functioning as well as in lipid metabolism, were up-regulated, although this cell response has not been enough to avoid or attenuate the abnormal ADP/ATP increase and cell death (fig. 2 and 3). On the other hand, deregulation of this pathway might have also resulted in reduced the levels of certain proteins, such as those involved in antioxidant defense, proteasome activity and protein repair, as discussed above.

TABLE 4. Ribosomal proteins and translation initiation factors differentially deregulated after 24 h exposure to the contaminants. Ratio represents the experimental group vs control mean log-ratio of three independent experiments.

Symbol	Gene Name	Accession Number	RATIO		
			AgNP	Cd	AgNP+Cd
EIF1AY	Eukaryotic translation initiation factor 1A. Y-chromosomal	O14602	-0.36		
EIF2A	eukaryotic translation initiation factor 2A	Q9BY44			0.29
EIF2AK3	eukaryotic translation initiation factor 2 alpha kinase 3	Q9NZJ5			-0.533
EIF2B1	eukaryotic translation initiation factor 2B subunit alpha	Q14232			-0.8
EIF3A	eukaryotic translation initiation factor 3 subunit A	Q14152			0.231
EIF3D	eukaryotic translation initiation factor 3 subunit D	O15371			0.208
EIF3G	eukaryotic translation initiation factor 3 subunit G	O75821			2.196
EIF3H	eukaryotic translation initiation factor 3 subunit H	O15372			-0.324
EIF3J	eukaryotic translation initiation factor 3 subunit J	O75822	-0.386		-0.64
EIF3L	eukaryotic translation initiation factor 3 subunit L	Q9Y262			-0.307
EIF3M	eukaryotic translation initiation factor 3 subunit M	Q7L2H7			0.511
EIF4	Eukaryotic initiation factor 4A-I	P60842			0.231
EIF4G1	eukaryotic translation initiation factor 4 gamma 1	Q04637			0.401
EIF4G2	eukaryotic translation initiation factor 4 gamma 2	P78344			0.162

Symbol	Gene Name	Accession Number	RATIO		
			AgNP	Cd	AgNP+Cd
RPL3	ribosomal protein L3	P39023			0.693
RPL10	ribosomal protein L10	P27635			0.616
RPL12	ribosomal protein L12	P30050	-0.358		-0.532
RPL15	ribosomal protein L15	P61313			0.367
RPL18	ribosomal protein L18	Q07020			0.165
RPL21	ribosomal protein L21	P46778			0.411
RPL29	ribosomal protein L29	P47914	-0.425		-0.352
RPL30	ribosomal protein L30	P62888			0.299
RPL32	ribosomal protein L32	P62910			0.27
RPL35	ribosomal protein L35	P42766	-0.382		-0.515
RPL38	ribosomal protein L38	P63173			-0.31
RPL39	ribosomal protein L39	P62891	-0.887		-0.826
RPL13A	ribosomal protein L13a	P40429			0.328
RPL18A	ribosomal protein L18a	Q02543			0.458
RPL37A	ribosomal protein L37a	P61513			0.376
RPLP0	ribosomal protein lateral stalk subunit P0	P05388	-0.463		-1.004
RPLP1	ribosomal protein lateral stalk subunit P1	P05386	-0.842		-1.443
RPLP2	ribosomal protein lateral stalk subunit P2	P05387	-0.652	-0.406	-0.863
RPS2	ribosomal protein S2	P15880			0.187
RPS3	ribosomal protein S3	P23396			0.172
RPS5	ribosomal protein S5	P46782			0.645
RPS7	ribosomal protein S7	P62081	-0.339		-0.445
RPS10	ribosomal protein S10	P46783	-0.296		-0.505
RPS12	ribosomal protein S12	P25398	-0.311		-0.355
RPS15	ribosomal protein S15	P62841	-0.569	-0.353	-0.559
RPS19	ribosomal protein S19	P39019	-0.616	-0.379	-0.765
RPS23	ribosomal protein S23	P62266			0.26
RPS24	ribosomal protein S24	P62847	-0.381		-0.877
RPS29	ribosomal protein S29	P62273			0.382
RPS27A	ribosomal protein S27a	P62979			0.401
RPS3A	ribosomal protein S3A	P61247			0.24
RPS4Y1	ribosomal protein S4. Y-linked 1	P22090		-0.408	0.449
RPSA	ribosomal protein SA	P08865			-0.427

Co-exposure to AgNP+Cd induces a metabolic reprogramming in HepG2 cells

Cancer cell lines are metabolic adapted for rapid growth under hypoxic and acidic conditions, being glycolysis the main process to synthesize ATP (Warburg effect) even in the presence of oxygen and functional mitochondria (Liberti and Locasale, 2016; Rodríguez-Enríquez *et al.,* 2001). HepG2 cells have the ability to utilize different routes of energy conversion allowing them to use glycolysis alongside oxidative phosphorylation (Kamalian *et al.,* 2015).

Downregulation of proteins involved in glycolysis (table 5) might have resulted in the harsh unbalance of ADP/ATP ratio observed after co-exposure to AgNP+Cd, despite the upregulation of proteins related with oxidative phosphorylation (table 6). Conversely, it is possible that, due to a not so harsh chemical stress, lone exposure to AgNP led to minor ADP/ATP unbalance compared to AgNP+Cd-exposed cells, even though downregulation of glycolytic proteins occurred in both groups.

In our previous study, we reported that 24 h-exposure to AgNP+Cd, but not to AgNP, resulted in the decrease of MTT metabolism, an assay that depends on the activity of mitochondrial succinate dehydrogenase. Therefore, it is possible that on cells with unaltered MTT metabolism (AgNP group) ATP supply was maintained, whereas on those exposed to AgNP+Cd it was not.

TABLE 5. Glycolysis related proteins differentially deregulated after 24 h-exposure to the contaminants. Ratio represents the experimental group vs control mean log-ratio of three independent experiments.

Symbol	Gene Name	Accession Number	RATIO		
			AgNP	Cd	AgNP+Cd
ALDOA	aldolase, fructose-bisphosphate A	P04075	-0,459		-0,527
ALDOC	aldolase, fructose-bisphosphate C	P09972			-0,462
ENO1	enolase 1	P06733	-0,578		-0,597
GAPDH	glyceraldehyde-3-phosphate dehydrogenase	P04406	-0,603		-0,739
GPI	glucose-6-phosphate isomerase	P06744	-0,62		-0,748
PGAM1	phosphoglycerate mutase 1	P18669	-0,36		-0,23
PGK1	phosphoglycerate kinase 1	P00558	-0,352		-0,314
PKM	pyruvate kinase, muscle	P14618	-0,303		-0,364
TPI1	triosephosphate isomerase 1	P60174	-0,644	-0,354	-0,716

TABLE 6. Oxidative phosphorylation related proteins differentially deregulated after 24 h-exposure to the contaminants. Ratio represents the experimental group vs control mean log-ratio of three independent experiments.

Symbol	Gene Name	Accession Number	RATIO		
			AgNP	Cd	AgNP+Cd
ATP5A1	ATP synthase. H+ transporting. mitochondrial F1 complex. alpha subunit 1	P25705			0.219
ATP5B	ATP synthase. H+ transporting. mitochondrial F1 complex. beta polypeptide	P06576			0.387
ATP5F1	ATP synthase. H+ transporting. mitochondrial Fo complex subunit B1	P24539			0.243
ATP5G3	ATP synthase. H+ transporting. mitochondrial Fo complex subunit C3	P48201			1.373
COX4I1	cytochrome c oxidase subunit 4I1	P13073			0.383
COX5A	cytochrome c oxidase subunit 5A	P20674			0.385
COX6B1	cytochrome c oxidase subunit 6B1	P14854			0.352
COX7A2	cytochrome c oxidase subunit 7A2	P14406			-0.657
COX8A	cytochrome c oxidase subunit 8A	P10176			0.636
CYB5A	cytochrome b5 type A	P00167			-0.29
CYC1	cytochrome c1	P08574			0.272
MT-CO2	cytochrome c oxidase subunit II	P00403			0.313
MT-CO3	cytochrome c oxidase III	P00414			0.527
NDUFA1	NADH:ubiquinone oxidoreductase subunit A1	O15239			0.342
NDUFA5	NADH:ubiquinone oxidoreductase subunit A5	Q16718			-0.983
NDUFA6	NADH:ubiquinone oxidoreductase subunit A6	P56556			-0.425
NDUFA8	NADH:ubiquinone oxidoreductase subunit A8	P51970			-1.437
NDUFA9	NADH:ubiquinone oxidoreductase subunit A9	Q16795			0.183
NDUFA12	NADH:ubiquinone oxidoreductase subunit A12	Q9UI09			0.368
NDUFB4	NADH:ubiquinone oxidoreductase subunit B4	O95168			0.292
NDUFB5	NADH:ubiquinone oxidoreductase subunit B5	O43674			0.359
NDUFB7	NADH:ubiquinone oxidoreductase subunit B7	P17568			0.851
NDUFS1	NADH:ubiquinone oxidoreductase core subunit S1	P28331			0.195
NDUFV1	NADH:ubiquinone oxidoreductase core subunit V1	P49821			0.306
SDHA	succinate dehydrogenase complex flavoprotein subunit A	P31040			0.554
SDHB	succinate dehydrogenase complex iron sulfur subunit B	P21912			0.245
UQCRC1	ubiquinol-cytochrome c reductase core protein I	P31930			0.247
UQCRC2	ubiquinol-cytochrome c reductase core protein II	P22695			0.193
UQCRFS1	ubiquinol-cytochrome c reductase. Rieske iron-sulfur polypeptide 1	P47985			0.193

In hepatocytes and HepG2 cells, under ideal nutritional conditions, ATP production occurs mainly through glucose oxidation (Iyer *et al.,* 2010). However, at nutrient deprivation, fatty acids can be oxidized in order to obtain ATP, through β-oxidation and tricarboxylic acid cycle (Houten and Wanders 2010, Iyer *et al.,* 2010, Carracedo *et al.,* 2013). Lipid metabolism related proteins were upregulated after co-exposure to AgNP+Cd (fig. 6D and table 7), suggesting that cells may be using an alternative nutrient to supply the metabolic demand, such as the lipids present in the culture medium (from fetal bovine serum).

Peroxisome proliferator-activated receptor gamma coactivator 1-alpha (PPARGC1A) and bile acid receptor (NR1H4 or FXR) increase transcriptional activity of the nuclear receptor PPARγ, having a central role in metabolic reprogramming in response to nutrient deprivation, through activation of gene expression related to glucose and lipid homeostasis (Mukherjee *et al.,*, 1997; Pineda Torra *et al.,*, 2003). Activation of these co-factors were pointed out as upstream regulators in the cells exposed to AgNP+Cd for 24 h (fig. 7A), suggesting that co-exposure to these

contaminants led to a metabolic reprogramming. Activation of β-oxidation regulator, carnitine O-palmitoyltransferase 1 (CPT1C) (Rinaldi *et al.,* 2015) and inactivation of NR1I2, an inhibitor of β-oxidation (Moreau *et al.,* 2008), were also indicated as upstream regulators (fig. 7A). In addition, canonical pathway analysis suggested alteration on glycolysis and gluconeogenesis in AgNP and AgNP+Cd groups, due to downregulation of proteins related to these pathways (fig. 7B). Taken together, these data reinforce the idea that co-exposure to AgNP+Cd induced a metabolic reprogramming in HepG2 cells due to the ADP/ATP ratio sharp increase in relation to control. Even so, this ratio remained disturbed in cells co-exposed to AgNP+Cd. As mentioned earlier, we have previously reported that 24 h of exposure to AgNP+Cd let to decrease of MTT metabolism, therefore, it is possible that metabolites produced by β-oxidation and TCA cycle (NADH, $FADH_2$ and acetyl-CoA) were not used in this pathway to efficiently restore ADP/ATP homeostasis.

TABLE 7. Tricarboxylic acid cycle (TCA) and lipid metabolism related proteins differentially deregulated after 24 h exposure to the contaminants. Ratio represents the experimental group *vs* control mean log-ratio of three independent experiments.

Symbol	Gene Name	Accession Number	RATIO		
			AgNP	Cd	AgNP+Cd
	TCA Cycle				
ACO2	aconitase 2	Q99798			0.453
DLD	dihydrolipoamide dehydrogenase	P09622			0.378
DLST	dihydrolipoamide S-succinyltransferase	P36957			0.374
FH	fumarate hydratase	P07954			0.168
IDH3A	isocitrate dehydrogenase 3 (NAD(+)) alpha	P50213	0.33		0.481
IDH3B	isocitrate dehydrogenase 3 (NAD(+)) beta	O43837			0.444
IDH3G	isocitrate dehydrogenase 3 (NAD(+)) gamma	P51553			0.478
MDH1	malate dehydrogenase 1	P40925	-0.667	-0.398	-1.046
OGDH	oxoglutarate dehydrogenase	Q02218			0.327
SDHA	succinate dehydrogenase complex flavoprotein subunit A	P31040			0.554
SDHB	succinate dehydrogenase complex iron sulfur subunit B	P21912			0.245
SUCLG1	succinate-CoA ligase alpha subunit	P53597			0.48

Symbol	Gene Name	Accession Number	RATIO		
			AgNP	Cd	AgNP+Cd
	Lipid metabolism				
DECR1	2.4-dienoyl-CoA reductase	Q16698			0.15
ECI1	Enoyl-CoA delta isomerase 1	P42126			0.359
PCCA	Propionyl-CoA carboxylase alpha chain	P05165			0.453
ACAA2	3-ketoacyl-CoA thiolase	P42765			0.398
ACADS	Short-chain specific acyl-CoA dehydrogenase	P16219			0.496
ACAT2	Acetyl-CoA acetyltransferase	O75908	-0.969	-0.695	-1.207
ACADM	Medium-chain specific acyl-CoA dehydrogenase	P11310			0.169
PCCB	Propionyl-CoA carboxylase beta chain	P05166			0.23
HADHB	Trifunctional enzyme subunit beta	P55084			0.371

4. Conclusion

Our results provide important information about the toxicological interaction of AgNP and cadmium in HepG2 cells, as well as some insights about possible toxicity mechanisms to be further studied. Co-exposure for 24 h to AgNP+Cd induced, in general, more toxic responses than individual exposures to AgNP or Cd. Total proteome profile of HepG2 cells changed substantially after 24 h of co-exposure to AgNP+Cd. Oxidative stress increase, previously observed, might be a result of downregulation of antioxidant defense system, due to the inhibition of the upstream regulator Nrf-2 activity, which may also have played a central role for downregulation of proteasome subunits. Another hallmark of the toxicity induced by AgNP+Cd was the upregulation of oxidative phosphorylation and lipid metabolism related proteins, suggesting that a metabolic reprogramming occurred, since HepG2 cells usually produce ATP mainly by glycolysis, and alternative nutrients, such as lipids, were possibly used to try to reestablish homeostatic ADP/ATP ratio. While cells exposed to individual contaminants exhibited downregulation of translation related proteins, cells co-exposed to AgNP+Cd showed both up and downregulation, resulting in a deep alteration of eIF2 canonical pathway. This situation might be the cause of downregulation of glycolytic, antioxidant and proteasomal proteins, and so have triggered cell adaptation mechanisms, i.e., metabolic reprogramming. However, this adaptation strategy was not enough to restore ADP/ATP homeostasis and to avoid cell death.

Conflict of interest statement

The authors declare that there are no conflicts of interest.

Acknowledgements

CAPES for the PhD scholarship. The authors also gratefully acknowledge financial support by the European Research Council (ERC) under the European Union's Horizon 2020 Research and Innovation Programme (grant agreement No 646603) as well the VILLUM Center for Bioanalytical Sciences at the University of Southern Denmark.

Supplementary table 1. List of all proteins identified in this study.

References

Davis, K., Ettinger, A.S., Fraser, W.D., 2016. Maternal and fetal exposure to cadmium, lead, manganese and mercury: The MIREC study. Chemosphere 163, 270–282. doi:10.1016/j.chemosphere.2016.08.023

Baird, T., Wek, R., 2012. Eukaryotic initiation factor 2 phosphorylation and translational control in metabolism. Adv. Nutr. 3, 307–321. doi:10.3945/an.112.002113.We

Capaldo, A., Gay, F., Scudiero, R., Trinchella, F., Caputo, I., Lepretti, M., Marabotti, A., Esposito, C., Laforgia, V., 2016. Histological changes, apoptosis and metallothionein levels in Triturus carnifex (Amphibia, Urodela) exposed to environmental cadmium concentrations. Aquat. Toxicol. doi:10.1016/j.aquatox.2016.01.009

Carracedo, A., Cantley, L.C., Pandolfi, P.P., 2013. Cancer metabolism: fatty acid oxidation in the limelight. Nat Rev Cancer 13, 227–32. doi:10.1038/nrc3483

Chapple, S.J., Siow, R.C.M., Mann, G.E., 2012. Crosstalk between Nrf2 and the proteasome: Therapeutic potential of Nrf2 inducers in vascular disease and aging. Int. J. Biochem. Cell Biol. doi:10.1016/j.biocel.2012.04.021

Cleveland, D., Long, S.E., Pennington, P.L., Cooper, E., Fulton, M.H., Scott, G.I., Brewer, T., Davis, J., Petersen, E.J., Wood, L., 2012. Pilot estuarine mesocosm study on the environmental fate of Silver nanomaterials leached from consumer products. Sci. Total Environ. 421–422, 267–272. doi:10.1016/j.scitotenv.2012.01.025

Cuypers, A., Plusquin, M., Remans, T., Jozefczak, M., Keunen, E., Gielen, H., Opdenakker, K., Nair, A.R., Munters, E., Artois, T.J., Nawrot, T., Vangronsveld, J., Smeets, K., 2010. Cadmium stress: An oxidative challenge. BioMetals 23, 927–940. doi:10.1007/s10534-010-9329-x

de Vries, H.E., Witte, M., Hondius, D., Rozemuller, a. J.M., Drukarch, B., Hoozemans, J., van Horssen, J., 2008. Nrf2-induced antioxidant protection: A promising target to counteract ROS-mediated damage in neurodegenerative disease? Free Radic. Biol. Med. 45, 1375–1383. doi:10.1016/j.freeradbiomed.2008.09.001

Della Torre, C., Balbi, T., Grassi, G., Frenzilli, G., Bernardeschi, M., Smerilli, A., Guidi, P., Canesi, L., Nigro, M., Monaci, F., Scarcelli, V., Rocco, L., Focardi, S., Monopoli, M., Corsi, I., 2015. Titanium dioxide nanoparticles modulate the toxicological response to cadmium in the gills of Mytilus galloprovincialis. J. Hazard. Mater. 297, 92–100. doi:10.1016/j.jhazmat.2015.04.072

Deville, S., Baré, B., Piella, J., Tirez, K., Hoet, P., Monopoli, M.P., Dawson, K.A., Puntes, V.F., Nelissen, I., 2016. Interaction of gold nanoparticles and nickel(II) sulfate affects dendritic cell maturation. Nanotoxicology 10, 1395–1403. doi:10.1080/17435390.2016.1221476

Donnelly, N., Gorman, A.M., Gupta, S., Samali, A., 2013. The eIF2?? kinases: Their structures and functions. Cell. Mol. Life Sci. 70, 3493–3511. doi:10.1007/s00018-012-1252-6

Elsaesser, A., Howard, C.V., 2012. Toxicology of nanoparticles ☆. Adv. Drug Deliv.

Rev. 64, 129–137. doi:10.1016/j.addr.2011.09.001

Ferreira, J.L.R., Lonn??, M.N., Fran??a, T. a., Maximilla, N.R., Lugokenski, T.H., Costa, P.G., Fillmann, G., Antunes Soares, F. a., de la Torre, F.R., Monserrat, J.M., 2014. Co-exposure of the organic nanomaterial fullerene C60 with benzo[a]pyrene in Danio rerio (zebrafish) hepatocytes: Evidence of toxicological interactions. Aquat. Toxicol. 147, 76–83. doi:10.1016/j.aquatox.2013.12.007

Fowler, B. a, 2009. Monitoring of human populations for early markers of cadmium toxicity: a review. Toxicol. Appl. Pharmacol. 238, 294–300. doi:10.1016/j.taap.2009.05.004

Franceschini, A., Szklarczyk, D., Frankild, S., Kuhn, M., Simonovic, M., Roth, A., Lin, J., Minguez, P., Bork, P., Von Mering, C., Jensen, L.J., 2013. STRING v9.1: Protein-protein interaction networks, with increased coverage and integration. Nucleic Acids Res. 41, 808–815. doi:10.1093/nar/gks1094

Furman, O., Usenko, S., Lau, B.L.T., 2013. Relative iFurman, O., Usenko, S., & Lau, B. L. T. (2013). Relative importance of the humic and fulvic fractions of natural organic matter in the aggregation and deposition of silver nanoparticles. Environ. Sci. Technol. 47, 1349–1356.

Glickman, M.H., Ciechanover, A., 2002. The Ubiquitin-Proteasome Proteolytic Pathway: Destruction for the Sake of Construction. Physiol. Rev. 82, 373–428. doi:10.1152/physrev.00027.2001

Gliga, A.R., Skoglund, S., Wallinder, I.O., Fadeel, B., Karlsson, H.L., 2014. Size-dependent cytotoxicity of silver nanoparticles in human lung cells: the role of cellular uptake, agglomeration and Ag release. Part. Fibre Toxicol. 11, 11. doi:10.1186/1743-8977-11-11

Glinski, A., Liebel, S., Pelletier, È., Voigt, C.L., Randi, M.A.F., Campos, S.X., Oliveira Ribeiro, C.A., Filipak Neto, F., 2016. Toxicological interactions of silver nanoparticles and organochlorine pesticides in mouse peritoneal macrophages. Toxicol. Mech. Methods 26, 251–259. doi:10.3109/15376516.2016.1159770

Goldoni, M., Johansson, C., 2007. A mathematical approach to study combined effects of toxicants in vitro: Evaluation of the Bliss independence criterion and the Loewe additivity model. Toxicol. Vitr. 21, 759–769. doi:10.1016/j.tiv.2007.03.003

Govindasamy, R., Rahuman, A.A., 2012. Histopathological studies and oxidative stress of synthesized silver nanoparticles in Mozambique tilapia (Oreochromis mossambicus). J. Environ. Sci. 24, 1091–1098. doi:10.1016/S1001-0742(11)60845-0

Guo, M., Xu, X., Yan, X., Wang, S., Gao, S., Zhu, S., 2013. In vivo biodistribution and synergistic toxicity of silica nanoparticles and cadmium chloride in mice. J. Hazard. Mater. 260, 780–788. doi:10.1016/j.jhazmat.2013.06.040

Han, X., Gelein, R., Corson, N., Wade-Mercer, P., Jiang, J., Biswas, P., Finkelstein, J.N., Elder, A., Oberdörster, G., 2011. Validation of an LDH assay for assessing nanoparticle toxicity. Toxicology 287, 99–104. doi:10.1016/j.tox.2011.06.011

Holmström, K.M., Finkel, T., 2014. Cellular mechanisms and physiological consequences of redox-dependent signalling. Nat. Rev. Mol. Cell Biol. 15, 411–21.

doi:10.1038/nrm3801

Houten, S.M., Wanders, R.J.A., 2010. A general introduction to the biochemistry of mitochondrial fatty acid β -oxidation 469–477. doi:10.1007/s10545-010-9061-2

Itoh, K., Wakabayashi, N., Katoh, Y., Ishii, T., O'Connor, T., Yamamoto, M., 2003. Keap1 regulates both cytoplasmic-nuclear shuttling and degradation of Nrf2 in response to electrophiles. Genes to Cells 8, 379–391. doi:10.1046/j.1365-2443.2003.00640.x

Iyer, V. V., Yang, H., Ierapetritou, M.G., Roth, C.M., 2010. Effects of glucose and insulin on HepG2-C3A cell metabolism. Biotechnol. Bioeng. 107, 347–356. doi:10.1002/bit.22799

Kamalian, L., Chadwick, A.E., Bayliss, M., French, N.S., Monshouwer, M., Snoeys, J., Park, B.K., 2015. The utility of HepG2 cells to identify direct mitochondrial dysfunction in the absence of cell death. Toxicol. Vitr. 29, 732–740. doi:10.1016/j.tiv.2015.02.011

Knasmüller, S., Mersch-Sundermann, V., Kevekordes, S., Darroudi, F., Huber, W.W., Hoelzl, C., Bichler, J., Majer, B.J., 2004. Use of human-derived liver cell lines for the detection of environmental and dietary genotoxicants; Current state of knowledge. Toxicology 198, 315–328. doi:10.1016/j.tox.2004.02.008

Lee, S., Hur, E. gene, Ryoo, I. geun, Jung, K.A., Kwak, J., Kwak, M.K., 2012. Involvement of the Nrf2-proteasome pathway in the endoplasmic reticulum stress response in pancreatic ??-cells. Toxicol. Appl. Pharmacol. doi:10.1016/j.taap.2012.08.021

Liberti, M. V., Locasale, J.W., 2016. The Warburg Effect: How Does it Benefit Cancer Cells? Trends Biochem. Sci. 41, 211–218. doi:10.1016/j.tibs.2015.12.001

Maurer-Jones, M. a., Gunsolus, I.L., Murphy, C.J., Haynes, C.L., 2013. Toxicity of engineered nanoparticles in the environment. Anal. Chem. 85, 3036–3049. doi:10.1021/ac303636s

Miranda, R.R., Bezerra, A.G., Ribeiro, C.A.O., Randi, M.A.F., Voigt, C.L., Skytte, L., Rasmussen, K.L., Kjeldsen, F., Neto, F.F., 2017. Toxicological interactions of silver nanoparticles and non-essential metals in human hepatocarcinoma cell line. Toxicol. Vitr. doi:10.1016/j.tiv.2017.01.003

Moreau, A., Vilarem, M.J., Maurel, P., Pascussi, J.M., 2008. Xenoreceptors CAR and PXR activation and consequences on lipid metabolism, glucose homeostasis, and inflammatory response. Mol. Pharm. doi:10.1021/mp700103m

Mukherjee, R., Jow, L., Croston, G.E., Paterniti, J.R., 1997. Identification, characterization, and tissue distribution of human peroxisome proliferator-activated receptor (PPAR) isoforms PPARgamma2 versus PPARgamma1 and activation with retinoid X receptor agonists and antagonists. J. Biol. Chem. 272, 8071–6. doi:10.1074/jbc.272.12.8071

Navarro, E., Piccapietra, F., Wagner, B., Marconi, F., Kaegi, R., Odzak, N., Sigg, L., Behra, R., 2008. Toxicity of silver nanoparticles to Chlamydomonas reinhardtii. Environ. Sci. Technol. 42, 8959–64.

Pineda Torra, I., Claudel, T., Duval, C., Kosykh, V., Fruchart, J.-C., Staels, B., 2003. Bile Acids Induce the Expression of the Human Peroxisome Proliferator-Activated Receptor α Gene via Activation of the Farnesoid X Receptor. Mol. Endocrinol. 17, 259–272. doi:10.1210/me.2002-0120

Rinaldi, C., Schmidt, T., Situ, A.J., Johnson, J.O., Lee, P.R., Chen, K.-L., Bott, L.C., Fadó, R., Harmison, G.H., Parodi, S., Grunseich, C., Renvoisé, B., Biesecker, L.G., De Michele, G., Santorelli, F.M., Filla, A., Stevanin, G., Dürr, A., Brice, A., Casals, N., Traynor, B.J., Blackstone, C., Ulmer, T.S., Fischbeck, K.H., 2015. Mutation in CPT1C Associated With Pure Autosomal Dominant Spastic Paraplegia. JAMA Neurol. 72, 561–70. doi:10.1001/jamaneurol.2014.4769

Riss, T.L., Moravec, R.A., 2004. Use of Multiple Assay Endpoints to Investigate the Effects of Incubation Time, Dose of Toxin, and Plating Density in Cell-Based Cytotoxicity Assays. Assay Drug Dev. Technol. 2, 51–62. doi:10.1089/154065804322966315

Rodríguez-Enríquez, S., Juárez, O., Rodríguez-Zavala, J.S., Moreno-Sánchez, R., 2001. Multisite control of the Crabtree effect in ascites hepatoma cells. Eur. J. Biochem. 268, 2512–2519. doi:10.1046/j.1432-1327.2001.02140.x

Schwämmle, V., León, I.R., Jensen, O.N., 2013. Assessment and improvement of statistical tools for comparative proteomics analysis of sparse data sets with few experimental replicates. J. Proteome Res. 12, 3874–3883. doi:10.1021/pr400045u

Urani, C., 2005. Cytotoxicity and induction of protective mechanisms in HepG2 cells exposed to cadmium 19, 887–892. doi:10.1016/j.tiv.2005.06.011

Vance, M.E., Kuiken, T., Vejerano, E.P., McGinnis, S.P., Hochella, M.F., Hull, D.R., 2015. Nanotechnology in the real world: Redeveloping the nanomaterial consumer products inventory. Beilstein J. Nanotechnol. 6, 1769–1780. doi:10.3762/bjnano.6.181

Vriend, J., Reiter, R.J., 2015. The Keap1-Nrf2-antioxidant response element pathway: A review of its regulation by melatonin and the proteasome. Mol. Cell. Endocrinol. doi:10.1016/j.mce.2014.12.013

Wildt, B.E., Celedon, A., Maurer, E.I., Casey, B.J., Nagy, A.M., Hussain, S.M., Goering, P.L., 2015. Intracellular accumulation and dissolution of silver nanoparticles in L-929 fibroblast cells using live cell time-lapse microscopy. Nanotoxicology 5390, 1–10. doi:10.3109/17435390.2015.1113321

Zhang, C., Hu, Z., Deng, B., 2016. Silver nanoparticles in aquatic environments: Physiochemical behavior and antimicrobial mechanisms. Water Res. 88, 403–427. doi:10.1016/j.watres.2015.10.0

4. DISCUSSÃO GERAL

Os resultados apresentados nesta tese fornecem as primeiras informações a respeito dos efeitos biológicos da coexposição entre AgNP e os metais tóxicos Cd e Hg em células HepG2.

No primeiro capítulo, observou-se que, de modo geral, apenas as associações entre as maiores concentrações de AgNP (AgNP II) e metais (Cd II e Hg II) induziram respostas que não poderiam ser previstas a partir das exposições individuais. Isto é, o somatório do efeito induzido pela mistura foi maior do que o induzido pelas exposições às AgNP ou metais isoladamente, sendo que a associação entre AgNP II com Cd II induziu mais efeitos deletérios do que a coexposição da AgNP com Hg II. Apesar disso, a concentração intracelular de Hg II, e não de Cd II, aumentou cerca de 2,8 vezes quando os as células foram coexpostas aos metais e NP.

As coexposições à AgNP e Cd, em especial à AgNP II + Cd II, levaram a redução da viabilidade celular (avaliada através do ensaio do vermelho neutro) de maneira tempo-dependente. No entanto, a situação inversa foi observada para AgNP II + Hg II: apesar desta mistura ter inicialmente reduzido a viabilidade de HepG2 (4 h de exposição), ela foi parcialmente recuperada após 24 h de exposição. A ativação de mecanismos de defesa ocorre de maneira tempo-dependente, sendo assim, é possível que um estresse inicial induzido por AgNP II + Hg II tenha sido contrabalançado. No entanto, se os mecanismos de defesa não forem capazes de reestabelecer a homeostase celular, a toxicidade aumenta, como observado nas células expostas à AgNP II + Cd II.

Tanto AgNP quanto os metais Cd e Hg são capazes de induzir a redução da atividade da succinato desidrogenase *in vitro* (YANO E MARCONDES, 2005; CHAIRUANGKITTI et al., 2013; AUEVIRIYAVIT et al., 2014), resultando na redução dos níveis intracelulares de ATP. O ensaio do MTT indicou que a redução do metabolismo mitocondrial após a exposição às AgNP ocorre de forma mais precoce (após 4 h) do que para os metais. Com relação às coexposições, a associação de AgNP II + Hg II resultou em uma redução maior do que a esperada, enquanto AgNP II + Cd II induziu um efeito similar ao somatório dos efeitos induzidos pelos contaminantes individuais.

A coexposição às maiores concentrações dos contaminantes resultou na alteração do mecanismo de morte celular: de apoptose para necrose. Enquanto células expostas aos contaminantes individuais iniciaram o processo apoptótico pela marcação positiva para fosfatidilserina (com anexina V-FITC), as células coexpostas parecem ter iniciado o programa apoptótico (*e.g.*, condensação da cromatina), no entanto, a membrana plasmática tornou-se permeável ao iodeto de propídio antes que a fosfatidilserina fosse marcada, caracterizando o processo necrótico. A apoptose é um evento que requer energia fornecida pela hidrólise de ATP e células coexpostas à AgNP II + Cd II apresentaram uma grande desbalanço (aumento) na relação ADP/ATP, como observado no capítulo 2. Desta forma, é possível que este estresse energético tenha levado ao processo necrótico, já que este é um evento passivo e independente de ATP. O decréscimo do *status* energético da célula também pode ser a causa da redução acentuada do número de células (ensaio de proliferação celular) após as coexposições.

O estresse oxidativo é um dos principais efeitos *in vitro* de AgNP, Cd e Hg (NZENGUE et al., 2008; LIU et al*.,* 2010; AGUADO et al., 2013). A elevação nos níveis citosólicos de EROs foi uma resposta inicial (já observada no ensaio de 2 h) após as coexposições às AgNP com ambos os metais, enquanto estes níveis mantiveram-se basais após exposição aos contaminantes individuais. Após exposições prolongadas (4 e 24 h), contaminantes individuais foram capazes de aumentar os níveis de EROs em HepG2, ao passo que células coexpostas apresentaram redução destes níveis ao longo do tempo. Após 24 h, somente grupos coexpostos às AgNP II + Cd II e AgNP I/II + Hg II mantiveram altos níveis de EROs. É possível que nestes grupos, o sistema de defesa antioxidante não tenha sido suficiente para reestabelecer a homeostase e, possivelmente, evitar a morte celular ao longo das 24 h de exposição.

Uma fonte importante de EROs podem ter sido as mitocôndrias, principalmente em células expostas às AgNP e Cd, bem como AgNP II + Cd II, já que ânion superóxido é convertido em peróxido de hidrogênio pela superóxido dismutase, e esta ERO pode difundir-se livremente para o citoplasma (FLEURY et al*.,* 2002). Além disso, o aumento desses níveis pode levar ao mal funcionamento mitocondrial e depleção de ATP.

Outro biomarcador analisado após as exposições foi a atividade dos transportadores de resistência a multixenobióticos, importantes no processo de destoxificação. Alguns trabalhos já demonstraram que nanopartículas, Cd e Hg podem interferir com o funcionamento e expressão destes transportadores (SALOMON E EHRHARDT, 2011; DELLA TORRE et al., 2012; CHEN et al., 2016). O acúmulo de rodamina B foi observado, especialmente após a coexposição às AgNP II + Cd II, o que pode ter resultado na presença prolongada dos contaminantes na célula e levado a uma maior sensibilidade.

Diferente do esperado, a concentração de Hg aumentou 2,8 vezes na presença de AgNP em relação ao observado em células expostas somente ao Hg, enquanto que a concentração intracelular de Cd se manteve a mesma tanto na presença ou ausência de AgNP. Metais, como Cd e Pb, podem adsorver à superfície de nanopartículas, devido a diferença entre cargas (ALQUDAMI et al., 2012). Como as nanopartículas utilizadas neste trabalho apresentam carga negativa e Cd e Hg, carga positiva, é possível que Hg tenha adsorvido à superfície de AgNP. Esse resultado explica, ao menos em parte, o aumento da toxicidade induzida por AgNP II + Hg II. No entanto, a mesma lógica não é válida para AgNP II + Cd II. É possível que esses contaminantes atuem em vias convergentes, ou ainda, que as células não sejam capazes de reestabelecer a homeostase em níveis muito altos de estresse.

Com base nos resultados obtidos no capítulo I, o segundo capítulo desta tese foi conduzido com a finalidade de investigar os mecanismos moleculares envolvidos na toxicidade de AgNP II + Cd II em HepG2. Para isso, foram realizadas análises de proteômica baseada em espectrometria de massas.

Como AgNP diferentes foram utilizadas, inicialmente foram realizadas análises bioquímicas para avaliar se as alterações na viabilidade celular eram similares entre AgNP de 2 nm + Cd (diâmetro utilizado no capítulo I) e AgNP de 10 nm + Cd (diâmetro utilizado no capítulo II). Após 4 h, os efeitos induzidos em após exposição às AgNP de 10 nm, isoladas ou combinadas com Cd, foram mais brandos do que o observado no capítulo I para AgNP de 2 nm. No entanto, os efeitos induzidos após 24 h de exposição pelos dois tamanhos de NP, tanto isoladamente como em combinação com Cd, foram bastante similares. Desta forma, os resultados obtidos no primeiro capítulo podem, com o devido cuidado, ser relacionados com os dados do capítulo II da tese.

A partir da análise proteômica, um total de 4522 proteínas foram identificadas e quantificadas de acordo com a máxima parcimônia. Células expostas aos contaminantes durante 24 h apresentaram uma maior alteração no perfil de proteínas em comparação às células expostas por apenas 4 h. Em particular, células coexpostas às AgNP+Cd apresentaram 43% do proteoma total regulado, o que não pode ser previsto a partir dos resultados observados após as exposições isoladas aos contaminantes (aproximadamente 6,5% e 2% do proteoma total foi alterado após 24 h exposição às AgNP e ao Cd, respectivamente).

Um dos efeitos toxicológicos mais característicos de AgNP e Cd *in vitro* é o aumento nos níveis de EROs (NEMMICHE et al., 2011; LEE et al., 2014; MIETHLING-GRAFF et al., 2014; LI *et* al., 2016). Como discutido anteriormente, a coexposição a esses contaminantes induziu um aumento precoce nos níveis de EROs em HepG2, o qual foi mantido ao longo das 24 h de exposição. Isto pode estar relacionado à inativação do fator de transcrição Nrf-2, resultando na depleção de enzimas e proteínas relacionadas à defesa antioxidante e, consequentemente, alteração do potencial redox intracelular.

A inativação de Nrf-2 também pode estar relacionada com outras respostas após 24 h de coexposição às AgNP+Cd, como a redução dos níveis de subunidades dos proteossomos. A redução da expressão ou da atividade do proteossomo pode levar não apenas ao acúmulo de proteínas danificadas, bem como alteração em diversos processos celulares, como proliferação, resposta ao estresse químico, transcrição gênica, inflamação etc., uma vez que esse sistema regula, de forma sincronizada e ordenada, a degradação de diversas proteínas (FALASCHETTI et al., 2013; GLICKMAN et al., 2002). Ainda, a redução nos níveis de proteínas envolvidas com ubiquitilação (ubiquitinas-conjugases, ubiquitinas-hidrolases, ubiquitinas-peptidases), tiorredoxinas, chaperonas e proteínas *heat-shock* podem ter contribuído para esse cenário, uma vez que proteínas danificadas ou mal dobradas não seriam eficientemente reparadas ou marcadas para degradação, ou ainda degradadas nos proteossomos.

Os níveis de proteínas envolvidas com a tradução, em especial subunidades ribossomais, foram significativamente reduzidos após 24 h de exposição às AgNP e Cd, levando a alteração significativa da via eIF2. Essa resposta sugere que células

expostas aos contaminantes individuais atenuaram a tradução de mRNA, em resposta à uma situação inicial de estresse, permitindo que as células poupem recursos energéticos enquanto um novo programa de expressão gênica é adotado (BAIRD E WEK 2012; DONNELLY et al., 2013). Apesar desta via também ter sido significativamente alterada após 24 h da co-exposição a AgNP+Cd, observou-se tanto aumento quanto redução nos níveis de um grande número de fatores de iniciação de transcrição e subunidades ribossomais. Essa situação pode ter facilitado a ativação da tradução de mRNA para proteínas-chave na resposta ao estresse celular, uma vez que proteínas envolvidas com o reestabelecimento do *status* energético da célula (*e.g.*, fosforilação oxidativa, proteínas mitocondriais e proteínas envolvidas com metabolismo de lipídios) tiveram sua abundância aumentada em relação ao controle. Por outro lado, é possível que o funcionamento inadequado dessa via tenha levado à redução nos níveis de fatores-chave para defesa contra o estresse químico, como a expressão de proteínas de defesa antioxidante, por exemplo.

A adaptação celular após a exposição às AgNP+Cd após 24 h parece estar envolvida com uma reprogramação ou adaptação metabólica. Em células tumorais, mesmo na presença de oxigênio e mitocôndrias funcionais, a glicólise é principal via de síntese de ATP (RODRÍGUEZ-ENRÍQUEZ et al., 2001; LIBERTI E LOCASALE, 2016). Talvez a redução nos níveis de proteínas envolvidas na glicólise, observada após 24 h de exposição às AgNP e AgNP+Cd, tenha gerado um desbalanço (aumento) inicial na relação ADP/ATP e as células tenham respondido com a aumento nos níveis de proteínas envolvidas na fosforilação oxidativa. Esse mecanismo de adaptação parece ter sido eficiente para células expostas apenas às AgNP, uma vez que a relação ADP/ATP foi pouco alterada em relação ao controle se comparadas às células coexpostas às AgNP+Cd.

Após 24 h de coexposição às AgNP+Cd também houve aumento de proteínas envolvida no metabolismo de lipídios e ciclo do ácido cítrico. Além disso, análise de reguladores *upstream* indicou que proteínas-chave envolvidas na reprogramação metabólica e metabolismo de lipídios podem estar ativadas (como PPARGC1A e NR1H4: envolvidas na ativação do receptor nuclear PPARγ que desempenha papel central na adaptação metabólica em resposta a falta de nutrientes; e CPT1C: ativador da β-oxidação) ou inibidas (NR1I2: inibidor da β-oxidação). Esses dados reforçam a

hipótese de que em resposta ao desbalanço acentuado na relação ADP/ATP após a coexposição aos contaminantes por 24 h, as células iniciam um processo de reprogramação metabólica que consiste no aumento de proteínas envolvidas na fosforilação oxidativa e no metabolismo de lipídios.

De maneira resumida, os dados obtidos no segundo capítulo desta tese dão suporte aos observados no primeiro capítulo em relação à toxicidade induzida por AgNP+Cd em HepG2.

Considerações finais

- De maneira geral, interações toxicológicas foram observadas apenas após as coexposições às maiores concentrações dos contaminantes, resultando numa alteração substancial em parâmetros bioquímicos e no mecanismo de morte celular.
- Na presença das AgNP, a concentração intracelular de Hg, mas não a de Cd, aumentou nas associações entre AgNP e metais. Ainda assim, a coexposição às AgNP+Cd induziu efeitos mais tóxicos em células HepG2 do que AgNP+Hg.
- A coexposição às AgNP+Cd por 24 h induziu uma profunda desregulação do proteoma celular, indicando que a toxicidade desta mistura está relacionada com a depleção das defesas antioxidantes, depleção de proteínas proteassomais e chaperonas, depleção de proteínas relacionadas com metabolismo da glicose. No entanto, a ativação de proteínas-chave para reprogramação metabólica sugere uma tentativa para reestabelecer a homeostase.
- Embora o conhecimento a respeito de interações entre nanopartículas e contaminantes ambientais esteja avançando, muitos estudos ainda são necessários para a compreensão de como essa interação ocorre a nível químico e quais os efeitos destas interações em organismos, particularmente, ao longo prazo.

REFERÊNCIAS

Adebambo, O.A., Ray, P.D., Shea, D., Fry, R.C., 2015. Toxicological responses of environmental mixtures: Environmental metal mixtures display synergistic induction of metal-responsive and oxidative stress genes in placental cells. Toxicol. Appl. Pharmacol. 289, 534–541. doi:10.1016/j.taap.2015.10.005

Aden, D.P., Vogel, A., Plotkin, S., Damjanov, I., Knowles, B.B., 1979. Controlled synthesis of HBS Ag in a differentiated human liver carcinoma-derived cell line. Nature 282, 615–616.Aebersold, R., Mann, M., 2003. Mass spectrometry-based proteomics 422.

Aguado, A., Galán, M., Zhenyukh, O., Wiggers, G.A., Roque, F.R., Redondo, S., Peçanha, F., Martín, A., Fortuño, A., Cachofeiro, V., Tejerina, T., Salaices, M., Briones, A.M., 2013. Mercury induces proliferation and reduces cell size in vascular smooth muscle cells through MAPK , oxidative stress and cyclooxygenase-2 pathways. Toxicol. Appl. Pharmacol. 268, 188–200. doi:10.1016/j.taap.2013.01.030

Ahamed, M., Ali, D., Alhadlaq, H. a., Akhtar, M.J., 2013. Nickel oxide nanoparticles exert cytotoxicity via oxidative stress and induce apoptotic response in human liver cells (HepG2). Chemosphere 93, 2514–2522. doi:10.1016/j.chemosphere.2013.09.047

Alqudami, A., Alhemiary, N. a., Munassar, S., 2012. Removal of Pb(II) and Cd(II) ions from water by Fe and Ag nanoparticles prepared using electro-exploding wire technique. Environ. Sci. Pollut. Res. 19, 2832–2841. doi:10.1007/s11356-012-0788-1

Arbuckle, T.E., Liang, C.L., Morisset, A.-S., Fisher, M., Weiler, H., Cirtiu, C.M., Legrand, M., Davis, K., Ettinger, A.S., Fraser, W.D., 2016. Maternal and fetal exposure to cadmium, lead, manganese and mercury: The MIREC study. Chemosphere 163, 270–282. doi:10.1016/j.chemosphere.2016.08.023

Asharani, P. V, Hande, M.P., Valiyaveettil, S., 2009. Anti-proliferative activity of silver nanoparticles. BMC Cell Biol. 10, 65. doi:10.1186/1471-2121-10-65

Asharani, P. V, Wu, Y.L., Gong, Z., Valiyaveettil, S., 2008. Toxicity of silver nanoparticles in zebrafish models 255102. doi:10.1088/0957-4484/19/25/255102

Aueviriyavit, S., Phummiratch, D., Maniratanachote, R., 2014. Mechanistic study on the biological effects of silver and gold nanoparticles in Caco-2 cells--induction of the Nrf2/HO-1 pathway by high concentrations of silver nanoparticles. Toxicol. Lett. 224, 73–83. doi:10.1016/j.toxlet.2013.09.020

Baird, T., Wek, R., 2012. Eukaryotic initiation factor 2 phosphorylation and translational control in metabolism. Adv. Nutr. 3, 307–321. doi:10.3945/an.112.002113.We

Benov, L., Sztejnberg, L., Fridovich, I., Enov, L.U.B., Ztejnberg, L.A.S., 1998. Critical evaluation of the use of hydroethidine as a measure of superoxide anion radical. Free Radic. Biol. Med. 25, 826–31. doi:10.1016/S0891-5849(98)00163-4

Birben, E., Murat, U., Md, S., Sackesen, C., Erzurum, S., Kalayci, O., 2012. Oxidative Stress and Antioxidant Defense. WAO J. 5, 9–19. doi:10.1097/WOX.0b013e3182439613

Blaauboer, B.J., Boekelheide, K., Clewell, H.J., Daneshian, M., Dingemans, M.M.L., Goldberg, A.M., Heneweer, M., Jaworska, J., Kramer, N.I., Leist, M., Seibert, H., Testai, E., Vandebriel, R.J., Yager, J.D., Zurlo, J., 2012. The use of biomarkers of toxicity for integrating in vitro hazard estimates into risk assessment for humans. ALTEX 29, 411–425. doi:10.14573/altex.2012.4.411

Broadhead, C.L., Combes, R.D., 2001. The current status for food additives toxicity testing and the potential for application of the Three Rs. ATLA 29, 471–485.

Bystrzejewska-Piotrowska, G., Golimowski, J., Urban, P.L., 2009. Nanoparticles: their potential toxicity, waste and environmental management. Waste Manag. 29, 2587–95. doi:10.1016/j.wasman.2009.04.001

C, P., Karlsson, H.L., Hedberg, J., Lowe, T.A., Winnberg, L., Elihn, K., Wallinder, I.O., Möller, L., 2013. Intracellular uptake and toxicity of Ag and CuO nanoparticles: A comparison between nanoparticles and their corresponding metal ions. Small 9, 970–982. doi:10.1002/smll.201201069

Canesi, L., Ciacci, C., Balbi, T., 2015. Interactive effects of nanoparticles with other contaminants in aquatic organisms: Friend or foe? Mar. Environ. Res. 111, 128–134. doi:10.1016/j.marenvres.2015.03.010

Capaldo, A., Gay, F., Scudiero, R., Trinchella, F., Caputo, I., Lepretti, M., Marabotti, A., Esposito, C., Laforgia, V., 2016. Histological changes, apoptosis and metallothionein levels in Triturus carnifex (Amphibia, Urodela) exposed to environmental cadmium concentrations. Aquat. Toxicol. doi:10.1016/j.aquatox.2016.01.009

Carlson, C., Hussain, S.M., Schrand, a M., Braydich-Stolle, L.K., Hess, K.L., Jones, R.L., Schlager, J.J., 2008. Unique cellular interaction of silver nanoparticles: size-dependent generation of reactive oxygen species. J. Phys. Chem. B 112, 13608–19. doi:10.1021/jp712087m

Carracedo, A., Cantley, L.C., Pandolfi, P.P., 2013. Cancer metabolism: fatty acid oxidation in the limelight. Nat Rev Cancer 13, 227–32. doi:10.1038/nrc3483

Chahrour, O., Cobice, D., Malone, J., 2015. Stable isotope labelling methods in mass spectrometry-based quantitative proteomics. J. Pharm. Biomed. Anal. 113, 2–20. doi:10.1016/j.jpba.2015.04.013

Chairuangkitti, P., Lawanprasert, S., Roytrakul, S., Aueviriyavit, S., Phummiratch, D., Kulthong, K., Chanvorachote, P., Maniratanachote, R., 2013. Silver nanoparticles induce toxicity in A549 cells via ROS-dependent and ROS-independent pathways. Toxicol. In Vitro 27, 330–8. doi:10.1016/j.tiv.2012.08.021

Chapple, S.J., Siow, R.C.M., Mann, G.E., 2012. Crosstalk between Nrf2 and the proteasome: Therapeutic potential of Nrf2 inducers in vascular disease and aging. Int. J. Biochem. Cell Biol. doi:10.1016/j.biocel.2012.04.021

Chen, M., Yin, H., Bai, P., Miao, P., Deng, X., Xu, Y., Hu, J., Yin, J., 2016. ABC transporters affect the elimination and toxicity of CdTe quantum dots in liver and kidney cells. Toxicol. Appl. Pharmacol. 303, 11–20. doi:10.1016/j.taap.2016.04.017

Chen, Y.Y., Zhu, J.Y., Chan, K.M., 2014. Effects of cadmium on cell proliferation , apoptosis , and proto-oncogene expression in zebrafish liver cells. Aquat. Toxicol. 157, 196–206. doi:10.1016/j.aquatox.2014.10.018

Christensen, F.M., Johnston, H.J., Stone, V., Aitken, R.J., Hankin, S., Peters, S., Aschberger, K., 2010. Nano-silver - feasibility and challenges for human health risk assessment based on open literature. Nanotoxicology 4, 284–295. doi:10.3109/17435391003690549

Cleveland, D., Long, S.E., Pennington, P.L., Cooper, E., Fulton, M.H., Scott, G.I., Brewer, T., Davis, J., Petersen, E.J., Wood, L., 2012a. Pilot estuarine mesocosm study on the environmental fate of Silver nanomaterials leached from consumer products. Sci. Total Environ. 421–422, 267–272. doi:10.1016/j.scitotenv.2012.01.025

Cleveland, D., Long, S.E., Pennington, P.L., Cooper, E., Fulton, M.H., Scott, G.I., Brewer, T., Davis, J., Petersen, E.J., Wood, L., 2012b. Pilot estuarine mesocosm study on the environmental fate of Silver nanomaterials leached from consumer products. Sci. Total Environ. 421–422, 267–272. doi:10.1016/j.scitotenv.2012.01.025

Contreras, J.E., Rodriguez, E.A., Taha-Tijerina, J., 2016. Nanotechnology applications for electrical transformers—A review. Electr. Power Syst. Res. 143, 573–584. doi:10.1016/j.epsr.2016.10.058

Cuypers, A., Plusquin, M., Remans, T., Jozefczak, M., Keunen, E., Gielen, H., Opdenakker, K., Nair, A.R., Munters, E., Artois, T.J., Nawrot, T., Vangronsveld, J., Smeets, K., 2010. Cadmium stress: An oxidative challenge. BioMetals 23, 927–940. doi:10.1007/s10534-010-9329-x

de Vries, H.E., Witte, M., Hondius, D., Rozemuller, a. J.M., Drukarch, B., Hoozemans, J., van Horssen, J., 2008. Nrf2-induced antioxidant protection: A promising target to counteract ROS-mediated damage in neurodegenerative disease? Free Radic. Biol. Med. 45, 1375–1383. doi:10.1016/j.freeradbiomed.2008.09.001

Della Torre, C., Balbi, T., Grassi, G., Frenzilli, G., Bernardeschi, M., Smerilli, A., Guidi, P., Canesi, L., Nigro, M., Monaci, F., Scarcelli, V., Rocco, L., Focardi, S., Monopoli, M., Corsi, I., 2015. Titanium dioxide nanoparticles modulate the toxicological response to cadmium in the gills of Mytilus galloprovincialis. J. Hazard. Mater. 297, 92–100. doi:10.1016/j.jhazmat.2015.04.072

Della Torre, C., Zaja, R., Loncar, J., Smital, T., Focardi, S., Corsi, I., 2012. Interaction of ABC transport proteins with toxic metals at the level of gene and transport activity in the PLHC-1 fish cell line. Chem. Biol. Interact. 198, 9–17. doi:10.1016/j.cbi.2012.04.008

Deville, S., Baré, B., Piella, J., Tirez, K., Hoet, P., Monopoli, M.P., Dawson, K.A., Puntes, V.F., Nelissen, I., 2016. Interaction of gold nanoparticles and nickel(II) sulfate affects dendritic cell maturation. Nanotoxicology 10, 1395–1403. doi:10.1080/17435390.2016.1221476

Donaldson, K., 2004. Nanotoxicology. Occup. Environ. Med. 61, 727–728. doi:10.1136/oem.2004.013243

Donnelly, N., Gorman, A.M., Gupta, S., Samali, A., 2013. The eIF2?? kinases: Their

structures and functions. Cell. Mol. Life Sci. 70, 3493–3511. doi:10.1007/s00018-012-1252-6

Eisenbrand, G., Pool-zobel, B., Baker, V., Balls, M., Blaauboer, B.J., Boobis, A., Carere, A., Kevekordes, S., Lhuguenot, J., Pieters, R., Kleiner, J., 2002. Methods of in vitro toxicology 40, 193–236.

Elsaesser, A., Howard, C.V., 2012a. Toxicology of nanoparticles. Adv. Drug Deliv. Rev. 64, 129–37. doi:10.1016/j.addr.2011.09.001

Elsaesser, A., Howard, C.V., 2012b. Toxicology of nanoparticles ☆. Adv. Drug Deliv. Rev. 64, 129–137. doi:10.1016/j.addr.2011.09.001

Eng, J.K., Searle, B.C., Clauser, K.R., Tabb, D.L., 2011. A face in the crowd: recognizing peptides through database search. Mol. Cell. Proteomics 10, R111.009522. doi:10.1074/mcp.R111.009522

Fabrega, J., Luoma, S.N., Tyler, C.R., Galloway, T.S., Lead, J.R., 2011. Silver nanoparticles: behaviour and effects in the aquatic environment. Environ. Int. 37, 517–31. doi:10.1016/j.envint.2010.10.012

Farré, M., Gajda-Schrantz, K., Kantiani, L., Barceló, D., 2009. Ecotoxicity and analysis of nanomaterials in the aquatic environment. Anal. Bioanal. Chem. 393, 81–95. doi:10.1007/s00216-008-2458-1

Feliu, N., Fadeel, B., 2010. Nanotoxicology: no small matter. Nanoscale 2, 2514–20. doi:10.1039/c0nr00535e

Ferreira, J.L.R., Lonn??, M.N., Fran??a, T. a., Maximilla, N.R., Lugokenski, T.H., Costa, P.G., Fillmann, G., Antunes Soares, F. a., de la Torre, F.R., Monserrat, J.M., 2014. Co-exposure of the organic nanomaterial fullerene C60 with benzo[a]pyrene in Danio rerio (zebrafish) hepatocytes: Evidence of toxicological interactions. Aquat. Toxicol. 147, 76–83. doi:10.1016/j.aquatox.2013.12.007

Filipič, M., 2012. Mechanisms of cadmium induced genomic instability. Mutat. Res. 733, 69–77. doi:10.1016/j.mrfmmm.2011.09.002

Fleury, C., Mignotte, B., Vayssière, J.-L., 2002. Mitochondrial reactive oxygen species in cell death signaling. Biochimie 84, 131–141. doi:10.1016/S0300-9084(02)01369-X

Foldbjerg, R., Irving, E.S., Hayashi, Y., Sutherland, D.S., Thorsen, K., Autrup, H., Beer, C., 2012. Global gene expression profiling of human lung epithelial cells after exposure to nanosilver. Toxicol. Sci. 130, 145–157. doi:10.1093/toxsci/kfs225

Fotakis, G., Timbrell, J. a, 2006. Role of trace elements in cadmium chloride uptake in hepatoma cell lines. Toxicol. Lett. 164, 97–103. doi:10.1016/j.toxlet.2005.11.016

Fowler, B. a, 2009. Monitoring of human populations for early markers of cadmium toxicity: a review. Toxicol. Appl. Pharmacol. 238, 294–300. doi:10.1016/j.taap.2009.05.004

Franceschini, A., Szklarczyk, D., Frankild, S., Kuhn, M., Simonovic, M., Roth, A., Lin, J., Minguez, P., Bork, P., Von Mering, C., Jensen, L.J., 2013. STRING v9.1: Protein-protein interaction networks, with increased coverage and integration. Nucleic Acids

Res. 41, 808–815. doi:10.1093/nar/gks1094

Furman, O., Usenko, S., Lau, B.L.T., 2013. Relative iFurman, O., Usenko, S., & Lau, B. L. T. (2013). Relative importance of the humic and fulvic fractions of natural organic matter in the aggregation and deposition of silver nanoparticles. Environ. Sci. Technol. 47, 1349–1356.

Gaillet, S., Rouanet, J.-M., 2015. Silver nanoparticles: their potential toxic effects after oral exposure and underlying mechanisms--a review. Food Chem. Toxicol. 77, 58–63. doi:10.1016/j.fct.2014.12.019

Gioria, S., Vicente, J.L., Barboro, P., Spina, R. La, Tomasi, G., Urbán, P., Kinsner-Ovaskainen, A., François, R., Chassaigne, H., 2016. A combined proteomics and metabolomics approach to assess the effects of gold nanoparticles in vitro. Nanotoxicology 10, 1743–5390. doi:10.3109/17435390.2015.1121412

Glickman, M.H., Ciechanover, A., 2002. The Ubiquitin-Proteasome Proteolytic Pathway: Destruction for the Sake of Construction. Physiol. Rev. 82, 373–428. doi:10.1152/physrev.00027.2001

Gliga, A.R., Skoglund, S., Wallinder, I.O., Fadeel, B., Karlsson, H.L., 2014. Size-dependent cytotoxicity of silver nanoparticles in human lung cells: the role of cellular uptake, agglomeration and Ag release. Part. Fibre Toxicol. 11, 11. doi:10.1186/1743-8977-11-11

Glinski, A., Liebel, S., Pelletier, È., Voigt, C.L., Randi, M.A.F., Campos, S.X., Oliveira Ribeiro, C.A., Filipak Neto, F., 2016. Toxicological interactions of silver nanoparticles and organochlorine pesticides in mouse peritoneal macrophages. Toxicol. Mech. Methods 26, 251–259. doi:10.3109/15376516.2016.1159770

Goldoni, M., Johansson, C., 2007. A mathematical approach to study combined effects of toxicants in vitro: Evaluation of the Bliss independence criterion and the Loewe additivity model. Toxicol. Vitr. 21, 759–769. doi:10.1016/j.tiv.2007.03.003

Govindasamy, R., Rahuman, A.A., 2012. Histopathological studies and oxidative stress of synthesized silver nanoparticles in Mozambique tilapia (Oreochromis mossambicus). J. Environ. Sci. 24, 1091–1098. doi:10.1016/S1001-0742(11)60845-0

Grainger, D.W., Castner, D.G., 2008. Nanobiomaterials and nanoanalysis: Opportunities for improving the science to benefit biomedical technologies. Adv. Mater. 20, 867–877. doi:10.1002/adma.200701760

Grosse, S., Evje, L., Syversen, T., 2013. Silver nanoparticle-induced cytotoxicity in rat brain endothelial cell culture. Toxicol. In Vitro 27, 305–13. doi:10.1016/j.tiv.2012.08.024

Guo, M., Xu, X., Yan, X., Wang, S., Gao, S., Zhu, S., 2013. In vivo biodistribution and synergistic toxicity of silica nanoparticles and cadmium chloride in mice. J. Hazard. Mater. 260, 780–788. doi:10.1016/j.jhazmat.2013.06.040

Han, X., Gelein, R., Corson, N., Wade-Mercer, P., Jiang, J., Biswas, P., Finkelstein, J.N., Elder, A., Oberdörster, G., 2011. Validation of an LDH assay for assessing nanoparticle toxicity. Toxicology 287, 99–104. doi:10.1016/j.tox.2011.06.011

Holmström, K.M., Finkel, T., 2014. Cellular mechanisms and physiological consequences of redox-dependent signalling. Nat. Rev. Mol. Cell Biol. 15, 411–21. doi:10.1038/nrm3801

Houten, S.M., Wanders, R.J.A., 2010. A general introduction to the biochemistry of mitochondrial fatty acid β -oxidation 469–477. doi:10.1007/s10545-010-9061-2

Hoyt, V.W., Mason, E., 2008. Nanotechnology. J. Chem. Heal. Saf. 15, 10–15. doi:10.1016/j.jchas.2007.07.015

Hsiao, I.L., Hsieh, Y.K., Wang, C.F., Chen, I.C., Huang, Y.J., 2015. Trojan-horse mechanism in the cellular uptake of silver nanoparticles verified by direct intra- and extracellular silver speciation analysis. Environ. Sci. Technol. 49, 3813–3821. doi:10.1021/es504705p

Hultin-Rosenberg, L., Forshed, J., Branca, R.M.M., Lehtiö, J., Johansson, H.J., 2013. Defining, comparing, and improving iTRAQ quantification in mass spectrometry proteomics data. Mol. Cell. Proteomics 12, 2021–31. doi:10.1074/mcp.M112.021592

Iliuk, A., Galan, J., Tao, W.A., 2009. Playing tag with quantitative proteomics. Anal. Bioanal. Chem. 393, 503–513. doi:10.1007/s00216-008-2386-0

Itoh, K., Wakabayashi, N., Katoh, Y., Ishii, T., O'Connor, T., Yamamoto, M., 2003. Keap1 regulates both cytoplasmic-nuclear shuttling and degradation of Nrf2 in response to electrophiles. Genes to Cells 8, 379–391. doi:10.1046/j.1365-2443.2003.00640.x

Iyer, V. V., Yang, H., Ierapetritou, M.G., Roth, C.M., 2010. Effects of glucose and insulin on HepG2-C3A cell metabolism. Biotechnol. Bioeng. 107, 347–356. doi:10.1002/bit.22799

Kamalian, L., Chadwick, A.E., Bayliss, M., French, N.S., Monshouwer, M., Snoeys, J., Park, B.K., 2015. The utility of HepG2 cells to identify direct mitochondrial dysfunction in the absence of cell death. Toxicol. Vitr. 29, 732–740. doi:10.1016/j.tiv.2015.02.011

Kang, J., 2012. Principles and Applications of LC-MS / MS for the Quantitative Bioanalysis of Analytes in Various Biological Samples. Tandem Mass Spectrom. - Appl. Princ. 794. doi:10.5772/1327

Karlsson, H.L., Gliga, A.R., Calléja, F.M.G.R., Gonçalves, C.S. a G., Wallinder, I.O., Vrieling, H., Fadeel, B., Hendriks, G., 2014. Mechanism-based genotoxicity screening of metal oxide nanoparticles using the ToxTracker panel of reporter cell lines. Part. Fibre Toxicol. 11, 41. doi:10.1186/s12989-014-0041-9

Kim, I., Lee, B.-T., Kim, H.-A., Kim, K.-W., Kim, S.D., Hwang, Y.-S., 2015. Citrate coated silver nanoparticles change heavy metal toxicities and bioaccumulation of Daphnia magna. Chemosphere. doi:10.1016/j.chemosphere.2015.06.046

Kim, S., Choi, J.E., Choi, J., Chung, K.-H., Park, K., Yi, J., Ryu, D.-Y., 2009. Oxidative stress-dependent toxicity of silver nanoparticles in human hepatoma cells. Toxicol. In Vitro 23, 1076–84. doi:10.1016/j.tiv.2009.06.001

Klaine, S.J., Alvarez, P.J.J., Batley, G.E., Fernandes, T.F., Handy, R.D., Lyon, D.Y.,

Mahendra, S., McLaughlin, M.J., Lead, J.R., 2008. Nanomaterials in the environment: behavior, fate, bioavailability, and effects. Environ. Toxicol. Chem.

Klein, I., Sarkadi, B., V??radi, A., 1999. An inventory of the human ABC proteins. Biochim. Biophys. Acta - Biomembr. 1461, 237–262. doi:10.1016/S0005-2736(99)00161-3

Knasmüller, S., Mersch-Sundermann, V., Kevekordes, S., Darroudi, F., Huber, W.W., Hoelzl, C., Bichler, J., Majer, B.J., 2004. Use of human-derived liver cell lines for the detection of environmental and dietary genotoxicants; Current state of knowledge. Toxicology 198, 315–328. doi:10.1016/j.tox.2004.02.008

Kumar, G., Degheidy, H., Casey, B.J., Goering, P.L., 2015. Flow cytometry evaluation of in vitro cellular necrosis and apoptosis induced by silver nanoparticles. Food Chem. Toxicol. 85, 45–51. doi:10.1016/j.fct.2015.06.012

Kumari, B., Singh, D.P., 2016. A review on multifaceted application of nanoparticles in the field of bioremediation of petroleum hydrocarbons. Ecol. Eng. 97, 98–105. doi:10.1016/j.ecoleng.2016.08.006

Lara, H.H., Garza-Treviño, E.N., Ixtepan-Turrent, L., Singh, D.K., 2011. Silver nanoparticles are broad-spectrum bactericidal and virucidal compounds. J. Nanobiotechnology 9, 1–8. doi:10.1186/1477-3155-9-30

Larance, M., Lamond, A.I., 2015. Multidimensional proteomics for cell biology. Nat. Rev. Mol. Cell Biol. 16, 269–280. doi:10.1038/nrm3970

Lee, S., Hur, E. gene, Ryoo, I. geun, Jung, K.A., Kwak, J., Kwak, M.K., 2012. Involvement of the Nrf2-proteasome pathway in the endoplasmic reticulum stress response in pancreatic ??-cells. Toxicol. Appl. Pharmacol. doi:10.1016/j.taap.2012.08.021

Lee, Y.-H., Cheng, F.-Y., Chiu, H.-W., Tsai, J.-C., Fang, C.-Y., Chen, C.-W., Wang, Y.-J., 2014. Cytotoxicity, oxidative stress, apoptosis and the autophagic effects of silver nanoparticles in mouse embryonic fibroblasts. Biomaterials 35, 4706–15. doi:10.1016/j.biomaterials.2014.02.021

Leslie, E.M., Deeley, R.G., Cole, S.P.C., 2005. Multidrug resistance proteins : role of P-glycoprotein , MRP1 , MRP2 , and BCRP (ABCG2) in tissue defense 204, 216–237. doi:10.1016/j.taap.2004.10.012

Li, J., Mao, H., Kawazoe, N., Chen, G., 2016. Insight into the interactions between nanoparticles and cells. Biomater. Sci. doi:10.1039/c6bm00714g

Liberti, M. V., Locasale, J.W., 2016. The Warburg Effect: How Does it Benefit Cancer Cells? Trends Biochem. Sci. 41, 211–218. doi:10.1016/j.tibs.2015.12.001

Liebel, S., 2015. UNIVERSIDADE FEDERAL DO PARANÁ Respostas de células de hepatocarcinoma humano (Hepg2) expostas à cilindrospermopsina Respostas de células de hepatocarcinoma humano (Hepg2) expostas à cilindrospermopsina.

Liebel, S., de Oliveira Ribeiro, C.A., de Magalhães, V.F., da Silva, R.D.C., Rossi, S.C., Randi, M.A.F., Filipak Neto, F., 2015. Low concentrations of cylindrospermopsin

induce increases of reactive oxygen species levels, metabolism and proliferation in human hepatoma cells (HepG2). Toxicol. Vitr. 29, 479–488. doi:10.1016/j.tiv.2014.12.022

Liu, W., Wu, Y., Wang, C., Li, H.C., Wang, T., Liao, C.Y., Cui, L., Zhou, Q.F., Yan, B., Jiang, G.B., 2010. Impact of silver nanoparticles on human cells: effect of particle size. Nanotoxicology 4, 319–30. doi:10.3109/17435390.2010.483745

Markus, a. a., Parsons, J.R., Roex, E.W.M., Kenter, G.C.M., Laane, R.W.P.M., 2013. Predicting the contribution of nanoparticles (Zn, Ti, Ag) to the annual metal load in the Dutch reaches of the Rhine and Meuse. Sci. Total Environ. 456–457, 154–160. doi:10.1016/j.scitotenv.2013.03.058

Massarsky, A., Trudeau, V.L., Moon, T.W., 2014. Predicting the environmental impact of nanosilver. Environ. Toxicol. Pharmacol. 38, 861–873. doi:10.1016/j.etap.2014.10.006

Maurer-Jones, M. a., Gunsolus, I.L., Murphy, C.J., Haynes, C.L., 2013. Toxicity of engineered nanoparticles in the environment. Anal. Chem. 85, 3036–3049. doi:10.1021/ac303636s

Maurer, M.M., Donohoe, G.C., Maleki, H., Yi, J., Mcbride, C., Nurkiewicz, T.R., Valentine, S.J., Bennett, C.E., 2016. Comparative plasma proteomic studies of pulmonary TiO 2 nanoparticle exposure in rats using liquid chromatography tandem mass spectrometry. doi:10.1016/j.jprot.2015.09.010

Mersch-Sundermann, V., Knasm??ller, S., Wu, X.J., Darroudi, F., Kassie, F., 2004. Use of a human-derived liver cell line for the detection of cytoprotective, antigenotoxic and cogenotoxic agents. Toxicology 198, 329–340. doi:10.1016/j.tox.2004.02.009

Messner, B., Ploner, C., Laufer, G., Bernhard, D., 2012. Cadmium activates a programmed, lysosomal membrane permeabilization-dependent necrosis pathway. Toxicol. Lett. 212, 268–75. doi:10.1016/j.toxlet.2012.05.026

Meyer, K., Selbach, M., 2015. Quantitative affinity purification mass spectrometry: a versatile technology to study protein–protein interactions. Front. Genet. 6, 1–7. doi:10.3389/fgene.2015.00237

Miethling-Graff, R., Rumpker, R., Richter, M., Verano-Braga, T., Kjeldsen, F., Brewer, J., Hoyland, J., Rubahn, H.-G., Erdmann, H., 2014. Exposure to silver nanoparticles induces size- and dose-dependent oxidative stress and cytotoxicity in human colon carcinoma cells. Toxicol. In Vitro 28, 1280–9. doi:10.1016/j.tiv.2014.06.005

Miranda, R.R., Bezerra, A.G., Ribeiro, C.A.O., Randi, M.A.F., Voigt, C.L., Skytte, L., Rasmussen, K.L., Kjeldsen, F., Neto, F.F., 2017. Toxicological interactions of silver nanoparticles and non-essential metals in human hepatocarcinoma cell line. Toxicol. Vitr. doi:10.1016/j.tiv.2017.01.003

Miranda, R.R., Damaso da Silveira, A.L.R., de Jesus, I.P., Grötzner, S.R., Voigt, C.L., Campos, S.X., Garcia, J.R.E., Randi, M.A.F., Ribeiro, C.A.O., Filipak Neto, F., 2016. Effects of realistic concentrations of TiO<inf>2</inf> and ZnO nanoparticles in Prochilodus lineatus juvenile fish. Environ. Sci. Pollut. Res. 23. doi:10.1007/s11356-015-5732-8

Misra, S.K., Dybowska, A., Berhanu, D., Luoma, S.N., Valsami-Jones, E., 2012. The complexity of nanoparticle dissolution and its importance in nanotoxicological studies. Sci. Total Environ. 438, 225–32. doi:10.1016/j.scitotenv.2012.08.066

Monfared, A.L., Bahrami, A.M., Hosseini, E., Soltani, S., Shaddel, M., 2015. Effects of Nano-particles on Histo-pathological changes of the fish. J. Environ. Heal. Sci. Eng. 13, 62. doi:10.1186/s40201-015-0216-9

Monroe, R.K., Halvorsen, S.W., 2009. Environmental toxicants inhibit neuronal Jak tyrosine kinase by mitochondrial disruption. Neurotoxicology 30, 589–98. doi:10.1016/j.neuro.2009.03.007

Moreau, A., Vilarem, M.J., Maurel, P., Pascussi, J.M., 2008. Xenoreceptors CAR and PXR activation and consequences on lipid metabolism, glucose homeostasis, and inflammatory response. Mol. Pharm. doi:10.1021/mp700103m

Morones, J.R., Elechiguerra, J.L., Camacho, A., Holt, K., Kouri, J.B., Ramírez, J.T., Yacaman, M.J., 2005. The bactericidal effect of silver nanoparticles. Nanotechnology 16, 2346–53. doi:10.1088/0957-4484/16/10/059

Mukherjee, R., Jow, L., Croston, G.E., Paterniti, J.R., 1997. Identification, characterization, and tissue distribution of human peroxisome proliferator-activated receptor (PPAR) isoforms PPARgamma2 versus PPARgamma1 and activation with retinoid X receptor agonists and antagonists. J. Biol. Chem. 272, 8071–6. doi:10.1074/jbc.272.12.8071

Nallanthighal, S., Chan, C., Bharali, D.J., Mousa, S.A., Vásquez, E., Reliene, R., 2017. Particle coatings but not silver ions mediate genotoxicity of ingested silver nanoparticles in a mouse model. NanoImpact. doi:10.1016/j.impact.2017.01.003

Navarro, E., Piccapietra, F., Wagner, B., Marconi, F., Kaegi, R., Odzak, N., Sigg, L., Behra, R., 2008. Toxicity of silver nanoparticles to Chlamydomonas reinhardtii. Environ. Sci. Technol. 42, 8959–64.

Nel, A., Xia, T., Mädler, L., Li, N., 2006. Toxic potential of materials at the nanolevel. Science 311, 622–7. doi:10.1126/science.1114397

Nemmiche, S., Chabane-Sari, D., Kadri, M., Guiraud, P., 2011. Cadmium chloride-induced oxidative stress and DNA damage in the human Jurkat T cell line is not linked to intracellular trace elements depletion. Toxicol. In Vitro 25, 191–8. doi:10.1016/j.tiv.2010.10.018

Nguyen, K.C., Willmore, W.G., Tayabali, A.F., 2013. Cadmium telluride quantum dots cause oxidative stress leading to extrinsic and intrinsic apoptosis in hepatocellular carcinoma HepG2 cells. Toxicology 306, 114–23. doi:10.1016/j.tox.2013.02.010

Nowack, B., Bucheli, T.D., 2007. Occurrence, behavior and effects of nanoparticles in the environment. Environ. Pollut. 150, 5–22. doi:10.1016/j.envpol.2007.06.006

Nzengue, Y., Steiman, R., Garrel, C., Lefèbvre, E., Guiraud, P., 2008. Oxidative stress and DNA damage induced by cadmium in the human keratinocyte HaCaT cell line: role of glutathione in the resistance to cadmium. Toxicology 243, 193–206. doi:10.1016/j.tox.2007.10.005

Peters, R.J.B., Bouwmeester, H., Gottardo, S., Amenta, V., Arena, M., Brandhoff, P., Marvin, H.J.P., Mech, A., Moniz, F.B., Pesudo, L.Q., Rauscher, H., Schoonjans, R., Undas, A.K., Vettori, M.V., Weigel, S., Aschberger, K., 2016. Nanomaterials for products and application in agriculture, feed and food. Trends Food Sci. Technol. 54, 155–164. doi:10.1016/j.tifs.2016.06.008

Pineda Torra, I., Claudel, T., Duval, C., Kosykh, V., Fruchart, J.-C., Staels, B., 2003. Bile Acids Induce the Expression of the Human Peroxisome Proliferator-Activated Receptor α Gene via Activation of the Farnesoid X Receptor. Mol. Endocrinol. 17, 259–272. doi:10.1210/me.2002-0120

Phillips, H. J., , 1973, Dye exclusion test for viability. In_____. Tissue culture: methods and applications. New York: Academic Press, p. 406-408.

Rajesh, K., Krishnamoorthy, J., Gupta, J., Kazimierczak, U., Papadakis, A.I., Deng, Z., Wang, S., Kuninaka, S., Koromilas, A.E., 2016. The eIF2α serine 51 phosphorylation-ATF4 arm promotes HIPPO signaling and cell death under oxidative stress. Oncotarget 7. doi:10.18632/oncotarget.10480

Regoli, F., Giuliani, M.E., 2014. Oxidative pathways of chemical toxicity and oxidative stress biomarkers in marine organisms. Mar. Environ. Res. 93, 106–17. doi:10.1016/j.marenvres.2013.07.006

Rinaldi, C., Schmidt, T., Situ, A.J., Johnson, J.O., Lee, P.R., Chen, K.-L., Bott, L.C., Fadó, R., Harmison, G.H., Parodi, S., Grunseich, C., Renvoisé, B., Biesecker, L.G., De Michele, G., Santorelli, F.M., Filla, A., Stevanin, G., Dürr, A., Brice, A., Casals, N., Traynor, B.J., Blackstone, C., Ulmer, T.S., Fischbeck, K.H., 2015. Mutation in CPT1C Associated With Pure Autosomal Dominant Spastic Paraplegia. JAMA Neurol. 72, 561–70. doi:10.1001/jamaneurol.2014.4769

Riss, T.L., Moravec, R.A., 2004. Use of Multiple Assay Endpoints to Investigate the Effects of Incubation Time, Dose of Toxin, and Plating Density in Cell-Based Cytotoxicity Assays. Assay Drug Dev. Technol. 2, 51–62. doi:10.1089/154065804322966315

Rodrigues, A.C., Curi, R., Hirata, M.H., Hirata, R.D.C., 2009. Decreased ABCB1 mRNA expression induced by atorvastatin results from enhanced mRNA degradation in HepG2 cells. Eur. J. Pharm. Sci. 37, 486–491. doi:10.1016/j.ejps.2009.04.006

Rodríguez-Enríquez, S., Juárez, O., Rodríguez-Zavala, J.S., Moreno-Sánchez, R., 2001. Multisite control of the Crabtree effect in ascites hepatoma cells. Eur. J. Biochem. 268, 2512–2519. doi:10.1046/j.1432-1327.2001.02140.x

Sahu, S.K., Bhangare, R.C., Tiwari, M., Ajmal, P.Y., Pandit, G.G., 2014. Depth profiles of lithogenic and anthropogenic mercury in the sediments from Thane Creek, Mumbai, India. Int. J. Sediment Res. doi:10.1016/S1001-6279(14)60057-3

Salomon, J.J., Ehrhardt, C., 2011. Nanoparticles attenuate P-glycoprotein/MDR1 function in A549 human alveolar epithelial cells. Eur. J. Pharm. Biopharm. 77, 392–397. doi:10.1016/j.ejpb.2010.11.009

Schwämmle, V., León, I.R., Jensen, O.N., 2013. Assessment and improvement of statistical tools for comparative proteomics analysis of sparse data sets with few

experimental replicates. J. Proteome Res. 12, 3874–3883. doi:10.1021/pr400045u

Segner, H., 1998. Isolation and primary culture of teleost hepatocytes 120, 71–81.

Seltenrich, N., 2013. Nanosilver: Weighing the risks and benefits. Environ. Health Perspect. 121, 220–225. doi:10.1289/ehp.121-a220

Sheng, Z.G., Li, Y., Fan, R.M., Chao, X.J., Zhu, B.Z., 2013. Lethal synergism between organic and inorganic wood preservatives via formation of an unusual lipophilic ternary complex. Toxicol. Appl. Pharmacol. 266, 335–344. doi:10.1016/j.taap.2012.11.013

Shvedova, A., Pietroiusti, A., Kagan, V., 2016. Nanotoxicology ten years later: Lights and shadows. Toxicol. Appl. Pharmacol. 299, 1–2. doi:10.1016/j.taap.2016.02.014

Sierra, M.I., Valdés, A., Fernandez, A.F., Torrecillas, R., Fraga, M.F., 2016. The effect of exposure to nanoparticles and nanomaterials on the mammalian epigenome. Int. J. Nanomedicine Volume 11, 6297–6306. doi:10.2147/IJN.S120104

Singh, R.P., Ramarao, P., 2012. Cellular uptake, intracellular trafficking and cytotoxicity of silver nanoparticles. Toxicol. Lett. 213, 249–59. doi:10.1016/j.toxlet.2012.07.009

Stacchiotti, A., Morandini, F., Bettoni, F., Schena, I., Lavazza, A., Giovanni, P., Apostoli, P., Rezzani, R., Francesca, M., 2009. Stress proteins and oxidative damage in a renal derived cell line exposed to inorganic mercury and lead 264, 215–224. doi:10.1016/j.tox.2009.08.014

Steen, H., Mann, M., 2004. The ABC's (and XYZ's) of peptide sequencing. Nat. Rev. Mol. Cell Biol. 5, 699–711. doi:10.1038/nrm1468

Syversen, T., Kaur, P., 2012. The toxicology of mercury and its compounds. J. Trace Elem. Med. Biol. doi:10.1016/j.jtemb.2012.02.004

Takeda, K., Suzuki, K., Ishihara, A., Kubo-irie, M., Fujimoto, R., Tabata, M., Oshio, S., Nihei, Y., Ihara, T., Sugamata, M., 2009. Nanoparticles Transferred from Pregnant Mice to Their Offspring Can Damage the Genital and Cranial Nerve Systems. Distribution 55, 95–102.

Tang, J., Xiong, L., Wang, S., Wang, J., Liu, L., Li, J., Wan, Z., Xi, T., 2008. Influence of silver nanoparticles on neurons and blood-brain barrier via subcutaneous injection in rats. Appl. Surf. Sci. 255, 502–504. doi:10.1016/j.apsusc.2008.06.058

Templeton, D.M., Liu, Y., 2010. Chemico-Biological Interactions Multiple roles of cadmium in cell death and survival. Chem. Biol. Interact. 188, 267–275. doi:10.1016/j.cbi.2010.03.040

Tomankova, K., Horakova, J., Harvanova, M., Malina, L., Soukupova, J., Hradilova, S., Kejlova, K., Malohlava, J., Licman, L., Dvorakova, M., Jirova, D., Kolarova, H., 2015. Cytotoxicity, cell uptake and microscopic analysis of titanium dioxide and silver nanoparticles in vitro. Food Chem. Toxicol. doi:10.1016/j.fct.2015.03.027

Urani, C., 2005. Cytotoxicity and induction of protective mechanisms in HepG2 cells exposed to cadmium 19, 887–892. doi:10.1016/j.tiv.2005.06.011

van der Oost, R., Beyer, J., Vermeulen, N.P.E., 2003. Fish bioaccumulation and biomarkers in environmental risk assessment: a review. Environ. Toxicol. Pharmacol. 13, 57–149.

Vance, M.E., Kuiken, T., Vejerano, E.P., McGinnis, S.P., Hochella, M.F., Hull, D.R., 2015. Nanotechnology in the real world: Redeveloping the nanomaterial consumer products inventory. Beilstein J. Nanotechnol. 6, 1769–1780. doi:10.3762/bjnano.6.181

Verano-Braga, T., Miethling-Graff, R., Wojdyla, K., Rogowska-Wrzesinska, A., Brewer, J.R., Erdmann, H., Kjeldsen, F., 2014. Insights into the cellular response triggered by silver nanoparticles using quantitative proteomics. ACS Nano 8, 2161–75. doi:10.1021/nn4050744

Vergilio, C.S., Carvalho, C.E. V, Melo, E.J.T., 2014. Mercury-induced dysfunctions in multiple organelles leading to cell death. Toxicol. In Vitro 29, 63–71. doi:10.1016/j.tiv.2014.09.006

Vinken, M., Blaauboer, B.J., 2016. In vitro testing of basal cytotoxicity: Establishment of an adverse outcome pathway from chemical insult to cell death. Toxicol. Vitr. doi:10.1016/j.tiv.2016.12.004

Vriend, J., Reiter, R.J., 2015. The Keap1-Nrf2-antioxidant response element pathway: A review of its regulation by melatonin and the proteasome. Mol. Cell. Endocrinol. doi:10.1016/j.mce.2014.12.013

Wang, Y., Zhao, Q., Han, N., Bai, L., Li, J., Liu, J., Che, E., Hu, L., Zhang, Q., Jiang, T., Wang, S., 2015. Mesoporous silica nanoparticles in drug delivery and biomedical applications. Nanomedicine Nanotechnology, Biol. Med. 11, 313–327. doi:10.1016/j.nano.2014.09.014

Weir, A., Westerhoff, P., Fabricius, L., von Goetz, N., 2012. Titanium Dioxide Nanoparticles in Food and Personal Care Products. Environ. Sci. Technol. 46, 2242–2250. doi:10.1021/es204168d

Wen, Y., Fa, C., Yao, C., Chieh, C., Sung, K., Hwa, S., 2010. Inorganic mercury causes pancreatic β -cell death via the oxidative stress-induced apoptotic and necrotic pathways. Toxicol. Appl. Pharmacol. 243, 323–331. doi:10.1016/j.taap.2009.11.024

Wildt, B.E., Celedon, A., Maurer, E.I., Casey, B.J., Nagy, A.M., Hussain, S.M., Goering, P.L., 2015. Intracellular accumulation and dissolution of silver nanoparticles in L-929 fibroblast cells using live cell time-lapse microscopy. Nanotoxicology 5390, 1–10. doi:10.3109/17435390.2015.1113321

Wu, Q., Nouara, A., Li, Y., Zhang, M., Wang, W., Tang, M., Ye, B., Ding, J., Wang, D., 2013. Comparison of toxicities from three metal oxide nanoparticles at environmental relevant concentrations in nematode Caenorhabditis elegans. Chemosphere 90, 1123–31. doi:10.1016/j.chemosphere.2012.09.019

Wu, Y., Zhou, Q., Li, H., Liu, W., Wang, T., Jiang, G., 2010. Effects of silver nanoparticles on the development and histopathology biomarkers of Japanese medaka (Oryzias latipes) using the partial-life test. Aquat. Toxicol. 100, 160–7. doi:10.1016/j.aquatox.2009.11.014

Yano, C.L., Marcondes, M.C.C.G., 2005. Cadmium chloride-induced oxidative stress in skeletal muscle cells in vitro. Free Radic. Biol. Med. 39, 1378–1384. doi:10.1016/j.freeradbiomed.2005.07.001

Yates, J.R., Ruse, C.I., Nakorchevsky, A., 2009. Proteomics by Mass Spectrometry: Approaches, Advances, and Applications. Annu. Rev. Biomed. Eng. 11, 49–79. doi:10.1146/annurev-bioeng-061008-124934

You, C., Han, C., Wang, X., Zheng, Y., Li, Q., Hu, X., Sun, H., 2012. The progress of silver nanoparticles in the antibacterial mechanism, clinical application and cytotoxicity. Mol. Biol. Rep. 39, 9193–9201. doi:10.1007/s11033-012-1792-8

Zanette, C., Pelin, M., Crosera, M., Adami, G., Bovenzi, M., Larese, F.F., Florio, C., 2011. Silver nanoparticles exert a long-lasting antiproliferative effect on human keratinocyte HaCaT cell line. Toxicol. Vitr. 25, 1053–1060. doi:10.1016/j.tiv.2011.04.005

Zhang, C., Hu, Z., Deng, B., 2016. Silver nanoparticles in aquatic environments: Physiochemical behavior and antimicrobial mechanisms. Water Res. 88, 403–427. doi:10.1016/j.watres.2015.10.025

RESULTADOS COMPLEMENTARES

Capítulo 1

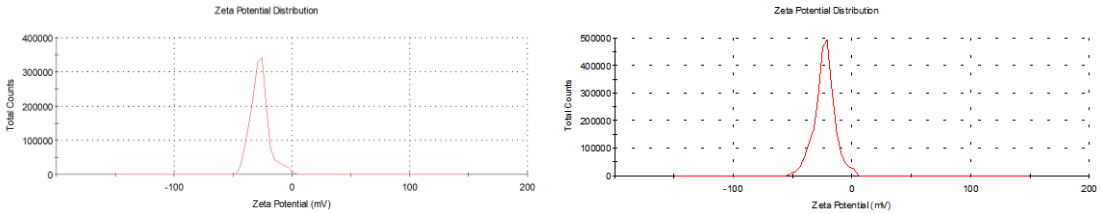

FIGURA 1. Caracterização das AgNP. Potencial zeta das duas soluções mãe de AgNP sintetizadas por ablação a laser.

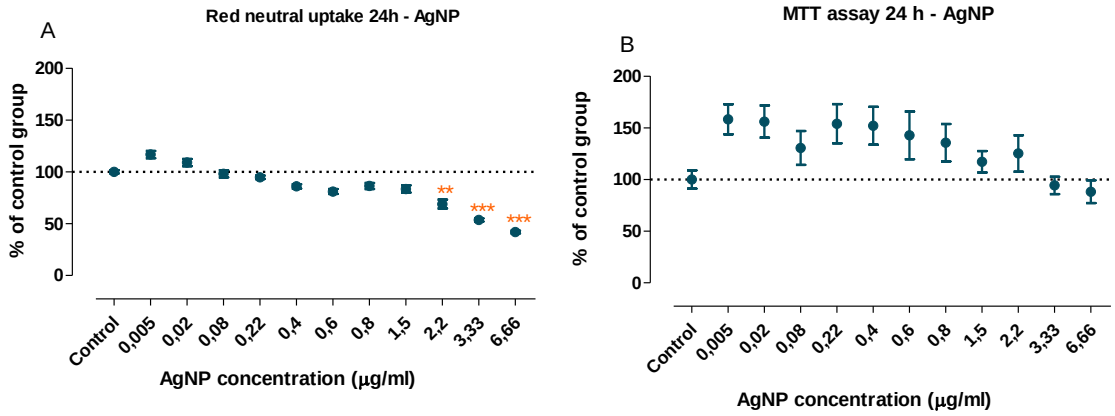

FIGURA 2. Screening de toxicidade após 24 h de exposição às AgNP. Ensaios de viabilidade celular (A e C vermelho neutro; B e D MTT) em porcentagem comparado ao controle em HepG2 após exposição às AgNP. Dados são apresentados em média + SEM de três réplicas biológicas independentes. Asteriscos indicam diferença em relação ao controle e sustenidos indicam efeito de interação *p<0,05, ***p<0,001. Sustenido (#) indica interação toxicológica.

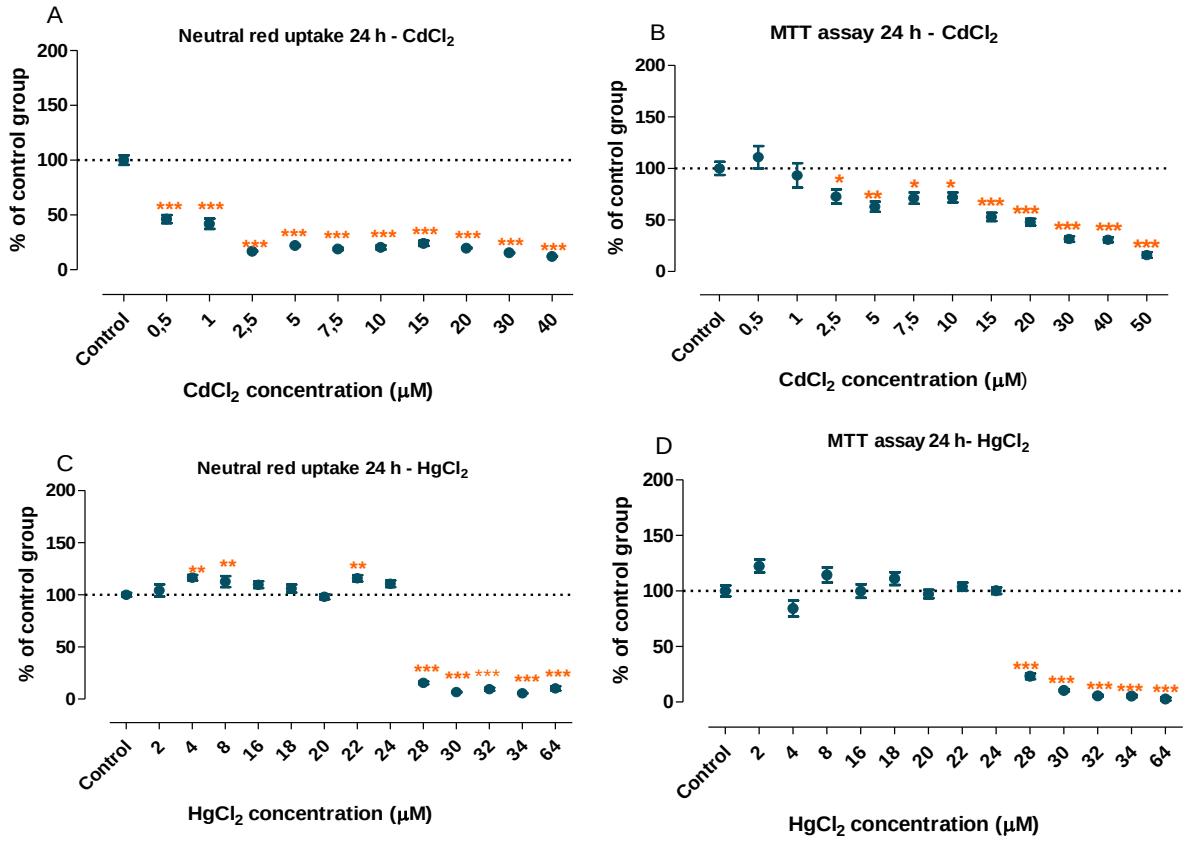

FIGURA 3. Screening de toxicidade após 24 h de exposição ao Cd e Hg. Ensaios de viabilidade celular (A e C vermelho neutro; B e D MTT) em porcentagem comparado ao controle em HepG2 após ao cadmio (A-B) e mercúrio (C-D). Dados são apresentados em média + SEM de três réplicas biológicas independentes. Asteriscos indicam diferença em relação ao controle e sustenidos indicam efeito de interação *p<0,05, ***p<0,001. Sustenido (#) indica interação toxicológica.

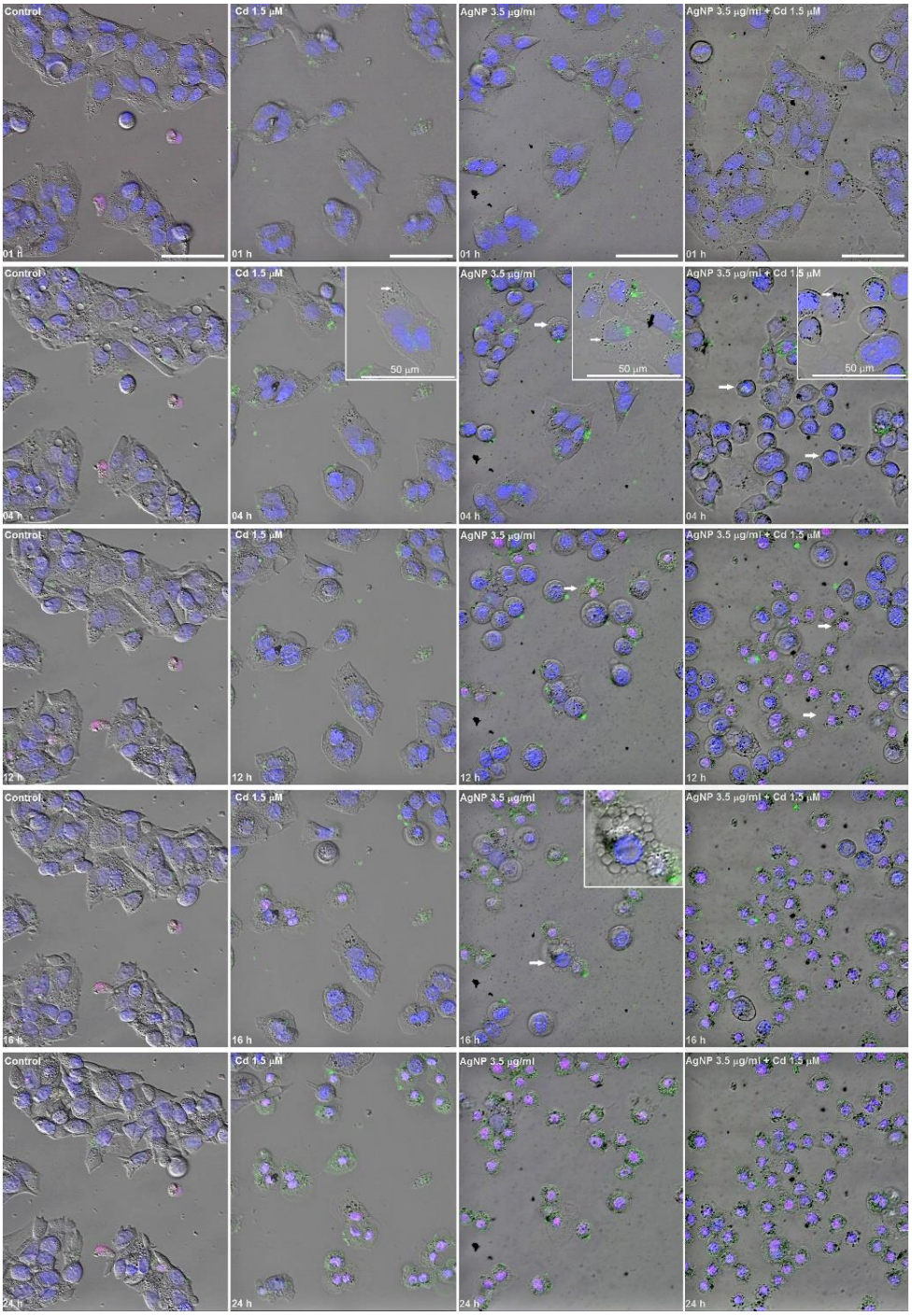

FIGURA 4. Ensaio de morte celular em time-lapse dos grupos: Controle, Cd II (1.5 µM), AgNP II (3.5 $\mu g.ml^{-1}$) and AgNP II+ Cd II. Células foram incubadas Hoechst (azul), anexina V-FITC (verde) e iodeto de propídio (vermelho) durante 24 h. Células viáveis apresentam o núcleo marcado em azul; células morrendo ou mortas apresentam o núcleo marcado em rosa/roxo (sobreposição das fluorescências vermelha e azul) e a superfície celular em verde (marcação da fosfatidilserina). Células do controle se mantem organizadas em grupos, aderidas à superfície e espraiadas durante o curso de 24h. Agregados de AgNP podem ser observados para exposição nos grupos que receberam AgNP II e AgNP II + Cd II, particularmente após 4 h de exposição. No entanto, essa observação deve ser feita com cuidado, pois os aspectos de agregados de AgNP são similares a organelas celulares (inserto 4 h; organela = seta em Cd II; AgNP = seta em AgNP II e AgNP II+ Cd II em imagens ajustadas. Células tornam-se arredondas a partir de 16 h no Cd II e anteriormente para exposição à AgNP II e AgNP II+ Cd II (setas

brancas em 4 h; setas pretas em insertos de AgNP II mostram perda do contato célula-célula). Taxa significativa de morte é observada a partir de 12 h, em grupos expostos à AgNP II e AgNP II+ Cd II (setas em 12 h), particularmente no último grupo. A maioria das células começa morrendo por apoptose, mas mudanças no modo de morte celular ocorrem (de apoptose para necrose), com dilatação/aumento celular e em seguida, ruptura (ver vídeo do material suplementar para mais detalhes). Células estão na mesma magnificação (exceto insertos).

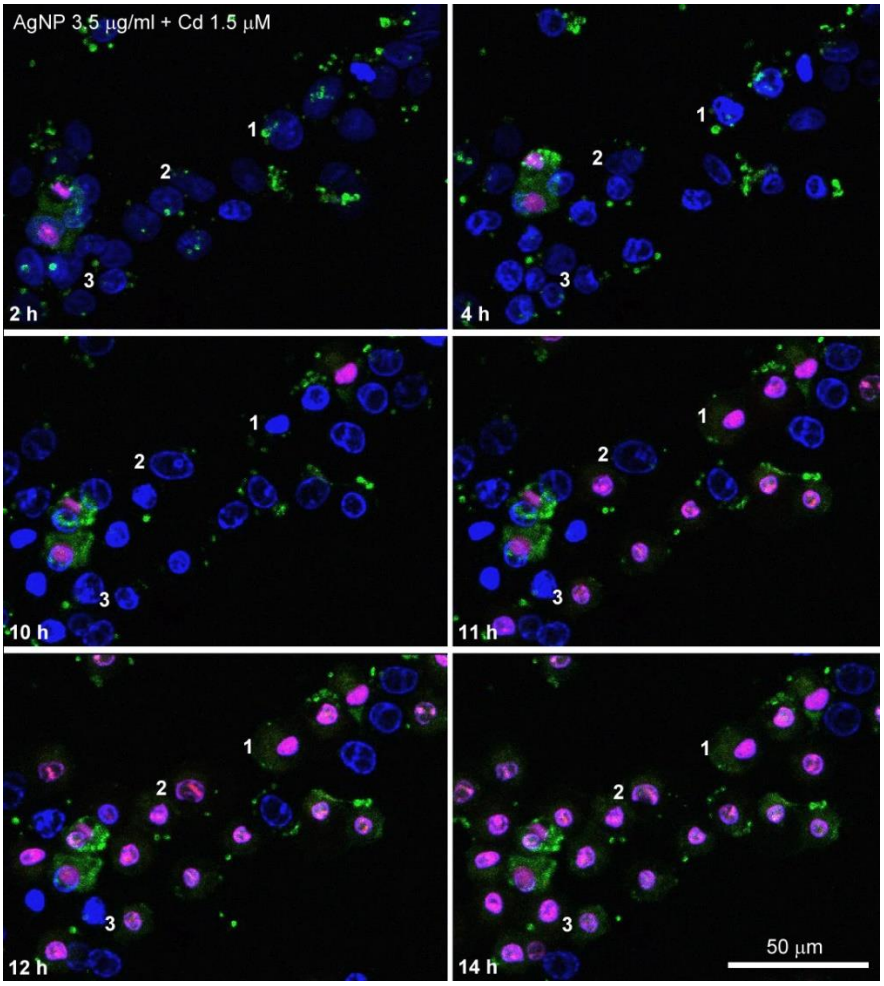

FIGURA 5. Ensaio de morte celular em time-lapse por microscopia confocal de células from HepG2 expostas à AgNP II + Cd II. Três células (1, 2 e 3) são indicadas por números. Modificações associadas com morte celular são descritas para a célula '1', mas também podem ser observadas para as outras células. Após 2 h de exposição, o núcleo da célula '1' está corado de azul (por Hoechst), indicando que a membrana plasmática ainda é uma barreira eficiente. A condensação da cromatina aumenta (característica de apoptose) durante o curso de 2-10 h de exposição. Em 11 h, a função de barreira da membrana plasmática é perturbada, de modo que o iodeto de propídio (laranja) e anexina V-FITC (verde) entram na célula e marcam o núcleo (azul + laranja = rosa/roxo) e a fosfatidilserina em verde, embora a última possa ainda estar na monocamada citosólica da membrana plasmática (característica de necrose). A marcação por fosfatidilserina torna-se mais intense após 12 h de exposição à AgNP+Cd.